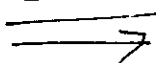


FREE CONVECTION HEAT TRANSFER ACROSS AIR LAYERS WITH ONE SURFACE SEMICIRCULAR CORRUGATED

Call no.



621.4022

2001

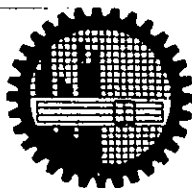
SHA



A. M. M. SHAMSUL ALAM



#94973#



DEPARTMENT OF MECHANICAL ENGINEERING

BANGLADESH UNIVERSITY OF ENGINEERING AND TECHNOLOGY, DHAKA

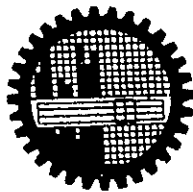
JANUARY, 2001

034

FREE CONVECTION HEAT TRANSFER ACROSS AIR LAYERS WITH ONE SURFACE SEMICIRCULAR CORRUGATED

By

A. M. M. SHAMSUL ALAM



A THESIS SUBMITTED TO THE DEPARTMENT OF MECHANICAL
ENGINEERING IN PARTIAL FULFILMENT OF THE DEGREE OF
MASTER OF SCIENCE IN MECHANICAL ENGINEERING

BANGLADESH UNIVERSITY OF ENGINEERING AND TECHNOLOGY, DHAKA

JANUARY, 2001

CERTIFICATE OF APPROVAL

The thesis titled "Free Convection Heat Transfer Across Air Layers with One Surface Semicircular Corrugated" submitted by A. M. M. Shamsul Alam, Roll Number 9610001F, Registration Number 86520 of M.Sc. Engineering (Mechanical) has been accepted as satisfactory in partial fulfillment of the degree of Master of Science in Engineering (Mechanical) on the 14th January, 2001.



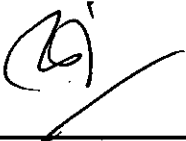
Dr. Chowdhury Md. Feroz (Supervisor)
Associate Professor
Mechanical Engineering Department
BUET, Dhaka.

Chairman



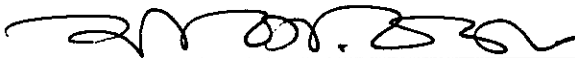
Dr. Md. Abdur Razzaq Akhanda
Professor
Mechanical Engineering Department
BUET, Dhaka.

Member



Dr. A.K.M. Sadrul Islam
Professor
Mechanical Engineering Department
BUET, Dhaka.

Member



Dr. Md. Abdur Rashid Sarkar
Professor & Head
Mechanical Engineering Department
BUET, Dhaka.

Member (Ex-officio)

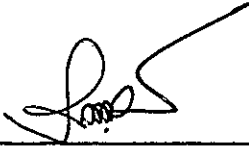


Dr. A. K. M. Iqbal Hussain
Professor
Mechanical & Chemical Engineering Department
Islamic Institute of Technology (IIT), Gazipur, Bangladesh.

Member (External)

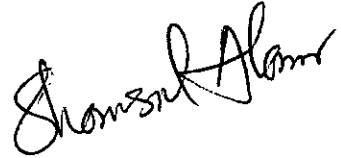
CERTIFICATE OF RESEARCH

This is to certify that the work presented in this thesis is an outcome of the investigation carried out by the author under the supervision of Dr. Chowdhury Md. Feroz, Associate Professor of Department of Mechanical Engineering, Bangladesh University of Engineering & Technology, Dhaka.



Dr. Chowdhury Md. Feroz

Supervisor



A. M. M. Shamsul Alam

Author

ACKNOWLEDGEMENT

The author hereby wish to express his heartiest and sincerest gratitude and indebtedness to Dr. Chowdhury Md. Feroz, Associate Professor of Department of Mechanical Engineering, Bangladesh University of Engineering & Technology, Dhaka, for his guidance, inspiration, constructive suggestions and close supervision throughout the entire period of the experimental investigation.

The author also expresses thankful gratitude to Dr. A. K. M. Iqbal Hussain, Professor of Department of Chemical & Mechanical Engineering, Islamic Institute of Technology, Gazipur, Dr. Md. Abdur Razzaq Akhanda, Professor of Department of Mechanical Engineering, Bangladesh University of Engineering & Technology, Dhaka, Dr. A. K. M. Sadrul Islam, Professor of Department of Mechanical Engineering, Bangladesh University of Engineering & Technology, Dhaka and Dr. Abdur Rashid Sarker, Professor & Head of Department of Mechanical Engineering, Bangladesh University of Engineering & Technology, Dhaka, for their cooperation, valuable suggestions and inspiration for completion of this thesis.

The author is indebted and highly grateful to his parent for giving continuous motivation for completion of this thesis, without their inspiration this thesis work would have not been possible. The author is also highly grateful to his wife for her continuous support throughout the research period.

A lot of thanks due for Mr. Amir Hossain, Senior Laboratory Instructor cum Store Keeper of Heat Transfer Laboratory of Mechanical Engineering Department for his cooperation and guidance all through the research work. Thanks are also given specially to Mr. Shahnewaz, Foreman Instructor, and Mr. Rahim of Welding & Sheet metal Shop and then to Mr. Halder, of Welding & Sheet metal Shop, Mr. Habib of Machine shop and Mr. Syed Shahadat Hossain Kazi & Mr. Mozammel Patwari of Carpentry Shop, BUET, for fabricating and assembling different parts and components of the experimental setup.

ABSTRACT

An experimental investigation on steady state natural convection heat transfer through air from hot semicircular corrugated plates to a cold flat plate placed above and parallel to it is carried out. The amplitude of corrugation is 10 mm and air pressure is atmospheric in the enclosure. The effects of angle of inclination, aspect ratio, temperature difference and Rayleigh number on average convective heat transfer co-efficient are investigated. This study covers the following ranges of parameters:

$$0^\circ \leq \theta \leq 75^\circ, 3.5 \leq A \leq 9.5, 10^\circ\text{C} \leq \Delta T \leq 35^\circ\text{C}, \text{ and } 3.40 \times 10^4 \leq Ra_L \leq 2.08 \times 10^6$$

where, side and bottom surfaces of enclosure surrounding the test section are adiabatic.

The experimental investigation gives the following results. The convective heat transfer coefficients increase with increasing of temperature potential but decrease with increasing of inclination for same aspect ratio. Moreover, convective heat transfer coefficients increase upto a certain aspect ratio and then decrease with a further increasing of aspect ratio and this limiting value of aspect ratio for maximum heat transfer coefficient is found to be 7.5.

The results are compared with those available in the literature and it is found that for Rayleigh number in the range of 3.0×10^5 to 1.0×10^6 , aspect ratio of 7.5 and the angle of inclination of $\theta = 0^\circ$ Nusselt number for semicircular corrugation is found to be higher by about 37%, 12%, 43% and 37% from those of vee, sinusoidal, flat and trapezoidal corrugation respectively.

Finally correlation for semicircular corrugation are developed which correlate almost all the experimental data within an error of $\pm 20\%$ by the following equations:

$$Nu_L = 0.0257 [Ra_L \text{Cos}\theta]^{0.5} \cdot [A]^{0.48}, \quad \text{for } 0^\circ \leq \theta < 60^\circ$$

$$Nu_L = 0.0105 [Ra_L \text{Cos}\theta]^{0.63} \cdot [A]^{0.67}, \quad \text{for } 60^\circ < \theta \leq 90^\circ$$

Through uncertainty analysis the uncertainty for the present calculation of the value of Nusselt number in semicircular corrugated enclosure is found to be 1.2526%.

	PAGES
CERTIFICATE OF APPROVAL	
CERTIFICATE OF RESEARCH	
ACKNOWLEDGEMENT	
ABSTRACT	
CONTENTS	
NOMENCLATURE	
CHAPTER 1: INTRODUCTION	1
1.1 General	1
1.2 Natural Convection in an enclosure	1
1.2.a Horizontal Fluid Layers	2
1.2.b Inclined Fluid Layers	3
1.3 Motivation behind the Selection of Present Work	4
1.4 The Present Study	5
CHAPTER 2: LITERATURE REVIEW	7
2.1 General	7
2.2 Natural Convective Heat Transfer in Plane Horizontal Fluid Layers	7
2.3 Natural Convective Heat Transfer in Plane Inclined Fluid Layers	10
CHAPTER 3: MATHEMATICAL MODEL	14
3.1 Description of the Problem	14
3.2 Mathematical Equations	15

CHAPTER 4:	EXPERIMENTAL SET-UP	16
	4.1 General Description of the Set-up	16
	4.2 The Test section	16
	4.2.1 The Hot Plate assembly	17
	4.2.2 The Outer Guard Heater Assembly	18
	a. The Upper Outer Guard Heater Ring	18
	b. The Lower Outer Guard Heater Ring	19
	4.2.3 The Cold Plate assembly	19
	4.2.4 The Rig Holder and Alignment Plate	20
	4.3 The Reverse Water tank	21
CHAPTER 5:	EXPERIMENTAL MEASUREMENT AND TEST PROCEDURE	22
	5.1 Instrumentation	22
	5.1.1 Temperature Measurement	22
	5.1.2 Heat Flux Measurement	23
	5.2 Test Procedure	23
	5.3 Reduction of Data	25
CHAPTER 6:	RESULTS AND DISCUSSION	26
CHAPTER 7:	CONCLUSIONS AND RECOMMENDATIONS	31
	7.1 Conclusions	31
	7.2 Recommendations	32
REFERENCES		33
<i>APPENDICES</i>		36
	<i>Appendix A</i> : Design of the Test Rig	36
	<i>Appendix B</i> : Conduction Correction	45
	<i>Appendix C</i> : Determination of Emissivity of Corrugated Surface	46
	<i>Appendix D</i> : Uncertainty Analysis	47
FIGURES		53

NOMENCLATURE

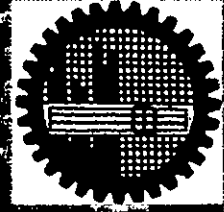
SYMBOL	MEANING	UNITS
A	Aspect ratio, L / H	dimensionless
A_{COR}	Projected area of the test section	m^2
A_{COLD}	Area of the cold plate	m^2
A_P	Area of any plane rectangular surface	m^2
A_i	Area of surface i	m^2
A_j	Area of surface j	m^2
A_s	Area of wooden surface	m^2
C	Constant	dimensionless
C_P	Specific heat of air at constant pressure	$kJ / kg K$
E_b	Emissive power of a black surface, σT^4	W / m^2
F	Shape factor	dimensionless
Gr	Grashof number, $g \beta \Delta T \cdot d^3 / \nu^2$	dimensionless
g	Acceleration due to gravity	m / sec^2
h	Average natural convective heat transfer coefficient	$W / m^2 K$
H	Amplitude of the corrugation	mm
I_{safe}	Safe current capacity of the heater coil	ampere
J	Radiosity [Emissive power for a black surface, E_b]	W / m^2
k	Thermal conductivity of air	$W / m K$
L_c	Characteristic length (= A_P)	m
L	Mean plate spacing	mm
m	Exponent	dimensionless
n	Exponent	dimensionless
Nu_L	Average Nusselt number, $h L / k$	dimensionless
Pr	Prandtl number, $\mu \cdot C_P / k$	dimensionless
q	Heat transfer rate	W / m^2
q''	Heat flux rate into the test hot plate	W / m^2

r	Unit electrical resistance	ohms/ m
Ra _L	Rayleigh number based on mean plate spacing (L), $g \cdot \beta \cdot \Delta T \cdot L^3 / \nu \alpha$	dimensionless
s	Maximum width of corrugation	mm
t	Time	sec
T	Temperature	K
T _a , T _∞	Ambient air temperature	K
T _f	Fluid film temperature, $[T_{COR} + T_{COLD}] / 2$	K
T _{COR}	Temperature of the hot corrugated plate	K
T _{COLD}	Temperature of the cold flat plate	K
ΔT	Temperature difference between the hot corrugated plate and flat cold plate	K
ΔT _c	Conduction correction	K
T _s	Temperature of the wooden surfaces	K
u, v, w	Velocity components in direction of x, y, z respectively	m / sec
V _{safe}	Safe voltage across the heater coil	Volts
W	Width of the enclosure	mm
x, y, z	Spatial coordinates	
X _{COR}	Longitudinal side of the test section of corrugated plate	mm
X _{COLD}	Longitudinal side of the cold flat plate	mm
ΔX	Thickness along x direction	mm
Y _{COR}	Lateral side of the test section of the corrugated plate	mm
Y _{COLD}	Lateral side of the cold flat plate	mm

GREEK ALPHABET:

α	Thermal diffusivity, $k / \rho C_p$	m ² / sec
β	Volumetric thermal expansion coefficient, $1 / T_f$	1 / K
Δ	Difference	
ε	Long wave emmissivities	dimensionless
ε _H	Hemispherical emmitance	dimensionless
ε _s	Long wave emmissivities of the wooden surface	dimensionless

θ	Tilt angle of inclination of the enclosed air layers with the horizontal	degree
ν	Kinematic viscosity of the convecting fluid (air)	m^2 / sec
ρ	Density	kg / m^3
σ	Stefan Boltzmann constant [= 5.67×10^{-8}]	$\text{W} / \text{m}^2 \text{K}^4$
ϕ	Phase angle of the current	degree



1

INTRODUCTION



1.1 GENERAL

In natural convection the fluid flow arises as a result of density variations caused by thermal expansion of the fluid in a non-uniform temperature distribution. The movement of fluid in natural convection whether it is a gas or liquid results from the buoyancy forces imposed on the fluid because of the decrease in its density in the proximity of the heat transfer surface caused as a result of a heating process. The buoyancy forces will not be present if the fluid is not acted upon by some external force field such as gravity, though it's not the only type of force field, which can produce free convection currents. A fluid enclosed in a rotating machine is acted upon by a centrifugal force field, and thus could experience natural convection currents provided one or more surfaces in contact with the fluid are heated. However, among these the presence of a temperature gradient has found to be the most common situation in which a mass density gradient may arise in a fluid. For gases and liquids density depends on temperature and generally it decreases as liquid expands with increasing temperature. As the temperature potential increases beyond a certain value, the viscous forces within the fluid can no longer sustain the buoyancy forces and a convective motion sets up, giving rise to circulation pattern thus occurs the natural convection. It is seen that the qualitative and quantitative analyses of natural convection heat transfer are quite difficult. That's why theoretical analysis of natural convection heat transfer for most of the practical situations are absent in the literature which necessitates the urgency of such experimental investigation at this present stage.

1.2 NATURAL CONVECTION IN AN ENCLOSURE

Heat transfer by free convection in enclosed spaces has numerous engineering applications. For example, free convection in wall cavities, between window glazing, in the annulus between concentric cylinders or spheres and in flat-plate solar collectors, nuclear reactor operation and safety, waste disposal and fire prevention and safety, cooling of microelectronic components are typical examples. The surfaces may be plan horizontal or vertical or inclined. The determination

of the onset of free convection and the heat transfer coefficient associated with free convection has been the subject of numerous investigations. Despite the vast amount of experimental and analytic studies of free convection in enclosed spaces, the heat transfer correlations covering all ranges of parameters are still not available.

Recently the heat transfer characteristics for non-plane (sinusoidal, rectangular and trapezoidal, square, vee corrugated) horizontal as well as inclined fluid layers have been reported. The main features of these types of natural convection heat transfer problems is that the boundary layer thickness, if there be any, is comparable with the dimensions of the enclosed fluid layers. Hence the development of the flow is often strongly influenced by the shape of the boundaries. Therefore, the heat transfer rate is also dependent on the shape of the boundary surfaces of the enclosure.

1.2a Horizontal fluid layers

The convective motion and heat transfer occurring in a horizontal layer of fluid heated from below have been the subject matter of a large number of research works in recent years. Fluids whose density decreases with increasing temperature, no natural convection currents occur in such a fluid when enclosed between two parallel horizontal plates as long as the temperature of the upper plate is higher than the temperature of the lower one. In that case heat will be transferred only by the conduction. The situation is different when the fluid is enclosed between two enclosed surfaces of which the upper surface is at lower temperature than the lower one. For such a situation fluids whose density decrease with increasing temperature leads to an unstable situation. Benard ^[1] mentioned this instability as a "top heavy" situation. Rayleigh ^[2] recognized that the unstable situation must break down at a certain value of Rayleigh number above which a convective motion must be generated. Jeffrey's ^[3] and Low ^[4] calculated this limiting value of Ra_L to be 1708, when the air layer is bounded on both sides by solid walls. They reported a value of 1108 with a free upper surface. Optical investigation in a trough filled with water carried out by Schmidt-Saunders ^[5] confirmed this limiting value [$Ra_L = 1708$]. Above the critical value of Ra_L a peculiar natural convection flow pattern arises. The flow field becomes a cellular structure with more or less regular hexagonal cells. In the interior of these cells the flow moves in upward direction and along the rim of the cells it returns down. According to Ostrach ^[6] when the top

and the bottom surfaces are rigid, the turbulence first appears at $Ra_L = 5380$ and the flow becomes fully turbulent at $Ra_L = 50,000$ for plane horizontal air layers but for water it occurs at lower values of Ra_L with same boundaries.

1.2b Inclined fluid layers

For an inclined layer heated from below, free convection flow pattern set in when a critical Grashof number is exceeded, but mechanism of heat transfer in various flow regimes is much more complicated than that of free convection in horizontal or vertical layers. Purely convective motion is gained after decaying of low distinct flow regimes: (i) Conductive regime and (ii) Postconductive regime. At very small Rayleigh number the motion is relatively simple and consists of one large cell that fills the whole slot, the fluid rising from the hot wall, falling down the cold and turning at the opposite ends of the slot. This flow pattern is known as base flow according to Ayyaswamy^[7]. The heat transfer in this flow regime is purely conductive [i.e., $Nu = 1$] except at the extreme ends where there is some convective heat transfer associated with the fluid turning. However, as the aspect ratio, A of the enclosure becomes increasingly large, the contribution of this convective heat transfer to the average Nusselt number becomes vanishingly small. For air this conductive regime exists if the Rayleigh number is less than a critical value Ra_C . This limit for plane fluid layers has been defined by Buchberg, *et al.*^[8] as follows:

$$Nu = 1 \quad \text{for } Ra_L < 1708 / \cos\theta \quad \text{i.e., } Ra_C = 1708 / \cos\theta$$

This value of critical Rayleigh number will be different for non-plane fluid layers (corrugated plates).

At Ra_C , the base flow becomes marginally unstable and the resulting flow begins to take the form of steady longitudinal rolls i.e., rolls with their axis along the up slope.

At $Ra_L \gg Ra_C$, the flow becomes convective. The resulting flow begins to take the boundary layer structure with the resistance to heat transfer lying exclusively in two boundary layers, one on each of the boundary surfaces.

1.3 MOTIVATION BEHIND THE SELECTION OF PRESENT WORK

Natural convective heat transfer across inclined fluid (air) layer heated from below is of importance in many engineering applications. In particular recently designers of flat-plate solar collectors are very much concerned about free convection heat loss from the absorber plate to the adjacent flat glass covers since a reduction of heat loss through the cover plates increase the collector's efficiency. A considerable number of investigations have already predicted the natural convection heat transfer across air layers bounded by two flat plates.

Dropkin-Somerscales^[9] investigated natural convection heat transfer in liquids confined with two parallel plates. Elsherbiny^[10] investigated free convection heat transfer for air layers bounded by a lower Vee-corrugated plate and an upper cold flat plate. He claimed that convective heat transfer across air layers bounded by Vee-corrugated plate and flat-plate are greater than those for two parallel flat plates by a maximum of 50%. Through experimental investigation, Kabir^[11] reported that the heat transfer coefficient for sinusoidal corrugation is lower than that for Vee-corrugation. Chowdhury^[12] reported that heat transfer coefficient for trapezoidal corrugation were lower than those for vee^[10] and sinusoidal^[11] corrugations on an average of 15% and 35%, respectively. But the values for trapezoidal corrugation are higher than those for rectangular corrugation by an average of 4%. Saiful^[13] reported that the heat transfer coefficient for square corrugation is lower than those for trapezoidal, rectangular and sinusoidal corrugations. Through experimental investigation Latifa^[14] concluded that the heat transfer coefficients for vee corrugation are higher than those for sinusoidal, trapezoidal, rectangular and square corrugations by 12%, 22%, 28% and 40%, respectively. Recently through experimental investigation, Stewart-Johnson^[15] reported the advantageous effect of spherical shaped surfaces in connection with convection heat transfer.

Works are reported on natural convection heat transfer across air layer in an enclosure bounded by two flat plates, from a hot sinusoidal, trapezoidal, rectangular, square and vee-corrugated plates to a cold flat plate. But no work is reported on natural convection heat transfer from hot semicircular corrugated plate to a cold flat plate. Hence through the present investigation an effort has been made to enrich the statistics on natural convection heat transfer concerned in an enclosure bounded by two plates.

1.4 THE PRESENT STUDY

Previously no work has been reported on the behavior of natural convection with the semicircular corrugated plates. So, the present study is an experimental investigation on the natural convection heat transfer rate from hot semicircular corrugated plates to a cold flat plate with air as the working fluid.

Main Objectives of the present work are:

- To redesign the existing experimental set-up for studying the natural convection heat transfer from semicircular corrugation.
- To determine the dependence of average natural convective heat transfer coefficient, h on aspect ratio, A .
- To study the variation of average natural convective heat transfer coefficient, h with the angle of inclination, θ of the semicircular corrugated plate with the horizontal.
- To observe the variation of average natural convective heat transfer coefficient, h with different thermal potential, ΔT .
- To compare the results of this study with earlier relevant investigations.
- To develop a correlation which will correlate all experimental data within reasonable limit.

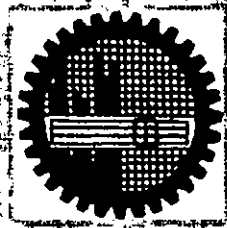
To meet the above objectives, the existing experimental set-up is redesigned for the present investigation. Supply of power to the experimental rig by electrical heater is varied by using a Variac with the variation of aspect ratio to keep a particular constant thermal potential (ΔT). The cold flat plate is cooled by continuous water circulation. In the fabrication of hot plate assembly, semicircular corrugated plates of depth (amplitudes, H) 10 mm is fabricated from G.I. sheets.

The aspect ratio is varied between 3.5 and 9.5 by changing the mean plate spacing, L . The angle of inclination, θ covering the range in between 0° and 75° and the range of temperature difference in this experiment is in between 10°C and 35°C .

The Rayleigh number in this study covers the range:

$$3.4 \times 10^4 \leq Ra_L \leq 2.08 \times 10^6$$

Correlation in the form of $Nu_L = C [Ra_L \cos\theta]^n [A]^m$ is developed to correlate the experimental data. The results obtained in the present study are compared with other studies related to the problem under investigation.



2

LITERATURE
REVIEW

2.1 GENERAL

Heat transfer by free convection in enclosed spaces has numerous engineering applications. The surface may be plane horizontal or vertical or inclined. In particular natural convection heat transfer through a layer of air bounded by two parallel plates heated from below is of interest to the designers of solar collectors. In a layer of fluid infinite in horizontal extent and enclosed by two horizontal surfaces; if the lower surface temperature is greater than the upper surface temperature, heat will transfer from the lower surface to the upper surface. For fluids whose density decrease with the increasing temperature there exists a "top heavy" unstable situation at a very small Rayleigh number. However, as long as the buoyancy is small as compared to viscous and conduction effects any disturbance will be driven out. In this state, the fluid is completely stationary and heat is transferred across the fluid layer by a conduction mechanism. This unstable state breaks down at a certain critical value of Rayleigh number (which depends on the boundary conditions).

At Ra_C , the unstable state becomes marginally unstable, as any disturbance in the fluid will result in fluid motion with no dampening. This flow state is known as post conductive state. It is laminar and has nearly hexagonal cell structure. The flow moves up in the interior of these cells and returns downward along its rim.

At $Ra_L \gg Ra_C$, the flow becomes convective with the breaking down of laminar flow into turbulent flow. The resulting flow begins to take the boundary layer structure with the resistance to heat transfer lying exclusively in two boundary layers, one on each of the boundary surfaces.

2.2 NATURAL CONVECTIVE HEAT TRANSFER IN PLANE HORIZONTAL FLUID LAYERS

Most of the researches on heat transfer in confined spaces have been carried out with parallel

plates in a horizontal position. A considerable number of experiments have been conducted on air, water and oil and the results have been reported by the investigators.

Thomson ^[16] performed an experimental investigation on natural convection heat transfer through a layer of soapy water between horizontal plates heated from below. He noted the presence of cellular pattern in soapy water whose mean temperature is greater than the ambient. Benard ^[11] also performed similar experimental investigation but his working fluid is paraffin oil and the published photographs are taken with a beam of parallel light that has passed through the layer of this paraffin oil. Those photographs clearly indicate the presence of hexagonal cellular convection patterns. Sterling-Scriven ^[17] concluded that the cellular convection patterns observed by Thomson and Benard are caused by surface tension rather than by thermal gradient.

Most elaborate experiment is performed by Mull-Reiher ^[18] on free convection heat transfer in horizontal air layer, who presented their experimental results by plotting k_e / k_C versus Gr_L and obtained a smooth curve in the range of $2.1 \times 10^3 < Gr_L < 8.89 \times 10^8$. Where according to their assumption k_e is an equivalent thermal conductivity that considers the effect of conduction, convection and radiation i.e., $k_e = k_C + k_r$, here k_C is the equivalent thermal conductivity which takes into effect both conduction and convection, and k_r is the equivalent thermal conductivity for radiation. Jakob ^[19] plotted the data of Mull-Reiher in log-log coordinates and showed that there is at least one point of inflection in the curve and finally developed the following correlation:

$$Nu = 0.195 (Gr_L)^{1/4} ; \text{ for } 10^4 < Gr_L < 4 \times 10^5 \quad (2.1a)$$

$$= 0.068 (Gr_L)^{1/3} ; \text{ for } Gr_L < 4 \times 10^5 \quad (2.1b)$$

Hollands, *et al.* ^[20] carried out an experimental investigation on natural convection through an air layer between two parallel copper plates, heated from below. They performed their experiment by varying pressure from 10 Pa to 700 kPa by inserting the plates in a pressure vessel. Actually the variation in \bar{Ra}_L over a wide range without altering the plate spacing or the temperature difference between the plates is attained through the variation of pressure. They carried out the test at mean plate spacing of 10 mm, 25 mm and 35 mm covering the range of Ra_L from subcritical to 4×10^6 . According to their report when their data along with the data of

Chu-Goldstein ^[21] for air are analyzed, the value of the index for Ra_L are more or less same as one third (1/3) while the correlation for the data of Chu and Goldstein are:

$$Nu \propto (Ra_L)^{0.294} ; \text{ for air} \quad (2.2a)$$

$$Nu \propto (Ra_L)^{0.278} ; \text{ for water} \quad (2.2b)$$

Rossby ^[22] also reported different power law for different Prandtl number fluids as follows:

$$Nu \propto (Ra_L)^{0.281} ; \text{ for silicon oil (Pr =11600)} \quad (2.3a)$$

$$Nu \propto (Ra_L)^{0.257} ; \text{ for mercury (Pr =0.025)} \quad (2.3b)$$

O'Toole-Silveston ^[23] developed the correlation equations for natural convection heat transfer across horizontal fluid layers by taking all the data available in the literature at that time. On the basis of Ra_L they differentiated the flow into the following three regions:

Initial region : $1700 < Ra_L < 3500$

Laminar region : $3500 < Ra_L < 10^5$

Turbulent region : $10^5 < Ra_L < 10^9$

They also developed the following correlation:

$$Nu = 0.229 (Ra_L \cos\theta)^{0.22} ; 5900 < Ra_L \cos\theta < 10^5 \quad (2.4a)$$

$$Nu \propto (Ra_L)^{0.305} ; \text{ for turbulent region} \quad (2.4b)$$

A number of investigators have also reported the 1/3 power law of dependency of Nusselt number on Rayleigh number. Malkus ^[24] and Globe, *et al.* ^[25] also found the asymptotic behavior of Nusselt number and obtained $Nu \propto (Ra_L)^{1/3}$. Through numerical solution of the governing differential equations Herrings ^[26] also predicted $Nu \propto (Ra_L)^{1/3}$ by neglecting the non linear interaction terms.

2.3 NATURAL CONVECTION HEAT TRANSFER IN PLANE INCLINED FLUID LAYER

Natural convection in inclined layers of fluid heated from below and cooled from above has received extensive attention owing to its importance in engineering applications, including solar heating, nuclear reactor operation and safety, energy efficient design of buildings, machinery and cooling of microelectronic components.

Graaf, *et al.* [27] performed investigations on heat transfer rate for the angles of inclination ranging from 0° to 90° in steps of 10° and covered the range, $10^3 < Ra_L \cos\theta < 10^5$.

Dropkin, *et al.* [28] performed an experimental investigation on natural convection heat transfer in liquids (water, silicon oils and mercury) confined in between two parallel plates, inclined at various angles with respect to the horizontal. They carried out their experiments in rectangular and circular containers having copper plates and insulated walls and covered the range, $5 \times 10^4 < Ra_L < 7.17 \times 10^8$ and $0.02 < Pr < 11560$. They reported the following correlation:

$$Nu = C (Ra_L)^{1/3} (Pr)^{0.074} \quad (2.5)$$

Where, the constant C is a function of the angle of inclination. It varies from $C = 0.069$ for the horizontal plates to $C = 0.049$ for vertical plates.

Ayyaswamy, *et al.* [29] carried out a theoretical investigation on natural convection heat transfer in an inclined rectangular region where their results are limited to $0^\circ < \theta < 120^\circ$, $0.2 < A < 20$ and Ra_L upto 10^6 . But Ayyaswamy, *et al.* [7] investigated the boundary layer domain and observed that:

$$Nu_{(\theta)} = Nu_{(\theta=90^\circ)} (\sin\theta)^{1/4}; \quad 0^\circ < \theta < 110^\circ \quad (2.6)$$

Hollands, *et al.* [30] performed an experimental investigation on free convection heat transfer rates through inclined air layers of high aspect ratio, heated from below. The covered range of Rayleigh number is from subcritical to 10^5 and angle of inclination as $0^\circ \leq \theta \leq 70^\circ$. They gave the following correlation:

$$\begin{aligned} Nu = & 1 + 1.44 [1 - 1708 / Ra_L \cos\theta]^* \times [1 - (\sin 1.8\theta)^{1.6} \times 1708 / Ra_L \cos\theta] \\ & + [\{ (Ra_L \cos\theta) / (5830) \}^{1/3} - 1]^* \end{aligned} \quad (2.7)$$

[* Denotes that when the arguments inside the bracketed terms become negative, the value of bracketed terms must be taken as zero].

Randall, et al. ^[31], carried out computation on natural convection heat transfer characteristics of flat enclosures, using interferometric techniques. The findings include the effects of Grashof number, tilt angle and aspect ratio on both the local and average heat transfer coefficients. Where the tested Grashof number ranges from 4×10^3 to 3.1×10^5 and the aspect ratio, which is the ratio of enclosure length to plate spacing, varies between 9 to 36. The angles of inclination of the enclosure are 45° , 60° , 75° and 90° . Their average heat transfer rate at an angle of inclination 90° show a decrease of 18% from that at 45° and the following shows their developed correlation:

$$Nu_L = 0.118 [Gr_L Pr \cos^2(\theta - 45)]^{0.29} \quad (2.8)$$

Experimental investigations on natural convection heat transfer from a horizontal lower vee corrugated plate to an upper cold flat plate for Rayleigh number from 7×10^3 to 7×10^5 were first carried out by Chinnappa ^[32]. In his experiment the vee angle is 60° and aspect ratios are 0.64, 0.931, 0.968, 1.1875 and 1.218. Experimental fluid is air in all the test runs. His obtained correlation is as follows:

$$Nu_L = 0.54 [Gr_L]^{0.36} ; \quad 7 \times 10^3 < Ra_L < 5.6 \times 10^4 \quad (2.9a)$$

$$Nu_L = 0.139 [Gr_L]^{0.278} ; \quad 5.6 \times 10^4 < Ra_L < 7 \times 10^5 \quad (2.9b)$$

Kabir ^[11] carried out experimental investigation on the natural convection heat transfer across air layer bounded by a lower horizontal sinusoidal corrugated plate and an upper cold flat plate for a range of Rayleigh number 5.50×10^3 to 2.34×10^6 , angle of inclination, θ from 0° to 75° and aspect ratios of 2.0 to 5.75. His experiment has the sinusoidal leading angle of 72° . His developed correlation which correlate all his experimental data within an error of $\pm 10\%$ is given below:

$$Nu_L = 0.0132 (Ra_L \cos\theta)^{0.51} (A)^{-0.35} \quad (2.10)$$

Chowdhury ^[12] conducted experimental investigation on natural convection heat transfer from a lower horizontal rectangular and trapezoidal corrugated plates to an upper cold flat plate for a range of Rayleigh number $9.84 \times 10^4 \leq Ra_L \leq 2.29 \times 10^6$, angle of inclination, θ from 0° to 75° covering aspect ratios $2.6 \leq A \leq 5.22$ and taking air as the working fluid. His recommended correlation which predicts the experimental data with an error of $\pm 15\%$ is shown below:

$$Nu_L = 0.0112 (Ra_L \cos\theta)^{0.521} (A)^{-0.4546} ; \text{ for Trapezoidal corrugation} \quad (2.11a)$$

$$Nu_L = 0.0102 (Ra_L \cos\theta)^{0.530} (A)^{-0.4923} ; \text{ for Rectangular corrugation} \quad (2.11b)$$

Saiful ^[13] conducted an experimental investigation on steady state natural convection heat transfer through air at atmospheric pressure from hot square corrugated plates to a cold flat plate placed above and parallel to it, where the surrounding are maintained at constant temperature. In his study the amplitudes of corrugation are $H = 10$ mm, 15 mm and 25 mm. His study covers the effects of angle of inclination, aspect ratio, temperature difference and Rayleigh number on average convective heat transfer co-efficient which covers the range of:

$$0^\circ \leq \theta \leq 75^\circ, 1.4 \leq A \leq 9.5, 10^\circ\text{C} \leq \Delta T \leq 35^\circ\text{C}, 3.294 \times 10^4 \leq Ra_L \leq 1.881 \times 10^6$$

The following shows the correlation he developed for square corrugation which correlates almost all his data within $\pm 20\%$:

$$Nu_L = 0.295 [Ra_L \cos\theta]^{0.265} . [A]^{-0.442} \quad (2.12)$$

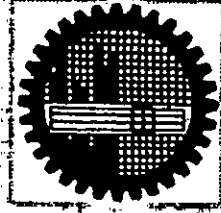
Latifa ^[14] carried out experimental investigation on the natural convection heat transfer from a lower horizontal vee-corrugated plate to an upper cold flat plate for a range of Rayleigh number 3.294×10^4 to 1.8814×10^6 , angle of inclination, θ from 0° to 75° and aspect ratio of 1.4 to 9.5 taking air as the working fluid. The following shows the correlation she developed which predicts her experimental data with an error of $\pm 12\%$:

$$Nu_L = 0.276 (Ra_L \cos\theta)^{0.294} (A)^{-0.331} \quad (2.13)$$

The review works on different types of corrugation is given in Table. 2.1.

Table 2.1: Review Works on Different Types of Corrugated Enclosures.

Type of Corrugated Enclosures	Correlation	Author
Vee corrugated enclosures	$Nu_L = 0.54 [Gr_L]^{0.36}$ $Nu_L = 0.139 [Gr_L]^{0.278}$	Chinnappa [1970]
Sinusoidal corrugated enclosures	$Nu_L = 0.0132 [Ra_L \cos\theta]^{0.51} [A]^{-0.35}$	Kabir [1988]
Trapezoidal corrugated enclosures	$Nu_L = 0.0112 [Ra_L \cos\theta]^{0.521} [A]^{-0.4546}$	Feroz [1992]
Rectangular corrugated enclosures	$Nu_L = 0.0102 [Ra_L \cos\theta]^{0.53} [A]^{-0.4923}$	Feroz [1992]
Square corrugated enclosures	$Nu_L = 0.295 [Ra_L \cos\theta]^{0.265} [A]^{-0.442}$	Saiful [1995]
Vee corrugated enclosures	$Nu_L = 0.276 [Ra_L \cos\theta]^{0.294} [A]^{-0.331}$	Latifa [1998]



3

**MATHEMATICAL
MODEL**

3.1 DESCRIPTION OF THE PROBLEM

Natural convection heat transfer in an inclined rectangular enclosure is a function of:

- Temperature difference between the hot and cold plates,
- Boundary conditions,
- Angles of inclination of the enclosure with the horizontal and
- The geometry of the hot plate.

Also the natural convection heat transfer is a function of geometry of the hot plate, which is the basis for sketching the present problem of variation of natural convection from hot semicircular corrugated plate to a cold flat plate.

The present investigation in rectangular region is carried out with bottom hot semicircular corrugated plates having amplitude of 10 mm where the upper cold plate is flat. The convective fluid is air. The side walls of the enclosure are made adiabatic and flat.

In the present experimental setup the spacing between the hot and cold plate is varied to get different aspect ratio, A defined as the mean plate spacing to amplitude of corrugation. The vertical side walls of the enclosure and the bottom hot corrugated plates are maintained at the same temperature. At the same time the upper wall of the lower guard heater assembly is maintained at the same temperature same as that of lower hot corrugated plate. At steady state the heat flux, q'' to the cold flat plate is by convection, conduction and radiation. But for Rayleigh number well above the critical value, conduction heat transfer is considered insignificant. So total heat flux, q'' have only two components: convection heat flux, q''_{CONV} and radiation heat flux, q_r'' . In case of fixed temperature potential, ΔT the radiative heat flux becomes constant and the convective heat transfer varies with aspect ratio, A and angle of inclination of the enclosure.

The radiative heat flux, q_r'' is calculated by using the formula derived in *Appendix-A* by considering hot corrugated plate and cold flat plate behaving as black bodies. The convective heat flux, q''_{CONV} is calculated by subtracting the value of q_r'' from the total heat flux, q'' . Heat flux from the hot corrugated plate is calculated by measuring the current and the voltage supply to the main heater (Heater 1). The mathematical equations required for calculating q_r'' , q''_{CONV} and natural convective heat transfer coefficient, h are shown in the following section:

3.2 MATHEMATICAL EQUATIONS

The mathematical equations that are used to calculate the natural convection heat transfer coefficient, Nusselt number, Nu_L and Rayleigh number, Ra_L are given below:

$$q_r'' = \sigma \cdot \epsilon_{COR} \cdot [(T_{COR})^4 - (T_{COLD})^4] \quad [3.2]$$

$$q'' = (VI \cos \phi) / A_{COR} \quad [3.3]$$

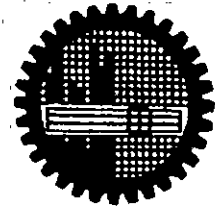
$$h = [q'' - q_r''] / [T_{COR} - T_{COLD}] \quad [3.4]$$

$$Nu_L = hL/k \quad [3.5]$$

$$Ra_L = g\beta[T_{COR} - T_{COLD}] \cdot L^3 / \nu\alpha \quad [3.6]$$

All properties of the air are evaluated at film temperature, T_f

$$\text{where, } T_f = [T_{COR} + T_{COLD}] / 2$$



4

**EXPERIMENTAL
SETUP**

4.1 GENERAL DESCRIPTION OF THE SETUP

The details of the experimental set up and test section are shown in Fig 4.1 and 4.2. There is a provision for the experimental set up to incline by an alignment plate in the range of 0° to 90° at steps of 15° . The air gap depth is varied by changing the position of the cold plate in relation to the hot plate from 35 mm to 95 mm. Experimental hot plate assembly is heated by the main electric heater sandwiched in between the hot corrugated plates by supplying a constant voltage from the voltage stabilizer. The guard heater assemblies are also heated by electric heaters sandwiched in between the inner and outer wooden strips. The cold flat plate is placed above the corrugated assembly by four vertical clamps, fixed on the upper guard heater. This cold plate assembly is cooled by passing a steady flow of cooling water from the overhead tank, where the head of overhead tank is always kept constant. A digital thermometer is used to measure the temperature of the test section of the hot plate and cold plate through thermocouples nos. 1 to 9 and 37 to 41 respectively. It is also used to monitor the surface temperatures of the guard heater assemblies through 27 chromel-alumel thermocouples. To obtain the total heat input to the experimental test section of the hot plate, the input current to the corresponding heater (main heater) and the voltage across the main heater is measured by a precision digital multimeter.

4.2 THE TEST SECTION

The test section consists of

- a. The hot plate assembly.
- b. The outer guard heater assembly.
- c. The cold plate assembly.
- d. The alignment plate and supporting frame.

Detail of the test section is shown in Fig. 4.3.

4.2.1 The Hot Plate Assembly

The main section of the hot plate assembly is the test section. The hot plate assembly is made of G.I. sheets having amplitude of semicircular corrugation of 10 mm with total dimension of 456 mm X 534 mm. An asbestos cloth of 12 mm thickness is placed on the upper side of the lower corrugated plate to insulate it electrically from the electrical heaters placed on this asbestos cloth as shown in Fig. 4.3. Another asbestos cloth is placed over the heaters to make the upper corrugated plates of the assembly well insulated from the sandwiched electrical heaters. There are three heaters on the hot plate assembly. One is used to heat the experimental test section and the other two heaters are used as end and side guard around the test section. These guard heaters are provided to reduce the end conduction losses from the experimental hot plate to a minimum level. For this purpose these guard heater sections are separated from the experimental hot plate section by cutting the top corrugated plate into five pieces forming separated guard sections and central experimental test section. The test section is 152 mm X 230 mm; 152 mm across the corrugation and 230 mm along the corrugation.

The end and side guard heater sections are 152 mm wide on all sides of the experimental hot plate section. Thus the overall dimensions of the hot plate assembly is 456 mm x 534 mm. This hot plate assembly is placed inside a rectangular ring of 483 mm x 560 mm. The rectangular ring is made of 76 mm wide and 19.05 mm thick wooden strip. Details of the hot plate assembly is shown Fig. 4.3 and details of the design and fabrication process of the heaters are given in the *Appendix – A*. The capacities of the main heater, end heater and side heater are 45, 45, 90 watts respectively.

The outer surfaces of both the test sections and the end and side guard heater sections are painted black with dull black plastic paint. The test section is separated from both the end and side guard section by asbestos powder to reduce conduction loss.

4.2.2 The Outer Guard Heater Assembly

The main feature of the outer guard heater assembly is to thermally isolate the hot test plate section from the surrounding surface except from the top. This assembly mainly consisted of upper guard heater ring and lower guard heater box. The heat input is varied by using Variacs 4, 5 and 6 to maintain the temperature difference between the hot test plate and its surrounding surfaces to zero. Under this condition all the heat input to the experimental hot plate section will be transferred only to the cold flat plate which is placed above the hot plate.

4.2.2a The Upper Outer Guard Heater Ring

The upper outer guard heater ring is a rectangular shaped structure, which consists of the following section:

- i. Inner wooden rectangular ring,
- ii. Inner asbestos rectangular ring,
- iii. Outer asbestos rectangular ring,
- iv. Outer wooden rectangular ring.

The inner wooden rectangular ring containing the test section is having a dimension of 483 mm x 564 mm. The inner and outer wooden rings are held together with wooden annular rings at the top of the outer guard heater assembly having 579 mm x 660 mm outside dimension and which is 19.05 mm thick and 48 mm wide. The height of the upper guard heater assembly is 139 mm. The inner and outer asbestos rectangular rings are fitted inside the annular space between the outer and inner rectangular wooden rings. The 127 mm wide outer asbestos ring is fitted inside the outer wooden rings. The outer dimension of outer asbestos ring is 555 mm x 635 mm and the outer dimension of the inner asbestos ring is 531 mm x 612 mm. The heater is made by wrapping 29 SWG Nichrome wire on the mica sheet sandwiched in between the inner and outer asbestos ring. The maximum capacity of the heater is 105 Watt. A cross section of the upper outer guard heater assembly is shown in Fig. 4.4. Both the outside and inside surfaces of the upper guard heater ring are painted with dull black plastic paint.

4.2.2b The Lower Outer Guard Heater Ring

The lower outer guard heater ring is a rectangular shaped structure, which consisted of the following sections:

- i. Inner wooden rectangular box,
- ii. Inner asbestos rectangular box,
- iii. Outer asbestos rectangular box,
- iv. Outer wooden rectangular box.

This assembly is a box-shaped structure. The wooden structures as well as asbestos sheets are 12 mm thick. The inner wooden box is 507 mm x 588 mm x 24 mm in outer dimension. The inner asbestos box is fitted over the inner wooden box. The outer dimension of inner wooden box is 531 mm x 612 mm x 40 mm. The outer asbestos box is fitted over the inner asbestos box and have the outer dimension of 555 mm x 636 mm x 52 mm. Two separate Nichrome heaters are sandwiched in between the inner and outer asbestos rings, one is lower bottom guard heater and the other is lower side guard heater. Finally an outer wooden box is fitted over the outer asbestos box whose outer dimension is 579 mm x 660 mm x 64 mm. A cross section of the lower guard heater is shown in Fig. 4.5. The outer surface of the outer wooden rectangular box is painted black with dull black plastic paint.

4.2.3 The Cold Plate Assembly

To receive the heat convected and radiated from the hot corrugated plate, a cold plate assembly is placed above the test hot plate. This cold plate assembly is a sealed 470 mm x 550 mm x 19.05 mm rectangular box made of 3.175 mm thick mild steel plates painted with dull black plastic paint. Provision of water circulation is made from a reserve tank through inlet and outlet connections. The outlet and inlet connections are placed on the upper surface of this box. The flat bottom surface of this assembly, facing the corrugated plate is acting as a receiver of heat that is convected and radiated from the hot corrugated plate. The whole cold plate assembly is placed above the hot corrugated plate and held by the vertical clamps, fixed on the upper outer guard heater assembly. These clamps have arrangements to change

the spacing between the hot corrugated plate and the cold flat plate from 19.5 mm to 109.5 mm in steps of 10 mm. The cold plate assembly is shown in Fig. 4.6.

4.2.4 The Rig Holder and Alignment Plate

a. The Rig Holders

There are two separate rig holders. One of them is the side rig holder and the other is the end rig holder. The side rig holder is a rectangular structure where the hot and cold plate assembly along with the guard heaters is placed. The two side supports of this frame is made of 38.1 mm x 38.1 mm x 6.35 mm mild steel angle bar, each of which is attached with the plate assembly by means of two bolts. Two other bolts are fixed at the center of the two opposite longitudinal sides of the frame and passed through the holes of the side supports so that the frame and the plate assembly with the guard heaters can swivel about a horizontal axis i.e. the lateral axis of the hot plate through these bolts. The rectangular frame is shown in Fig. 4.7.

The function of the end rig holder is to carry the bulk load of the whole experimental section. It is also fabricated from 38.1 mm x 38.1 mm x 6.35 mm mild steel angle bar. The supporting stand consisting of two pairs of leg 915 mm apart connected by a flat mild steel bar. The height of the stand is 460 mm. The rectangular frame along with the two alignment plates is connected with this stand at the top center of its legs by means of two bolts. These two bolts pass through the 16 mm diameter central holes of the alignment plates and the two holes located at the center of the two lateral sides of the frame. Due to this type of fixing the frame and the plate assembly with the guard heaters can also swivel about a horizontal axis i.e. the longitudinal axis of the hot plate. The connection between the rectangular frame and the supporting stand is shown in Fig. 4.8.

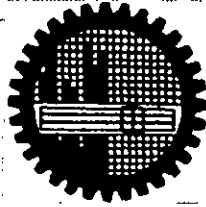
The angle of inclination of the test section of the hot corrugated plate can set at a desired value by means of two screws passing through the corresponding peripheral holes of diameter 6.5 mm of the alignment plates as mentioned above and the two holes 76 mm apart located at the top of the two legs of the supporting stand. The supporting stand is shown in Fig. 4.9.

b. The Alignment Plate

The alignment plate is a circular disc of mild steel having diameter of 102 mm and thickness of 6.35 mm. Two alignment plates are connected at the center of the two opposite lateral sides of the rectangular frame by means of two screws passing through 6.5 mm diameter holes located on each disc at 40 mm apart. These matches with the holes of the two 57 mm x 57 mm hanging side supports made of 6.35mm thick mild steel sheet that are welded with the supporting frame at its center. These discs have also several holes of diameter 6.5 mm along a circle of radius 38 mm. The angle of inclination of the test section is varied by means of these holes by changing the inclination angle from 0° to 90° in steps of 15°. One of the alignment plates is shown in Fig. 4.10.

4.3 THE WATER RESERVE TANK

The water reserve tank is an overhead tank – a simple cylindrical drum made of galvanized iron sheet. The water level in the tank is kept constant during experiments by controlling the water flow using the inlet and outlet valves of this tank. The water from the tank is used to cool the cold plate assembly by passing a steady flow of cooling water from this tank through pipes of 12.5 mm diameter.



5

**EXPERIMENTAL
MEASUREMENT &
TEST PROCEDURE**

EXPERIMENTAL MEASUREMENT & TEST PROCEDURE

5.1 INSTRUMENTATION

In the present investigation provisions are made for measuring angle of inclination, air gap between the hot and the cold plates and the temperatures at different points of the experimental setup. There are five variacs and one stabilizer to supply regulated voltage at different sections of the experimental set-up. Each variac have graduated scale on it to measure the voltage supplied to the heaters. Also the voltage and current supplied by the stabilizer to the test section is measured by a precision multimeter. Details of the instrumentation and measurement procedure is given below:

5.1.1 Temperature Measurement

The accuracy of the value of natural convection is dependent on the accuracy of the measurement of temperature and input power (voltage and current values). For this reason, precision instruments are used. Temperature at different sections of the experimental set-up are measured by forty-one 36 SWG chromel-alumel thermocouples connected to two thermometers [OMEGA, Model: DP 116-TC2, Input Signal: T, Input voltage: 220 volt, Watt: 2 W, Display: - 199.9 to + 199.9 °C, Made in U.S.A.] to show the temperature directly through two selector switches each having 24 points. Out of these, nine thermocouples of number 1 to 9, are fixed on the bottom surface of the test section of the hot corrugated plate and five thermocouples of number 37 to 41, are fixed on the bottom surface of the cold plate facing the corrugated plate and the rest are fixed on the guard heater sections. The positions of the thermocouples are shown in Fig. 5.1 to 5.5. These thermocouples are calibrated in between 0°C (melting ice temperature) and 100°C (saturated steam temperature). There is a maximum variation of 0.10% between the actual and the standard reading within the working range of the experiment. The calibration curve for the thermocouple number 5 is shown in Fig. 5.6.

Since the thermocouples are fixed to the bottom surface of the experimental hot plate hence for greater accuracy, the actual temperature of the exposed top surface of the experimental hot corrugated plate [T_{COR}] is determined after necessary conduction correction. *Appendix-B* contains the outline of the procedure for calculating the conduction correction.

5.1.2 Heat Flux Measurement

Amount of heat supplied per unit area of the test section through heater is the heat flux. Heat flux from the hot corrugated plate is calculated by measuring the current and voltage to the main heater.

A digital multimeter, model: "ALDA CE, AVD 890D" is employed to measure the voltage across the stabilizer, which supplies the necessary heat to the test section of the hot plate assembly. The meter has the range of 200 mV - 700 Volts for measurement of AC voltage.

The same digital meter is employed to measure the current supplied to the test section of the hot plate. This has the range for AC current of 20 mA - 20 amps.

5.2 TEST PROCEDURE

Semicircular corrugation having amplitudes, $H = 10$ mm are used. The experimental fluid is air at atmospheric pressure. Experiments are carried out under steady state condition. Experimental measurements are recorded for four values of ΔT , four inclination angles, θ of the air layer and four different air gaps, L . The test is carried out according to the following procedure:

- a. The room temperature is recorded before starting the experiment for selecting T_{COR} to maintain a steady ΔT [say, $\Delta T = T_{COR} - T_{COLD} = 10^\circ\text{C}$] since $T_{COLD} \cong T_{ROOM}$.
- b. In the next step the spacing between the hot corrugated plate and the cold flat plate is set to 95 mm. Here the distance is measured between the bottom surface of the cold plate and the centerline of the semicircular corrugated plate (Fig. 4.2). The spacing L i.e., air gap of 95

mm is set by fixing the cold plate to the appropriate holes of the clamps fixed on the upper outer guard heater assembly.

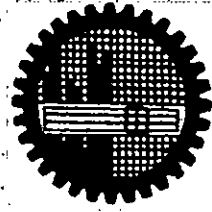
- c. Then the rig is aligned to horizontal position for angle of inclination $\theta = 0^\circ$.
- d. Then all the heater circuits are switched on and at the same time, the waterline of the cold flat plate and the reserve tank are opened.
- e. By regulating the stabilizer and variacs, the temperatures of thermocouples are monitored. Thermocouple readings of nos. 1 to 36 are made equal. The cold plate is maintained at the room temperature by controlling the water flow through it to maintain ΔT constant during a particular test run.
- f. As the steady state is reached (i.e. $T_{COR} - T_{COLD} = 10^\circ C$) readings of temperatures of thermocouples Nos. 1 to 9 and 37 to 41 are recorded. At the same time readings of ampere and voltage supplied to the test section of the hot plate is also noted to obtain the heat input.
- g. Next all the operations of the steps [e] and [f] are repeated for inclination angles $\theta = 30^\circ$, 45° , and 75° keeping air gap, $L = 95$ mm constant throughout.
- h. Subsequently air gap, L is changed to the other values of 75 mm, 55 mm and 35 mm and operations from step [c] to step [g] are repeated.
- i. Then for other values of ΔT i.e. for 18° , $26^\circ C$ and $35^\circ C$ all the operations illustrated in step [b] to [h] are repeated. Thus full set of readings are completed.

The ranges of parameters are as follows:

- Rayleigh number, $Ra_L = 3.40 \times 10^4 \leq Ra_L \leq 2.08 \times 10^6$
- Heat flux, $q'' = 77.80$ to 360.41 W/m²
- Temperature difference
between hot and cold plate, $\Delta T = 10^\circ C$ to $35^\circ C$
- Temperature of the hot plate, $T_{COR} = 40^\circ C$ to $65^\circ C$
- Amplitude of corrugation, $H = 10$ mm
- Inclination angle, $\theta = 0^\circ$ to 75°
- Air gap, $L = 35$ mm to 95 mm

5.3 REDUCTION OF DATA

Convective heat transfer coefficient is calculated from convective heat flux. The heat flux, q'' is obtained from readings of voltage and current input to Heater.1. This heat flux, q'' is the combination of convective and radiative heat flux. So in calculating convective heat flux, the radiative heat flux is deducted from this measured heat flux. To find out the radiative heat flux the Stefan-Boltzman equation for gray surface [Equation 3.1] is used. The outline for obtaining the emissivity of the test section of the hot corrugated plate is given in *Appendix-C* and the emissivity for the semicircular corrugated plates having opening angle of 65° has been considered to be 0.975.



6

RESULTS & DISCUSSION

RESULTS & DISCUSSION

This is an experimental investigation involving the steady state free convection heat transfer from hot semicircular corrugated plate to a cold flat plate placed above the former and parallel to it. The experiment is carried out in a finite rectangular enclosure in which the assembly is being inclined at various angles with respect to the horizontal. The rectangular enclosure between the hot and the cold plate contained air. Moreover, the enclosure have adiabatic surroundings, therefore, it is expected that the heat transfer rate from the test plate will remain unaffected by the presence of surrounding surfaces as there shall be no heat loss through the surroundings from the experimental hot corrugated plate. The amplitude of corrugation of hot plate is 10 mm. Experiment covered a wide range of Rayleigh number from 3.4×10^4 to 2.08×10^6 , angle of inclination from 0° to 75° and the temperature difference between hot and cold plates of 10°C , 18°C , 26°C and 35°C .

Fig. 6.1 to 6.4 and 6.5 to 6.8 show the temperature distribution over the experimental hot corrugated plate and cold flat plate, respectively. From the curves it is clear that the temperature distribution over the experimental hot corrugated plate and cold plate is fairly uniform for different aspect ratios (A or L/H) and different inclination angles, θ . Here it can be mentioned that Figs. 6.1 to 6.8 represent curves only for $A = 7.5$, this is because for the other aspect ratios the curves are found to be similar. The presence of an isothermal temperature distribution over the surface enabled the calculation of the test surface temperature to be made from the average measured temperature at the bottom corrugated plate. This is achieved by a correction term using one dimensional heat conduction equation as described in the *Appendix B*.

Figs 6.9 to 6.16 are the graphical representation of the effect of aspect ratio, A ($A = L/H$) on average free convective heat transfer coefficients, h across rectangular regions for various angles of inclination, θ and temperature difference, ΔT . Figs. 6.9 to 6.12 are drawn for a particular θ with different values of ΔT and Figs. 6.13 to 6.16 are drawn for a particular ΔT with different values of θ . From these graphs it is observed that for $0^\circ \leq \theta \leq 75^\circ$ heat transfer coefficients increase with the increase of aspect ratio, A upto a certain value of A. For angles of inclination and different temperature potentials with in the range of present study the limiting value of aspect ratio is found to be 7.5. Beyond this value of aspect ratio, the heat transfer coefficients decrease with the increase of

aspect ratio for all angles of inclination, θ and temperature differences, ΔT . The increasing trend in heat transfer coefficient is observed for the range of aspect ratio 3.5 to 7.5 and after this it showed a decrease in its value. This is due to the fact that as the aspect ratios are increased, the gap between the hot corrugated plate and the cold flat plate is also increased. As the gap increases better mixing of the fluid occurs and this enhances the heat transfer rate. But this enhancement of heat transfer rate has got a limitation and after certain limit heat transfer coefficients are found to decrease with increasing aspect ratio. This is due to the fact that, as the aspect ratio exceeded a limiting value, the convection currents appeared to be weak to reach the cold flat plate by crossing a higher distance. Hence heat transfer coefficients decrease with the increase of aspect ratio beyond its limiting value. These figures also indicate that heat transfer coefficients increase with increase in temperature potentials and decrease with increase of inclination angle, θ . The differences in heat transfer coefficients at different temperature potentials gradually increase with increase of aspect ratios.

Figs. 6.17 to 6.20 show the variation of heat transfer coefficients with angles of inclination and temperature potentials at a particular aspect ratio. These figures indicate that at a particular aspect ratio and inclination angle, heat transfer coefficient gradually increases with increase in temperature potential. But with the increase in angle of inclination, the rate of increase in heat transfer coefficient decreases. Within the experimental range $0 \leq \theta \leq 75^\circ$, the heat transfer coefficient is found to be maximum at horizontal condition. This is due to the fact that at a constant gap between the hot and cold plates, the convective fluid particles in inclined position have to cross larger vertical distance in transferring heat energy than in horizontal. Figs. 6.17 to 6.20 also show the variation of heat transfer coefficient with aspect ratio, A each of which is drawn for a particular value of ΔT . The figures indicate that for a particular temperature potential the dependence of heat transfer coefficient on angle of inclination is same as that for temperature potentials as mentioned at the beginning of this paragraph. This is perhaps due to the fact that the Rayleigh number for breaking down the unstable situation in order to set convective motion within the fluid increases with the increase of angle of inclination. Again the effect of fluid stagnation in the corrugation cavity at higher angle of inclination may also not be ruled out, as the fluid flow direction appears to be perpendicular to the corrugation channel.

Figs. 6.21 to 6.24 show the relationship between the Nusselt number and $Ra_l \cos\theta$ for different values of aspect ratio, A and angle of inclination, θ . From these figures it is observed that Nusselt number increases with increasing Rayleigh number at a particular aspect ratio, A and angle of inclination. This is due to the fact that at a constant A and angle of inclination, Rayleigh number

increases with the increase of temperature potential, ΔT . Again increase of Rayleigh number leads to the increase of Nusselt number.

The experimental results showing the effects of inclination angle on Nusselt number for different aspect ratios and Rayleigh number are shown in Figs. 6.25 to 6.28. From these figures it is observed that at constant aspect ratio and Rayleigh number, Nusselt number decreases with increase of inclination angle. For a constant Rayleigh number, Nusselt number is found to be maximum at inclination angle $\theta = 0^\circ$. The reason for such behavior is due to the fact that at high and moderate Ra_L (greater than 5×10^4) as θ approaches 90° , the hydrodynamic instabilities begin to interfere with the motion induced by thermal instabilities. The thermal instabilities are dominant at lower angles of inclination as mentioned by Arnold^[33]. Moreover the fact that at a constant gap between the hot and cold plates, the convective fluid particles in inclined position have to cross larger vertical distance in transferring heat energy than in horizontal.

COMPARISON

Fig. 6.29 shows the comparison of Nusselt number of the present study with the Nusselt number of other works available in literature. From this figure it is observed that for an aspect ratio of 7.5, inclination, $\theta = 0^\circ$ and for Rayleigh numbers in the range of 3.0×10^5 to 1.0×10^6 , the values of Nusselt number for semicircular corrugation ($H = 10\text{mm}$) are higher by about 37%, 12%, 43%, and 37% than those of vee, sinusoidal, flat and trapezoidal corrugations respectively.

CORRELATION

In natural convection system the average Nusselt number is related in the following way:

$$Nu = f(Re, Gr, Pr)$$

And because of small velocities in free-convection system, the significance of Reynolds number, Re is neglected. So in natural convection system the average Nusselt number is:

$$Nu = f(Gr, Pr)$$

In the present experiment the investigation is carried out with only one confined convective fluid (air). So Prandtl number is assumed as a constant property in above equation. Now when the value

of Prandtl number is 1, the velocity and thermal distribution becomes equal. Therefore, the Nusselt number, in natural convection system, which measures the thermal convective property of the fluid mainly depends on Grashof number i.e. Rayleigh number, Ra_L . It is experimentally found that Nusselt number increases with the increase of Rayleigh number. For analysis of natural convection from inclined surface because of buoyancy force, Ra_L is generally substituted by its vertical component i.e. $Ra_L \cos\theta$. So, $Ra_L \cos\theta$ must include the contribution of the fluid property in natural convection. Again the aspect ratio describing the geometry of the confined space is also found to have influence on Nusselt number as it is experimentally observed that average convective heat transfer coefficient for all of the corrugations mentioned in this paper increase upto a certain limit with the increase of aspect ratio.

In the light of the above knowledge in earlier studies of Kabir^[11], Feroz^[12], Saiful^[13] and Latifa^[14] a correlation equation is developed in terms of Nu_L , $Ra_L \cos\theta$ and A in the form:

$$Nu_L = C (Ra_L \cos\theta)^n (A)^m.$$

Kabir^[11], Feroz^[12], Saiful^[13] and Latifa^[14] determined the exponents 'n' and 'm' by plotting Nu_L vs $(Ra_L \cos\theta)$ and $Nu_L / (Ra_L \cos\theta)^n$ vs A respectively. The value of constant 'C' is determined from the graphical representation of Nu_L vs $(Ra_L \cos\theta)^n (A)^m$. Experimental investigation of El Sherbiny, S. M. et al^[34] on free convection across inclined air layers with one surface vee corrugated correlated their data by the following two equations:

$$Nu_\theta = 1 + 1.44 \left[1 - \frac{1708}{Ra_L \cos\theta} \right] \times \left[1 - \frac{1708(\sin 1.8\theta)^{1.6}}{Ra_L \cos\theta} \right] + \left[\left(\frac{Ra_L \cos\theta}{5830} \right)^{1/3} - 1 \right], \quad \text{for } 0^\circ \leq \theta < 60^\circ$$

$$Nu_\theta = \frac{(90^\circ - \theta)Nu_{60^\circ} + (\theta - 60^\circ)Nu_{90^\circ}}{30^\circ}, \quad \text{for } 60^\circ < \theta \leq 90^\circ$$

In present experimental investigation while correlating it is observed that the values of Nusselt number for 75° behave differently than those for $0^\circ \sim 45^\circ$ as is observed in Figs. 6.25 – 6.28. So it is decided to develop two separate correlations: one for $0^\circ \sim 45^\circ$ and another for 75° .

From the best fit curve of linear regression the correlating equations are found out.

The values of 'C', 'n' and 'm' are found to be as follows:

$$C = 0.0257, n = 0.5, m = -0.48, \text{ for } 0^\circ \leq \theta < 60^\circ$$

$$C = 0.0105, n = 0.63, m = -0.67, \text{ for } 60 < \theta \leq 90^\circ$$

All the experimental data for semicircular corrugation of the present study are correlated by the following equations within an error of $\pm 20\%$.

$$Nu_L = 0.0257 [Ra_L \cos\theta]^{0.5} \cdot [A]^{-0.48}, \quad \text{for } 0^\circ \leq \theta < 60^\circ$$

$$Nu_L = 0.0105 [Ra_L \cos\theta]^{0.63} \cdot [A]^{-0.67}, \quad \text{for } 60 < \theta \leq 90^\circ$$

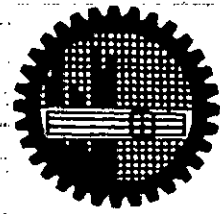
where,

$$3.40 \times 10^4 \leq Ra_L \leq 2.08 \times 10^6$$

$$3.5 \leq A \leq 9.5,$$

$$0^\circ \leq \theta \leq 75^\circ,$$

These are shown graphically in Figs. 6.30 and 6.31.



7

CONCLUSIONS & RECOMMENDATIONS

CONCLUSIONS & RECOMMENDATIONS

The conclusions that can be drawn from this experimental investigation of free convection heat transfer from hot semicircular corrugated plate to cold flat plate is included in this chapter. Recommendations are also made for further future investigation on the present topic.

7.1 CONCLUSIONS

The significant conclusions as a consequence of the present investigation are enumerated below:

- The natural convection heat transfer coefficient is found to be dependent on the Rayleigh number, Ra_L , aspect ratio, A and the inclination angle, θ .
- The average heat transfer coefficient increases with the increase of aspect ratio up to a value of 7.5 for $\Delta T = 35^\circ$ and $\theta = 0^\circ$. Beyond this critical aspect ratio a further increase of aspect ratio results in the decrease of the heat transfer coefficient within the present experimental setup.
- As the inclination angle increases from the horizontal plane, the average heat transfer coefficients decrease for a constant aspect ratio and constant ΔT . The average heat transfer coefficients are found to be maximum at $\theta = 0^\circ$.
- The average Nusselt number decreases with the increase of inclination angle for a constant Rayleigh number and aspect ratio. The average Nusselt numbers are found to be maximum for horizontal layers ($\theta = 0^\circ$) for all aspect ratios and Rayleigh numbers investigated.
- Plots of the average Nusselt number versus $Ra_L \cos\theta$ for all aspect ratios are found to be linear in log-log graph paper.
- The average Nusselt number can be correlated by the correlation:

$$Nu_L = 0.0257 [Ra_L \cos\theta]^{0.5} \cdot [A]^{-0.48}, \quad \text{for } 0^\circ \leq \theta < 60^\circ$$

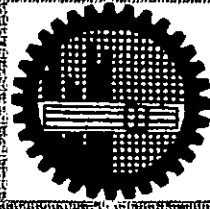
$$Nu_L = 0.0105 [Ra_L \cos\theta]^{0.63} \cdot [A]^{-0.67}, \quad \text{for } 60 < \theta \leq 90^\circ$$

Which correlate all experimental data within $\pm 20\%$. The correlation are found to be valid for $3.4 \times 10^4 \leq Ra_L \leq 2.08 \times 10^6$, $3.5 \leq A \leq 9.5$ and $0^\circ \leq \theta \leq 75^\circ$.

- Comparison of the present obtained result with other relevant works in the literature shows that, for the same plate spacing the Nusselt number for the present semicircular geometry is higher by about 37%, 12%, 43% and 37% than those of vee, sinusoidal, flat and trapezoidal corrugation respectively at aspect ratio of 7.5 and angle of inclination of 0° .

7.2 RECOMMENDATIONS

- Further investigations can be carried out with semicircular corrugated plates of different amplitudes or pitches to ascertain the effect of aspect ratio on heat transfer rate.
- For comprehensive investigation of the natural convection heat transfer of the similar type, a test rig consisting of a pressure as well as a vacuum vessel will be helpful. For finding out the effect of Prandtl number experiments may be carried out with different fluids e.g. water, silicon oil etc.
- A comprehensive investigation of natural convection heat transfer of the similar type may be carried out over a wide range of Rayleigh number.
- An experimental investigation can be performed with very high temperature potential i.e. $\Delta T \gg 35^\circ\text{C}$ and also the velocity field can be investigated.
- Numerical simulation of natural convection heat transfer from hot corrugated plates to a cold flat plate can also be predicted.



REFERENCES

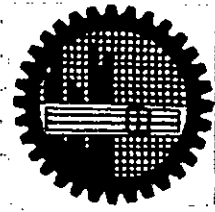
REFERENCE

REFERENCE

- [1] Benard, H., Rev. Gen. Sci. Pures Appl. Vol. 11, pp. 1261~1271.
- [2] Rayleigh, L., 1916, "On Convection Currents in a Horizontal Layer of Fluid when the Higher Temperature is on the Underside", Phil. Magh. Vol. 32, p. 529.
- [3] Jeffreys, H., 1928, "Some Cases of Instability in Fluid Motion", Proc. Roy. Soc. (London), (A), Vol. 118, p.195.
- [4] Low, A.R., 1929, "On the Criterion for Stability of a Layer of Viscous Fluid Heated from Below", Proc. Roy. Soc. (London), (A), Vol. 125, p.180.
- [5] Schluter, A., Lortz, D., Busse, F., 1965, "On the Stability of Steady Finite Amplitude Convection", Journal of Fluid Mechanics, Vol. 23, pp. 129~144.
- [6] Ostrach, S., 1957, "Convective Phenomenon Fluids Heated from Below", Trans ASME, Vol. 79, pp. 299~305.
- [7] Ayyaswamy, P.S., and Cotton, I., 1973, "The Boundary Layer Regime for Natural Convection in a Differentially Heated, Tilted Rectangular Cavity", J. Heat Transfer, Trans. ASME Series C, Vol.95, pp. 543~545.
- [8] Buchberg, H., Catton, I., and Edwards, D.K., 1976, "Natural Convection in Enclosed Spaces; A Review of Application to Solar Energy Collection", J. Heat Transfer, Vol. 98, No.2, pp. 182~188.
- [9] Dropkin, D., and Somerscales, F., 1965, "Heat Transfer by Natural Convection in Liquids Confined by Two Parallel Plates which are Inclined at Various Angles with Respect to the Horizontal", Journal of Heat Transfer, Series C, Vol. 87, pp. 77~81.
- [10] Elsherbiny, S.M., Hollands, K.G.T. and Raithby, G.D., 1977, "Free Convection Across Inclined Air Layers with One Surface Vee Corrugated", Heat Transfer Solar Energy Systems, Howell, J.R. and Min, T., (eds), American Society of Mechanical Engineers, New York.
- [11] Kabir, H., 1988, "An Experimental Investigation of Natural Convection Heat Transfer from a Hot Corrugated Plate to a Flat Plate", M.Sc. Engineering (Mechanical) Thesis, BUET.
- [12] Chowdhury, M.F., 1992, "Natural Convection from Hot Corrugated Plates to a Cold Flat Plate", M. Sc. Engineering (Mechanical) Thesis, BUET.

- [13] Saiful, K. M., 1995, "An Experimental Investigation of Natural Convection Heat Transfer from Hot Square Corrugated Plate to a Cold Flat plate," M. Sc. Engineering (Mechanical) Thesis, BUET.
- [14] Latifa, B., 1998, "An Experimental Investigation of Natural Convection from Hot Vee Corrugated Plates to a Cold Flat Plate", M.Sc. Engineering (Mechanical) Thesis, BUET.
- [15] Stewart, W.T., and Johnson, J.C., 1985, "Experimental Natural Convection Heat Transfer from Spherical Natural Zones", ASME Journal, Heat Transfer, Vol. 107, pp. 463~465.
- [16] Thomson, J.J., 1882, Proc. Glasgow Phil. Soc., Vol. 13, pp. 464.
- [17] Sterling, C.V., and Scriven, L.E., 1964, "Journal of Fluid Mechanics", Vol. 19, p.321.
- [18] Mull, W., and Reiher, H., 1930, "Experimental Investigation of Free Convection Heat Transfer in Horizontal air Layers", Gesundh-Ing. 28(1), pp. 1~28.
- [19] Jakob, M., 1946, Trans. ASME, Vol. 68, pp. 189.
- [20] Hollands, K.G.T., and Konicek, L., 1973, "Experimental Study of the Stability of Differentially Heated Inclined Air Layers", International Journal of Heat and Mass Transfer, Vol. 16, pp. 1467~1476.
- [21] Chu, T.Y., and Goldstein, R.J., 1969, "Thermal Convection in a Horizontal Layer of Air", Prog. Heat and Mass Transfer, Vol. 2, pp. 55~75.
- [22] Rossby, H.T., 1969, "A Study of Benard Convection with and without Rotation", Journal of Fluid Mechanics, Vol. 36(2), pp.309~335.
- [23] O'Toole, J.L., and Siveston, P.L., 1961, "Correlations of Convective Heat transfer in Confined Horizontal Layers", A.I.Ch.E. Chem.Engg. Prog. Symp. Ser. Vol. 57(32), pp. 81~86.
- [24] Malkus, W.V.R., 1963, "Outline of a Theory of Turbulent Convection", Theory and Fundamental Research in Heat Transfer, Edited by J.A.Clark, Pergamon Press, New York, pp. 203~212.
- [25] Globe, S., and Dropkin, D., 1959, "Natural Convection Heat Transfer in Liquids Confined by Two Horizontal Plates and Heated from below", Journal of Heat Transfer, Vol. 81, Series C, pp. 24~28.
- [26] Herring, J.R., 1965, "Investigation of Problems in Thermal Convection", Journal Atoms Sci., Vol. 20, p. 325.
- [27] Graff, J.G.A., and E.F.M. Van der Held, 1952, "The Relation between the Heat Transfer and Convection Phenomena in Enclosed Air Layers", Appl. Sci. Res., Vol. 3, p. 393.

- [28] Dropkin, D., and Somerscales, F., 1965, "Heat Transfer by Natural Convection in Liquids Confined by Two Parallel Plates which are Inclined at Various Angles with Respect to the Horizontal", *Journal of Heat Transfer, Series C*, Vol. 87, pp. 77-81.
- [29] Ayyaswamy, P.S., and Cotton, I., 1974, "Natural Convection Flow in a Finite rectangular Slot Arbitrarily oriented with Respect to Gravity Vector", *International Journal of Heat and Mass Transfer*, Vol. 17, pp. 173-184.
- [30] Hollands, K.G.T., Raithby, G.D., and Konicek, L., 1975, "Correlation Equations for Free Convection Heat Transfer in Horizontal Layers of Air and water", *International Journal of Heat and Mass Transfer*, Vol. 18, pp. 879-884.
- [31] Randall, K.R., et. Al., 1977, "Interferometric Investigation of Convection in Slat-Flat Plate and Vee-Corrugated Solar Collectors", *Solar Energy International Progress*, pp. 447-460.
- [32] Chinnappa, J.C.V., 1970, "Free Convection in Air Between a 60° Vee-Corrugated Plate and Flat Plate", *International Journal of Heat and Mass Transfer*, Vol. 13, pp. 117-123.
- [33] Arnold, J.N., Catton, I., and Edwards, D.K. 1976, "Experimental Investigation of Natural Convection in Inclined Rectangular Regions of Differing Aspect Ratios" *J. Heat Transfer*, Vol. 98, pp. 67-71.
- [34] El Sherbiny, S. M., G. D. Raithby and K. G. T. Hollands, 1982, "Heat Transfer by Natural Convection across Vertical and Inclined Air Layers," *J. Heat Transfer*, Vol. 104C, pp. 96 ~ 102.
- [35] Jakob, M., 1949, "Heat Transfer", Vol. 1, John Wiley and Sons, Inc. N.Y.
- [36] Gryzagoridis, J., 1971, "Natural Convection from a Vertical Plate in Low Grashof Number Range", *International Journal of Heat and Mass Transfer*, Vol. 14, pp. 162-164.
- [37] McAdams, W.H., 1949, "Heat Transmission", Third Edition, McGraw-Hill Book Company, Inc.
- [38] Hollands, K.G.T., 1963, "Directional Selectivity, Emittance and Absorptance Properties of Vee-Corrugated Surfaces", *Solar energy*, Vol. 7, pp. 108-116.
- [39] Grag, H.P., 1982, "Treaties of Solar Energy", John Wiley and Sons Ltd., Vol. 1.



APPENDICES: A - D

DESIGN OF THE TEST RIG

Design of the test rig considers the following two aspects:

- (1) Heat transfer calculations,
- (2) Electrical heater design.

Heat transfer calculation consists of the determination of the steady state heat transfer rate from different exposed heated surfaces of the experimental rig under different design conditions. It also requires the estimation of the steady state heat transfer rate from the experimental hot corrugated plate to the cold plate.

Next, heaters are designed to the required capacity so that the designed operating condition can be achieved. It is to be noted that there are six heaters. Heater no. 1 (main heater) is test plate heater and the rest are guard heaters.

A1 HEAT TRANSFER CALCULATIONS

In the process of determining the rates of heat input to different exposed surfaces of the experimental rig under different designed operating conditions it is necessary to calculate as furnished below:

- Calculation of the rate of heat transfer from the hot corrugated plate to the cold flat plate by convection and radiation.
- Calculation of rate of heat transfer from the exposed surfaces of the upper guard heater assembly to the ambient air by convection and radiation.
- Calculation of rate of heat transfer from the exposed surfaces of the lower guard heater assembly to the ambient air by convection and radiation.

For proper design the above three items are estimated for two extreme design temperatures namely the maximum and the minimum design temperatures. From the previous available experimental data it is found that maximum heat transfer will occur when the rig is in horizontal position and mean plate spacing is moderate and rig operates under maximum design temperature. Consequently minimum heat transfer will occur when rig is in vertical position, mean plate spacing is moderate and rig operates under minimum design temperature.

Guard heaters are provided to ensure no heat loss in any direction, other than required (towards cold plate). For this reason temperature of guard heating surfaces are maintained at T_{COR} thus there is no heat transfer among guard heater and experimental hot plate. The heat supplied to the guard heaters is dissipated to the ambient air through convection and radiation. Here conduction heat losses from inner surface of guard heaters to the outer surfaces of the same and radiation heat losses from its outer surface are independent of the physical alignment of the experimental rig. But convection heat losses are strongly influenced by physical alignment of the experimental rig.

A1.1 Calculation of Rate of Heat Transfer from the Hot Corrugated Plate to the Cold Flat Plate

Heat transfer from the hot corrugated plate to the cold flat plate takes place by two different modes (conduction is negligible);

- Natural convection and
- Radiation.

A1.1a Calculation of Natural Convection Heat Transfer

In order to compute the heat transfer rate it is necessary to know natural convection heat transfer coefficient that is unknown for this configuration. Virtually this has to be found out experimentally. For design purpose it is assumed that the corrugated plate is a flat one. For computing heat transfer co-efficient approximately the following correlations Jakob^[35] for

horizontal [Fig. A.1] and vertical [Fig. A.2] positions of the test rig heated from below are used.

For Horizontal Position:

$$Nu_L = 0.195 [Gr_L]^{1/4}, \quad 10^4 < Gr_L < 4 \times 10^5 \quad (A1a)$$

$$Nu_L = 0.068 [Gr_L]^{1/3}, \quad Gr_L < 4 \times 10^5 \quad (A1b)$$

For Vertical Position:

$$Nu_L = 1 \quad Gr_L < 2000 \quad (A2a)$$

$$Nu_L = 0.18 [Gr_L]^{1/4} [H/L]^{1/9}, \quad 2 \times 10^3 < Gr_L < 2 \times 10^5 \quad (A2b)$$

$$Nu_L = 0.065 [Gr_L]^{1/3} [H/L]^{1/9}, \quad 2 \times 10^5 < Gr_L < 11 \times 10^6 \quad (A2c)$$

After knowing Nu_L convective heat transfer co-efficient, h is found by using the following equation:

$$h = Nu_L \cdot k/L \quad (A3)$$

And finally convective heat transfer rate is calculated by using the following equation:

$$Q_{CONV} = A_{COR} \cdot h \cdot [T_{COR} - T_{COLD}] \quad (A4)$$

A1.1b Calculation of Radiation Heat Transfer

The radiation heat transfer rate is found by the following approximation:

- Interior surfaces i.e. the hot corrugated plate and the cold flat plates behave like black bodies.
- Heat transfer by convection is not taken into account.

➤ Side walls of the test rig are adiabatic.

Since the interior surfaces as mentioned above are assumed to be black, the radiation emitted is absorbed without any reflection. Defining Q_{i-j} as the rate at which radiation is emitted by black surface i , and is intercepted by black surface j , [Fig. A3] i.e.,

$$Q_{i-j} = [A_i J_j] F_{ij} \quad (A5)$$

Since radiosity equals emissive power for a black surface [$J_i = E_{bi}$], hence

$$Q_{i-j} = A_i F_{ij} E_{bj} \quad (A6a)$$

$$Q_{j-i} = A_j F_{ji} E_{bi} \quad (A6b)$$

The net radiation exchanged between two black surfaces:

$$\begin{aligned} Q_{ij} &= Q_{i-j} - Q_{j-i} \\ \text{or, } Q_{ij} &= A_i F_{ij} E_{bi} - A_j F_{ji} E_{bi} \end{aligned} \quad (A7)$$

$$\text{By reciprocity, } A_i F_{ij} = A_j F_{ji} \quad (A8)$$

According to Stefan – Boltzman law:

$$E_{bi} = \sigma T_i^4 \quad (A9a)$$

$$E_{bj} = \sigma T_j^4 \quad (A9b)$$

Now from Eqs. [A7], [A8], [A9a] and [A9b]:

$$Q_{ij} = A_i F_{ij} \sigma [T_i^4 - T_j^4] \quad (A10)$$

Considering surfaces i and j as corrugated and flat plate respectively and assuming that the radiation emitted by the corrugated surface is intercepted by the cold flat plate [$F_{ij} = 1$], the Eq. [A10] takes the following form:

$$Q_{\text{rad}} = A_{\text{COR}} \sigma [T_{\text{COR}}^4 - T_{\text{COLD}}^4] \quad (\text{A11})$$

From Eq. [A11] the radiation heat transfer is estimated.

A1.2 Calculation of Rate of Heat Transfer from the Exposed Surfaces of the Upper Guard Heater Assembly to the Ambient Air by Convection and Radiation

When the experimental rig is kept horizontal, the exposed surfaces of the upper guard heater assembly consist of two pairs of parallel vertical plane surfaces facing outward having dimensions of 660 mm x 127 mm and 579 mm x 127 mm.

When the experimental rig is kept vertical, one of the pair of dimensions 660 mm x 127 mm of the exposed surfaces of the upper guard heater assembly became horizontal; one facing upward and another facing downward. But the other pair of the exposed heated surfaces of dimensions 579 mm x 127 mm remains vertical facing outward.

For design the following correlation are used to estimate the rate of heat transfer from the exposed surfaces of the upper guard heater assembly:

- For computing convective heat transfer co-efficient approximately the following correlating equation recommended by Gyrzagoridis ^[36] for vertical heated surfaces of height H (Fig. A.4) is used:

$$\text{Nu}_H = 0.555 [\text{Gr}_H \text{Pr}]^{1/4}, \quad 10 < \text{Gr}_H < 10^9 \quad (\text{A12})$$

where, Nu_H and Gr_H are based on length of the vertical surface.

- For computing convective heat transfer co-efficient approximately for heated horizontal surfaces (Figs. A.5 and A.6) of characteristic length $L_c = \sqrt{(\text{Area of the plate})} = A_p$ the following correlating equations recommended by McAdams ^[37] are used.

$$\begin{aligned} \text{Nu}_{L_c} &= 0.54 [\text{Gr}_{L_c} \cdot \text{Pr}]^{1/4}, \quad 10^5 < \text{Gr}_{L_c} < 2 \times 10^7, \text{ for upward facing} \quad [\text{A13a}] \\ &= 0.14 [\text{Gr}_{L_c} \cdot \text{Pr}]^{1/3}, \quad 2 \times 10^7 < \text{Gr}_{L_c} < 3 \times 10^{10} \end{aligned}$$

$$\text{Nu}_{L_c} = 0.27 [\text{Gr}_{L_c} \cdot \text{Pr}]^{1/4}, \quad 3 \times 10^5 < \text{Gr}_{L_c} < 3 \times 10^7, \text{ for downward facing} \quad [\text{A13b}]$$

where, Nu_{L_c} and Gr_{L_c} are based on the characteristic length L_c of the plane mentioned above.

The radiation heat transfer from these exposed heated surfaces are estimated by the following equation:

$$Q_{\text{rad}} = A_s \cdot \epsilon_s \cdot \sigma [T_g^4 - T_s^4] \quad (\text{A14})$$

A1.3 Calculation of Rate of Heat Transfer from the Exposed Surfaces of the Lower Guard Heater Assembly to the Ambient Air by Convection and Radiation

When the experimental rig is kept horizontal, the exposed surfaces of the lower guard heater assembly consisted of two pairs of parallel plane surfaces facing outward and having dimension of 660 mm x 64 mm and 579 mm x 64 mm and the surface 660 mm x 579 mm facing downward become vertical.

When the experimental rig is kept vertical, one of the pairs of surface having the dimensions 660 mm x 64 mm of the lower guard heater assembly becomes horizontal; one facing upward and another facing downward. But the other pair of exposed heated surfaces of dimensions 579 mm x 64 mm remains vertical facing outward. The bottom face became vertical.

For estimating both convective and radiative heat transfer rate from the exposed surfaces of the lower guard heater assembly the correlating equation are the same as described in the preceding section A1.2.

For both the lower and upper guard heater assembly the sum of the heat convected and radiated from the exposed surfaces must be equal to the amount of heat conducted from guard heaters through asbestos and wooden strip layers. But during the design the exposed surface temperature, T_s of the guard heater assembly is not known. So T_s is assumed and estimation of conduction heat transfer is made. Then by using this surface temperature the amount of convective and radiative heat transfer are calculated. The iterated solutions are continued until the conduction heat transfer rate becomes equal to the sum of convective and radiative heat transfer. Thus the equation for estimating conduction heat transfer rate is given as below:

$$q_{\text{Cond}} = A_s \cdot \sum_{j=1}^{j=2} K_j / L_j [T_g - T_s] \quad (\text{A15})$$

where,

k_1 : The thermal conductivity of asbestos cloth = 0.192 W / m K

k_2 : The thermal conductivity of wooden strip = 0.130 W / m K

L_1 : The thickness of the asbestos cloth = 12 mm

L_2 : The thickness of the wooden strip = 12 mm

T_s : Temperature of the guard heating element = T_{COR}

Now substituting the above values into Eq. (A15) the conduction heat transfer rate is found to be:

$$Q_{\text{Cond}} = 26.833 A_s [T_g - T_s] \quad (\text{A16})$$

A2 HEATER DESIGN

The total numbers of heater are six in this experimental setup. Among the heaters one heater is in the experimental test section and the other five heaters acted as guard heaters. Each of the heaters has separate controlling variac through which power input to the heaters are controlled during experiment. Power required for each heater is estimated from the heat transfer calculations shown in section A1.

The details of the heater design are given below:

Power (P) taken by the electric heater of resistance R can be determined by the following equation:

$$P = I_{\text{safe}}^2 \cdot R \quad (\text{A17})$$

If 'r' be the resistance of the heating wire per meter of length, then for a heater of power P the length of the heating wire will be:

$$L = R / r \quad (\text{A18})$$

By knowing I_{safe} and P taken by each electric heater the required resistance, R is calculated from Eq. (A17). For particular heating wire, resistance 'r' is fixed. So, by putting the value of R and r into equation (A18) required length for each heater is determined.

The ratings of the heating wires are as follows:

Type 1: Resistance, $r = 39.37$ ohms/m
Current carrying capacity = 0.75 amps

Type 2: Resistance, $r = 26.25$ ohms/m
Current carrying capacity = 1.5 amps.

The particulars of the heating arrangement that are used in the experimental set up are given in Table A1.

Table A1: The particulars of the heating arrangement that are used are given in following tabular form.

Heater Number and Name	Maximum Power Requirement (Watt)	Type	Length of Wire (cm)	Location	Variat Connected with Heater	
					Safe Installed Capacity (Watt)	Safe Voltage (Volt)
Experimental hot corrugated plate heater	12.50	1-Nichrome Wire	97.40	Experimental test section Figure 4.3	22.5	30
Outer side guard heater	83.40	1-Nichrome Wire	376.60	Longitudinal sides of the test section Figure 4.3	22.5	30
Outer end guard heater	20.79	1-Nichrome Wire	93.87	Lateral sides of the test section Figure 4.3	90	120
Upper outer guard heater	97.60	1-Nichrome Wire	165.24	Upper guard heater ring Figure 4.4	180	120
Bottom guard heater	113.02	1-Nichrome Wire	510.34	Lower guard heater ring Figure 4.4	90	120
Lower outer guard heater	43.17	1-Nichrome Wire	194.93	Lower guard heater ring Figure 4.5	45	60

CONDUCTION CORRECTION

One-dimensional conduction equation of Fourier is expressed as:

$$q'' = K \cdot \Delta T_C / \Delta x, \quad \text{for one layer of conduction zone} \quad (\text{B1a})$$

$$= T_C / \sum(\Delta x_i / k_j), \quad \text{for two or more layers of conduction zone} \quad (\text{B1b})$$

According to the present investigation it is observed that under steady state heat conduction the resistance to the heat conduction will consist of resistance offered by the upper asbestos cloth layer and upper corrugated plate (G.I. Sheet).

The thermal conductivity of asbestos cloth, $k_1 = 0.157 \text{ W / m K.}$

The thermal conductivity of G.I. sheet, $k_2 = 70 \text{ W / m K.}$

The thickness of asbestos cloth, $x_1 = 2.15052 \times 10^{-3} \text{ m.}$

The thickness of G.I. sheet, $x_2 = 7.9375 \times 10^{-4} \text{ m.}$

It is assumed that there is no temperature difference at the interface of lower corrugated plate and the interface of the lower guard heater box. So that the heat only goes up toward the cold plate. It is also assumed that the temperature at the bottom surface of the lower corrugated plate is equal to the temperature at the interface of the two asbestos cloths.

Now by substituting the above values into equation (B1a) the conduction correction in temperature measurements are found to be:

$$\Delta T_C = 0.0137089 q'' \quad (\text{B2})$$

where, q'' will be taken as electrical heat input (W / m^2) per unit projected surface area of the experimental section of the hot corrugated plate.

DETERMINATION OF EMISSIVITY OF THE CORRUGATED SURFACE

Accurate prediction of the radiation heat transfer from the experimental hot corrugated plate to the cold flat plate largely depends on the precise determination of the long wave emissivity and hemispherical emissivity of the corrugated surface, so the emissivity of the semicircular corrugated plate is determined as accurate as possible.

The semicircular corrugated plate is painted with dull black plastic paint. Hollands^[38] developed the method of determining the hemispherical emissivities of the vee corrugated surfaces using the plane emissivities of the corrugating surfaces. When a plane G.I. sheet is uniformly painted to dull black with black paint, its emissivity can be taken as the emissivity of the black paint. From Table 3.6 of "Treatise of Solar Energy," of Grag^[38] the emissivity of the black paint is found to be 0.94. So it is assumed that the plane emissivity of the G.I. corrugated plate (painted black) be same as that of when uncorrugated. Considering this value of the emissivity, the hemispherical emissivity of semicircular corrugated plate having opening angle of 65° is found to be 0.975 (using Fig. C2).

UNCERTAINTY ANALYSIS

D1 GENERAL

Errors will creep into all experiments regardless of the care being exerted. If the experimenter knows what the error is, he will correct what will be no longer an error. But in most situations, the experimenter can not talk very confidently about what the error in a measurement is. He can only talk about what it 'might be,' about the limits that he feels bound the possible error. The term 'uncertainty' is used to refer to a possible value that an error may have. Kline-McClintock^[40] attributed this definition and it still seems an appropriate and valuable concept.

According to Thasher and Binder^[41] for single sample measurement it is proposed that the experimenter describes the uncertainty of his measurements in terms of what he believes would happen if measurement are repeated a larger number of times. In this way one can estimate the standard error and uncertainty interval and can give odds that the error would be less than the uncertainty interval. The reliability of a result described in this manner is indicated by the size of the uncertainty interval and the magnitude of the odds.

This chapter is devoted to determine the interval around each measurement parameter within which its true value is believed to lie and it will lead to the ultimate goal, that is, to estimate how great an effect of uncertainties in the individuals measurements have on the calculated results. An uncertainty estimate is only as good as the equation(s) it is based on. If those equations are incomplete and do not acknowledge all the significant factors that affect the results then the analysis will either underestimate or overestimate the uncertainty in the results. In the present experiment the uncertainty of calculation in average natural heat transfer coefficient and Nusselt number is influenced by variation of heat input, measurement in temperature, aspect ratio, area of the test section, angle of inclination and geometry of the enclosure.

D2 BASIC MATHEMATICS

In this experiment, each test point is run only once, and hence they are single sample experiments. A precise method of single sample uncertainty analysis has been described in the engineering literature by the works of Kline-McClintock^[40] and Moffat^[42].

If a variable x_1 , has a uncertainty U_1 , then the form of representing this variable and its uncertainty is,

$$x_1 = x_1 (\text{measured}) \pm U_1 \quad (\text{D1})$$

This statement should be interpreted to mean the following:

- The best estimate of x_1 is x_1 (measured),
- There is an uncertainty in x_1 that may be as large as $\pm U_1$,
- The odds are 20 to 1 against the uncertainty of being larger than $\pm U_1$.

It is important to note that such specifications can only be made by the experimenter based on the total laboratory experience. Let us suppose, a set of measurement is made and the uncertainty in each measurement may be expressed with the same odds. These measurements are then used to calculate some desired result R using the independent variables $x_1, x_2, x_3, \dots, x_n$, where,

$$R = R (x_1, x_2, x_3, \dots, x_n) \quad (\text{D2})$$

If $U_1, U_2, U_3, \dots, U_n$ be the uncertainties in the independent variables given with the same odds, then the uncertainty U_R in the result having these odds is given in Kline-McClintock^[40] as,

$$U_R = [\{ (\partial R / \partial x_1) U_1 \}^2 + \{ (\partial R / \partial x_2) U_2 \}^2 + \dots + \{ (\partial R / \partial x_n) U_n \}^2]^{1/2} \quad (\text{D3})$$

where, the partial derivative of R with respect to x_i is the sensitivity coefficient for the result R with respect to the measurement x_i . In most situations, the overall uncertainty in a given result is dominated by only a few of its terms. Terms in the uncertainty equation that are smaller than

the largest term by a factor of 3 or more can usually be ignored. This is a natural consequence of the Root-Sum -Square (RSS) combination: small terms have very small effects.

Sometimes the estimate is required as a function of reading, rather than in engineering units. While this can always be calculated using equation (D2), it is also possible to do the calculation of relative uncertainty directly. In particular, whenever the equation describing the result is a pure product form such as equation (D4), then the relative uncertainty can be found directly.

That is, if

$$R = x_1^a x_2^b x_3^c \dots x_m^n \quad (D4)$$

Then,

$$U_R / R = [\{ a (U_1 / x_1)^2 + b (U_2 / x_2)^2 + \dots + n (U_m / x_m)^2 \}] \quad (D5)$$

D3 UNCERTAINTY FOR AVERAGE NATURAL CONVECTION HEAT TRANSFER COEFFICIENT MEASUREMENT

Let the experimental investigation deals with the steady state natural convection heat transfer through air at atmospheric pressure from hot semicircular corrugated plates to a cold flat plate placed above and parallel to it, where the surroundings are maintained at constant temperature. Let the heat q'' is transferred through hot semicircular corrugated plate to cold flat plate by using a heater then the mathematical equations for total heat will be:

$$q'' = VI \cos \phi / A_{COR} \quad (D6)$$

that is, the total heat flux from the hot semicircular corrugated plate is calculated by measuring the current and voltage supply of the main heater.

Average natural convection heat transfer coefficient will be

$$h = [q'' - q_r''] / [T_{COR} - T_{COLD}] \quad (D7)$$

where, q_r'' is the heat transfer by radiation.

In case of a fixed temperature potential the radiative heat flux becomes constant and the convective heat transfer varies on aspect ratio and angle of inclination of the enclosure. For calculating the uncertainty of natural convective heat transfer coefficient the equation may be written in the following way with ignoring the effect of estimated uncertainty for fixed radiative heat flux, because the amount of total radiative heat flux is 15 to 20% of the total heat flux, which is found from experiment. Therefore, the amount is considered as a small quantity compared to the total convective heat flux. So the average natural convective heat transfer coefficient will be;

$$h = [q''] / [T_{COR} - T_{COLD}] = (VI \cos \phi) / \{A_{COR} (T_{COR} - T_{COLD})\} \quad (D8)$$

where, V and I are the supply voltage and current to the hot corrugated plate, A_{COR} is the area of the hot test section, T_{COR} and T_{COLD} are the average temperature of the test section and cold plate which are measured through fourteen (14) Chromel Alumel thermocouples.

Let us suppose the enclosure is deviated by an angle β from the horizontal and different angle of inclination due to wrong adjustment. Then the measured natural convective heat transfer coefficient will be;

$$h = \{(VI \cos \phi).(\cos\beta)\} / \{A_{COR} (T_{COR} - T_{COLD})\} \quad (D9)$$

Now differentiating both the sides of equation (D9) with respect to V, I, A_{COR} , $(T_{COR} - T_{COLD})$, β respectively, we get;

$$\partial h / \partial V = \{(I \cos \phi). (\cos\beta)\} / \{A_{COR} (T_{COR} - T_{COLD})\} \quad (D10)$$

$$\partial h / \partial I = \{(V \cos \phi). (\cos\beta)\} / \{A_{COR} (T_{COR} - T_{COLD})\} \quad (D11)$$

$$\partial h / \partial A_{COR} = - \{(VI \cos \phi). (\cos\beta)\} / \{A_{COR}^2 (T_{COR} - T_{COLD})\} \quad (D12)$$

$$\partial h / \partial (T_{COR} - T_{COLD}) = - \{(VI \cos \phi). (\cos\beta)\} / \{A_{COR} (T_{COR} - T_{COLD})^2\} \quad (D13)$$

$$\partial h / \partial \beta = - \{(VI \cos \phi).(\sin\beta)\} / \{A_{COR} (T_{COR} - T_{COLD})\} \quad (D14)$$

Let U_h be the uncertainty in the result and U_V , U_I , $U_{A_{COR}}$, $U_{(T_{COR} - T_{COLD})}$ and U_β be the uncertainty in the voltage, current, area of the test section and temperature of the hot and cold plate reading and angle of deviation of the enclosure respectively. So, from equation (D5) we get;

$$U_h = \{[(\partial h / \partial V)U_V]^2 + [(\partial h / \partial I)U_I]^2 + [(\partial h / \partial A_{COR}) U_{ACOR}]^2 + [(\partial h / \partial (T_{COR} - T_{COLD}))]^2 \times \{U_{(T_{COR} - T_{COLD})}\}^2 + [(\partial h / \partial \beta) U_\beta]^2\}^{1/2} \quad (D15)$$

Putting the values of partial derivatives, the above equation can be written as follows:

$$U_h = [U_V^2 \{[(I \cos \phi) \cdot (\cos \beta)] / \{A_{COR} (T_{COR} - T_{COLD})\}\}^2 + U_I^2 \{[(V \cos \phi) \cdot (\cos \beta)] / \{A_{COR} (T_{COR} - T_{COLD})\}\}^2 + U_{ACOR}^2 \{[- (VI \cos \phi) \cdot (\cos \beta)] / \{A_{COR}^2 (T_{COR} - T_{COLD})\}\}^2 + \{U_{(T_{COR} - T_{COLD})}\}^2 \{[- (VI \cos \phi) \cdot (\cos \beta)] / \{A_{COR} (T_{COR} - T_{COLD})\}\}^2 + U_\beta^2 \{[- (VI \cos \phi) \cdot (\sin \beta)] / \{A_{COR} (T_{COR} - T_{COLD})\}\}^2]^{1/2} \quad (D16)$$

$$= \{[(VI \cos \phi) \cdot (\cos \beta)] / \{A_{COR} (T_{COR} - T_{COLD})\}\} [(U_V / V)^2 + (U_I / I)^2 + (U_{ACOR} / A_{COR})^2 + \{U_{(T_{COR} - T_{COLD})}\}^2 / (T_{COR} - T_{COLD})^2 + U_\beta^2 \tan^2 \beta]^{1/2} \quad (D17)$$

Dividing equation (D17) by equation (D8), we get;

$$U_h / h = \{[(U_V / V)^2 + (U_I / I)^2 + (U_{ACOR} / A_{COR})^2 + \{U_{(T_{COR} - T_{COLD})}\}^2 / (T_{COR} - T_{COLD})^2 + U_\beta^2 \tan^2 \beta]^{1/2} \quad (D18)$$

For room temperature, (30 ± 1)°C and atmospheric pressure, 14.7 Psi, we have;

$$V = (700 \pm 0.012) \text{ volts}$$

$$I = (20 \pm 0.03) \text{ amps}$$

$$A_{COR} = 34960 \text{ mm}^2 \pm 382 \text{ mm}^2 \text{ [Nominal dimension } (152 \pm 1) \times (230 \pm 1)]$$

$$(T_{COR} - T_{COLD}) = 35^\circ\text{C} \pm 0.006^\circ\text{C}$$

$$\beta = 0^\circ \pm 3^\circ$$

$$\text{So, } U_h / h = [(0.012 / 700)^2 + (0.03 / 20)^2 + (382 / 34960)^2 + (0.006 / 35)^2 + (3\pi / 180)^2 \tan^2 3^\circ]^{1/2}$$

$$= [(2.94 \times 10^{-10}) + (2.25 \times 10^{-6}) + (1.194 \times 10^{-4}) + (2.74 \times 10^{-8}) + (7.53 \times 10^{-6})]^{1/2}$$

$$= 0.011367$$

$$= 1.1367\%$$

D4 UNCERTAINTY FOR AVERAGE NUSSELT NUMBER

$$\text{Let } Nu_L = (h L) / k \quad (D19)$$

where,

- Nu_L : Average Nusselt number
- h : Average natural heat transfer coefficient
- L : Mean plate spacing
- k : Thermal conductivity of air

$$\text{So, } \partial Nu_L / \partial h = L / k \quad (D20)$$

$$\partial Nu_L / \partial L = h / k \quad (D21)$$

If U_{NuL} , U_h and U_L be the uncertainty of Nu_L , h and L respectively, we get from equation (D5);

$$U_{NuL} = [\{ (\partial Nu_L / \partial h) U_h \}^2 + \{ (\partial Nu_L / \partial L) U_L \}^2]^{1/2} \quad (D22)$$

$$= [\{ (hL / k) (U_h / h) \}^2 + \{ (hL / k) (U_L / L) \}^2]^{1/2}$$

$$= hL / k [(U_h / h)^2 + (U_L / L)^2]^{1/2} \quad (D23)$$

So, dividing equation (D23) by equation (D19), we have;

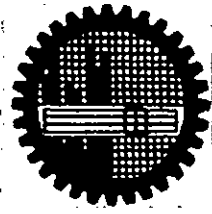
$$U_{NuL} / Nu_L = [(U_h / h)^2 + (U_L / L)^2]^{1/2} \quad (D24)$$

For room temperature, $(30 \pm 1)^\circ\text{C}$ and atmospheric pressure, 14.7 Psi, we have;

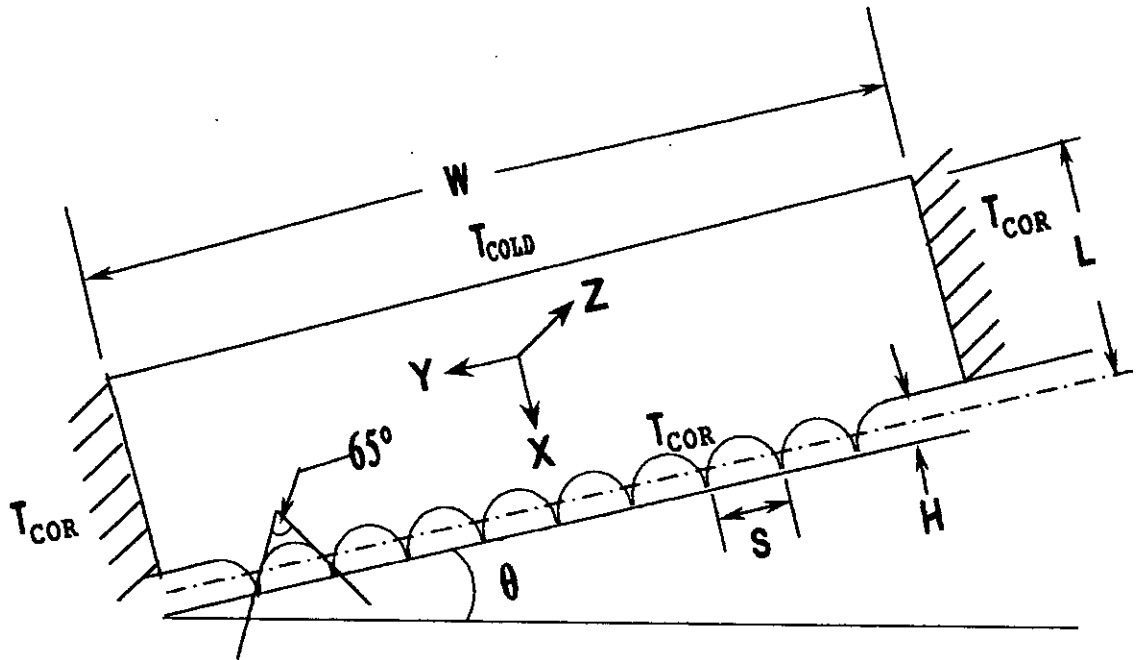
$$L = 95 \text{ mm} \pm 0.5 \text{ mm}$$

$$U_h / h = 0.011367$$

$$\begin{aligned} \text{So, } U_{NuL} / Nu_L &= [(0.011367)^2 + (0.5 / 95)^2]^{1/2} \\ &= [0.0001279 + 0.0000277]^{1/2} \\ &= 0.012526 \\ &= 1.2526\% \end{aligned}$$



FIGURES
(All dimensions are in mm)



$$\theta = 0^\circ - 75^\circ$$

$$L = 35 \text{ mm} - 95 \text{ mm}$$

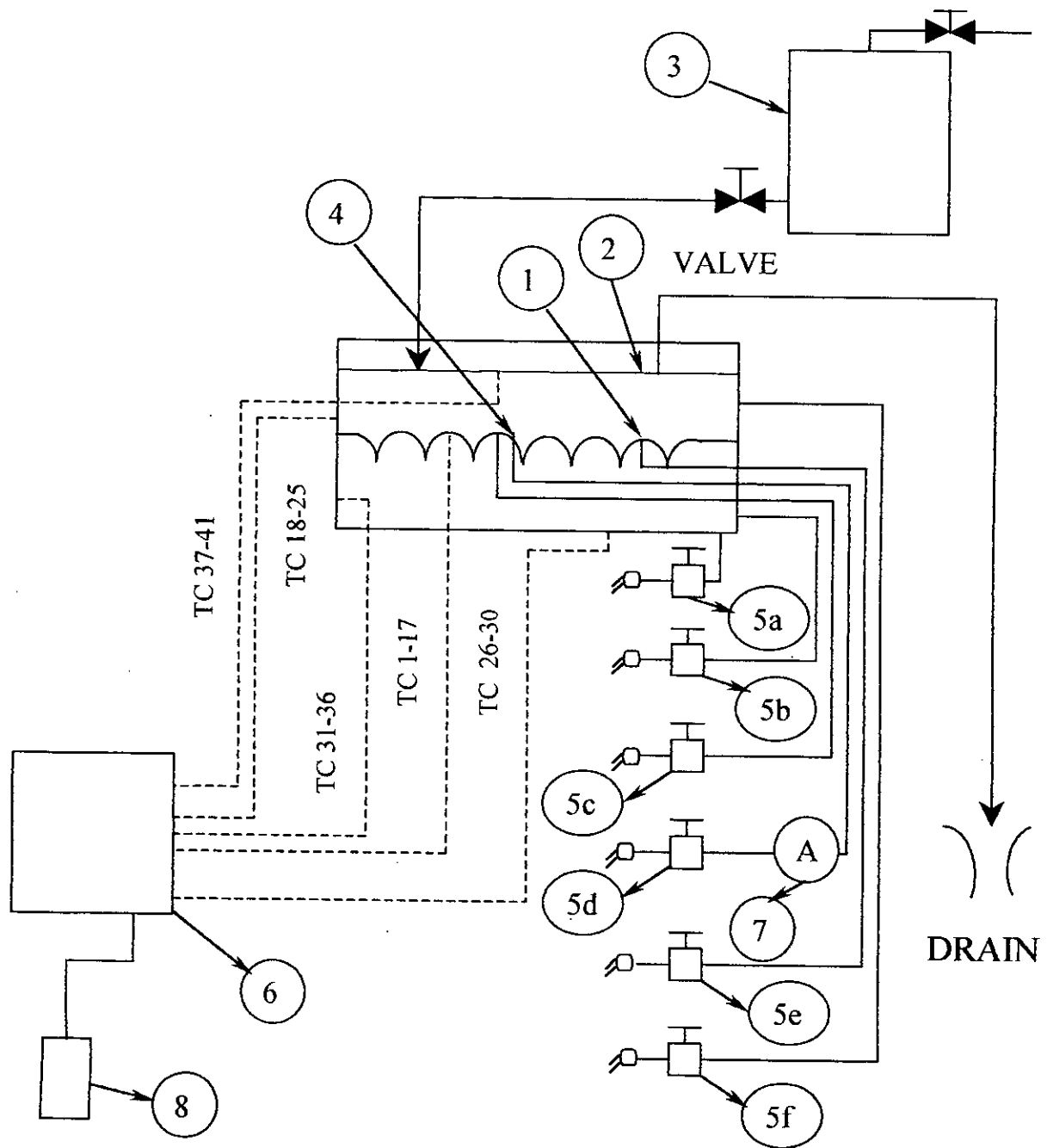
$$H = 10 \text{ mm}$$

$$S = 20 \text{ mm}$$

$$W = 635 \text{ mm}$$

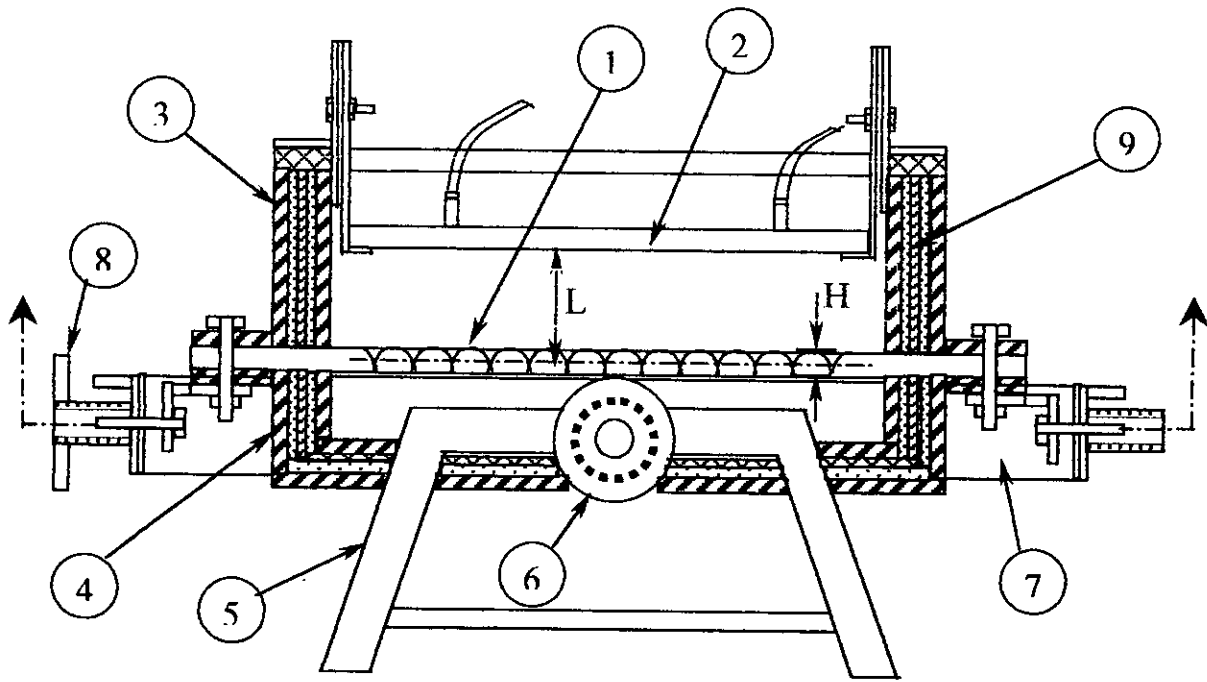
$$\text{Angle of Corrugation} = 65^\circ$$

Fig. 3.1: Sketch of the inclined air layer bounded by semicircular corrugated plate and flat plate.



- | | | |
|-----------------------------|-------------------------------------|---|
| 1. EXPERIMENTAL HOT PLATE | 5d. STABILIZER FOR HEATER | 1 |
| 2. COLD PLATE | 5e. VARIAC FOR HEATER | 2 |
| 3. CONSTANT HEAD WATER DRUM | 5f. VARIAC FOR HEATER | 4 |
| 4. TEST SECTION | 6. THERMOCOUPLE SELECTOR SWITCH | |
| 5a. VARIAC FOR HEATER | 7. DIGITAL MULTIMETER (FOR CURRENT) | |
| 5b. VARIAC FOR HEATER | 8. DIGITAL THERMOMETER | |
| 5c. VARIAC FOR HEATER | | |

Fig. 4.1: Schematic Diagram of the Experimental Set-up.



1. HOT PLATE ASSEMBLY
2. COLD PLATE
3. UPPER GUARD HEATER
4. LOWER GUARD HEATER
5. END RIG HOLDER
6. ALIGNMENT PLATE
7. SIDE RIG HOLDER
8. ALIGNMENT INDICATOR
9. NICHROME HEATERS

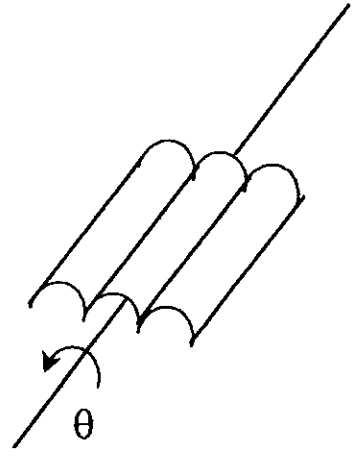
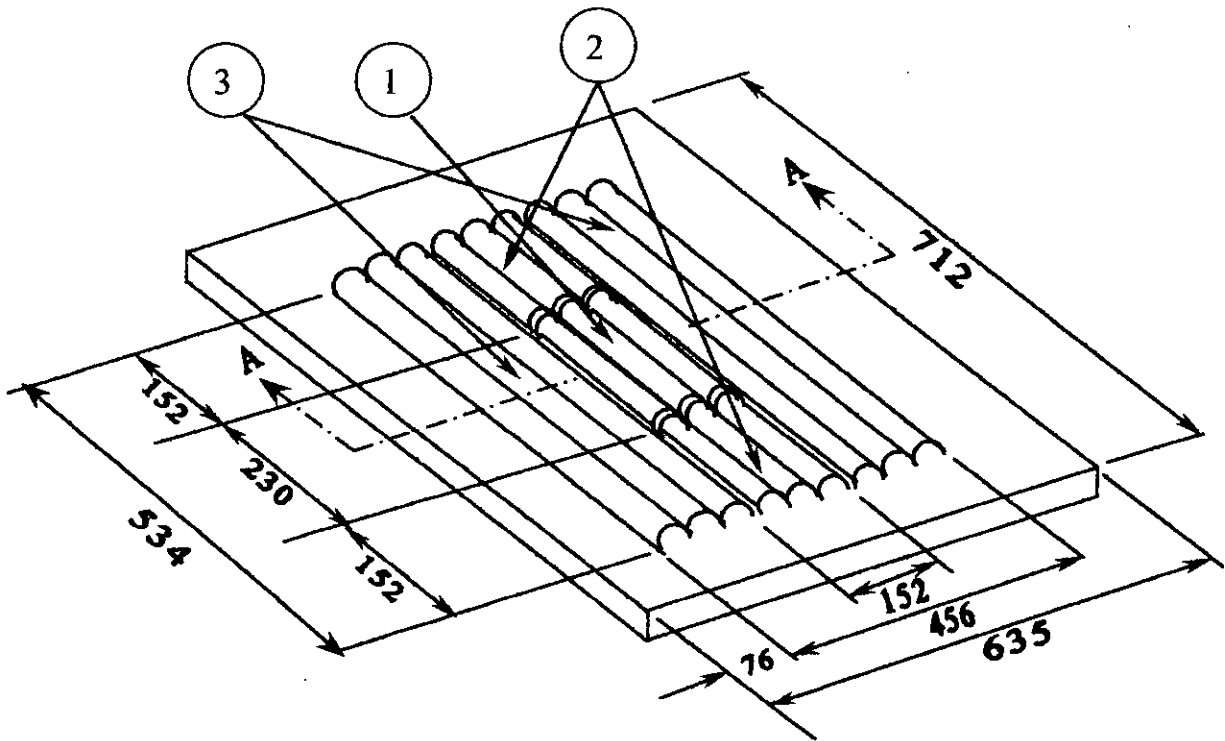


Fig. 4.2: Details of Test Section.



1. EXPERIMENTAL HOT PLATE (152 mm x 230 mm)
2. OUTER SIDE GUARD HEATER (Each 152 mm x 152 mm)
3. OUTER END GUARD HEATER (Each 152 mm x 534 mm)

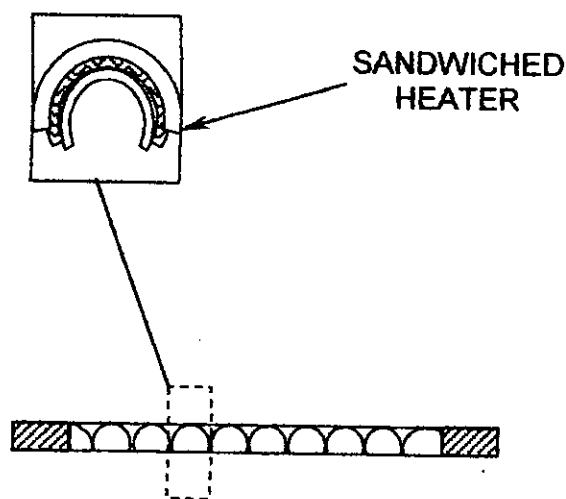
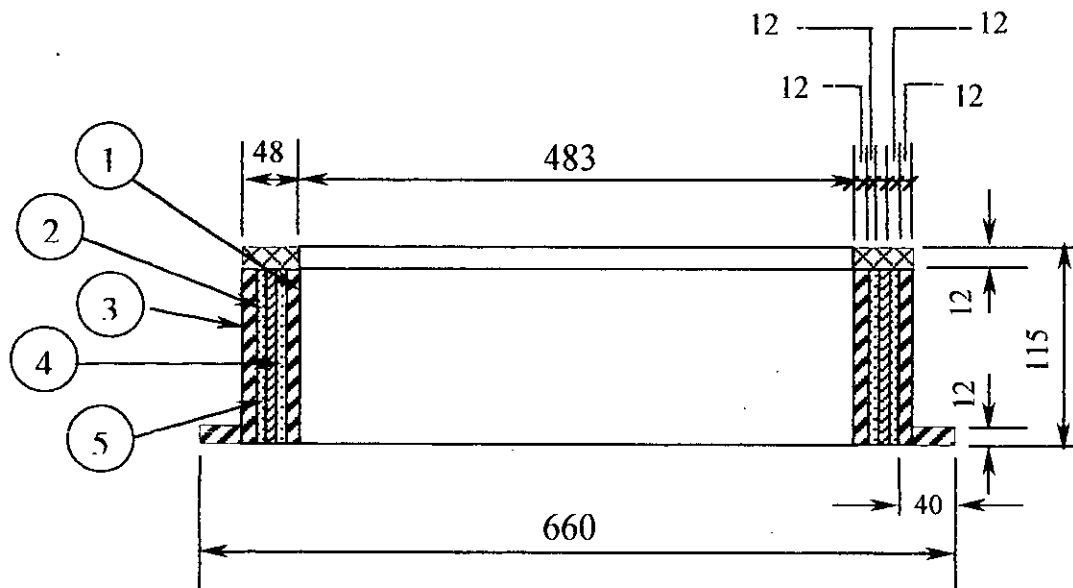
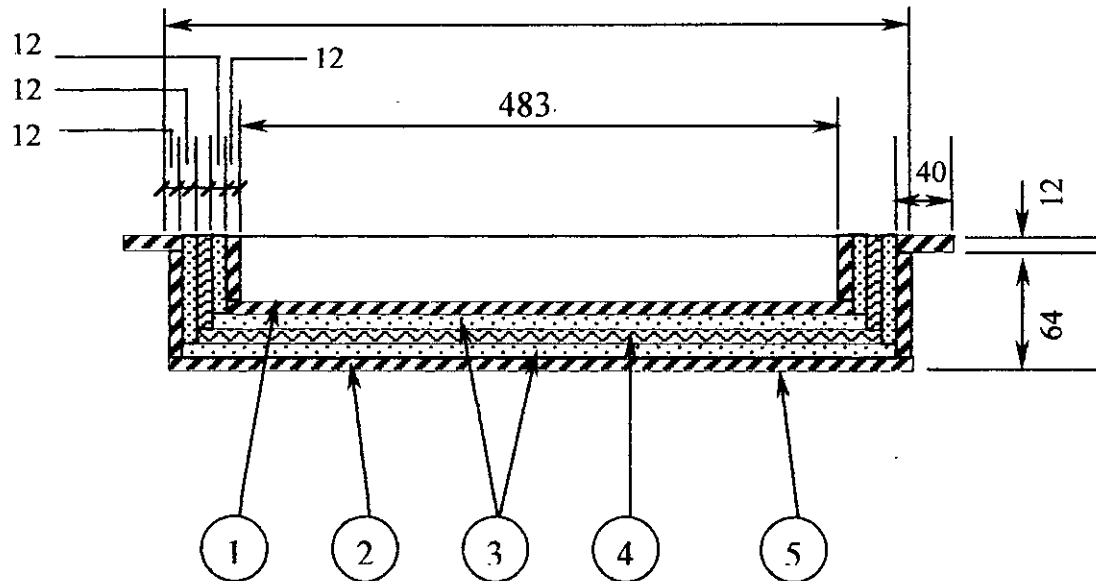


Fig. 4.3: Details of the Hot Plate Assembly.



1. INNER WOODEN RING (12 mm thick)
2. OUTER WOODEN RING (12 mm thick)
3. UPPER OUTER GUARD HEATER (660 mm X 579 mm X 48 mm
outer dimension)
4. INNER ASBESTOS RING (12 mm thick)
5. OUTER ASBESTOS RING (12 mm thick)

Fig. 4.4: Details of Upper Guard Heater Ring.



1. INNER WOODEN BOX (507 mm X 588 mm X 24 mm outer dimension)
2. OUTER WOODEN BOX (555 mm X 636 mm X 52 mm outer dimension)
3. ASBESTOS INSULATION (12 mm thick)
4. BOTTOM GUARD HEATER (29 SWG Nichrome wire)
5. LOWER OUTER GUARD HEATER RING

Fig. 4.5: Details of Lower Outer Guard Heater Ring.

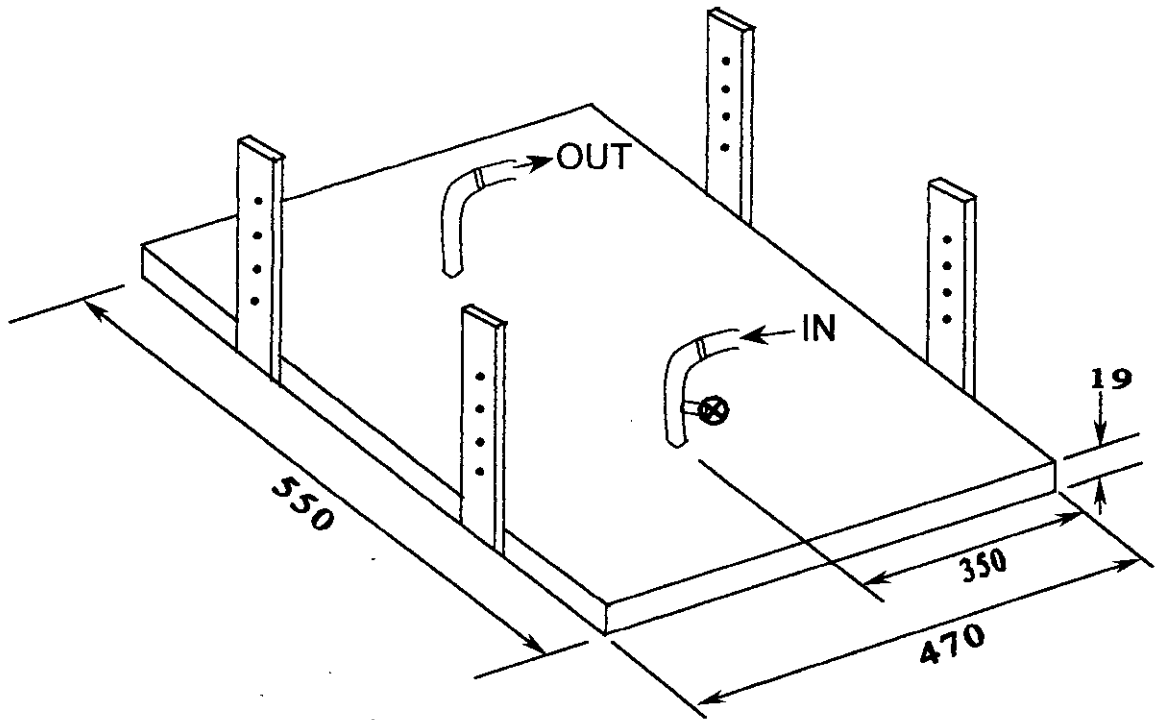


Fig. 4.6: Details of the Cold Plate Assembly.

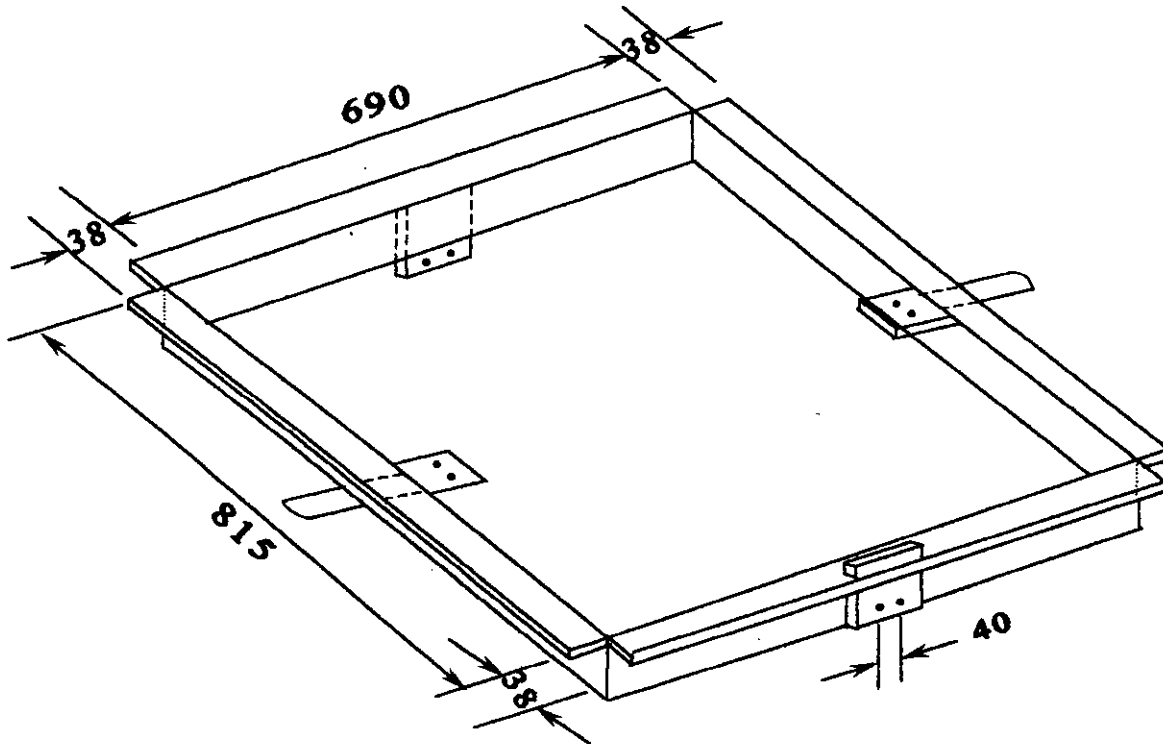


Fig. 4.7: The Rectangular Supporting Frame.

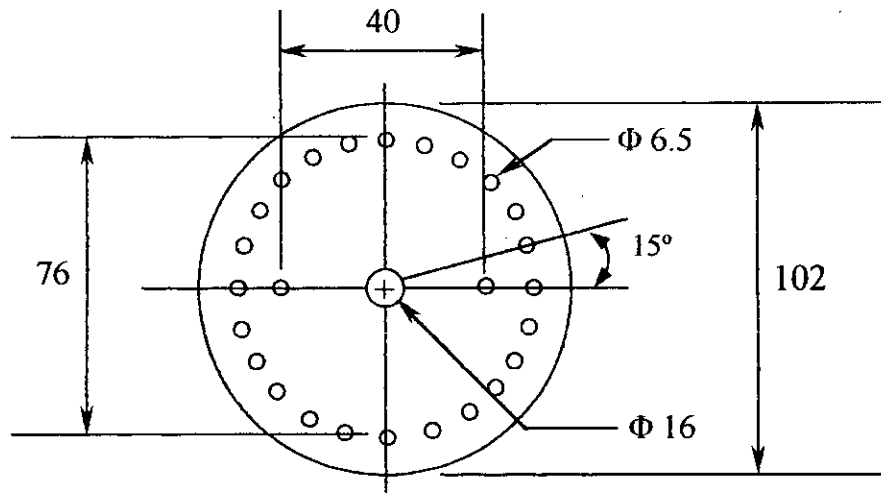
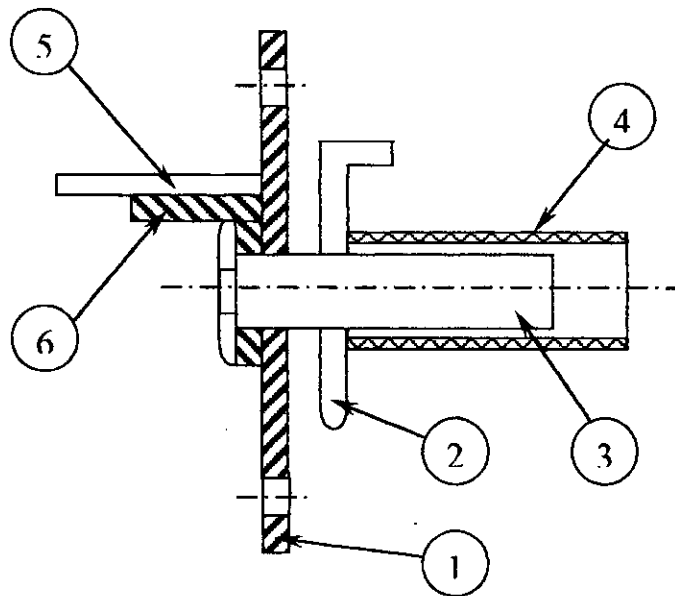


Fig. 4.10: Alignment Plate.



1. ALIGNMENT PLATE
2. SUPPORTING FRAME
3. SUPPORTING BOLT
4. SUPPORTING BOLT HOLDER
5. SUPPORTING FRAME
6. OVER HANGING SIDE SUPPORT

Fig. 4.8: Connecting Assembly of Rectangular Supporting Frame and Supporting Stand.

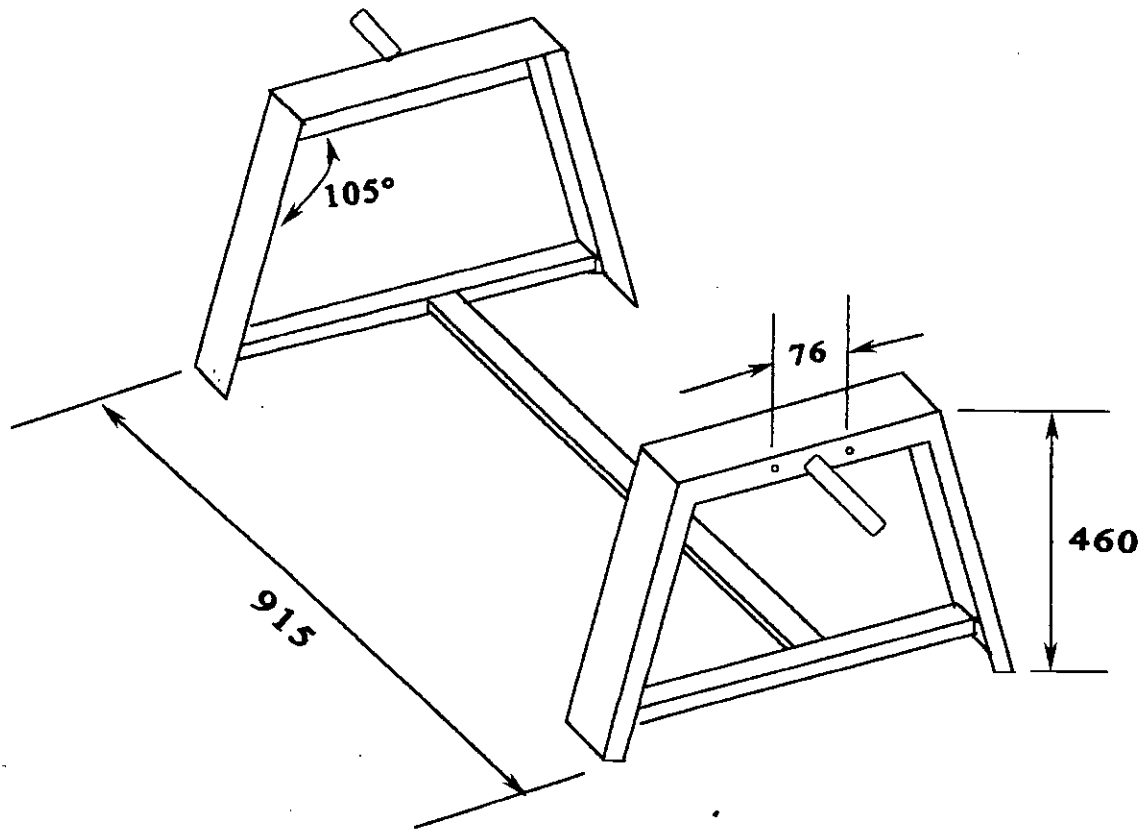
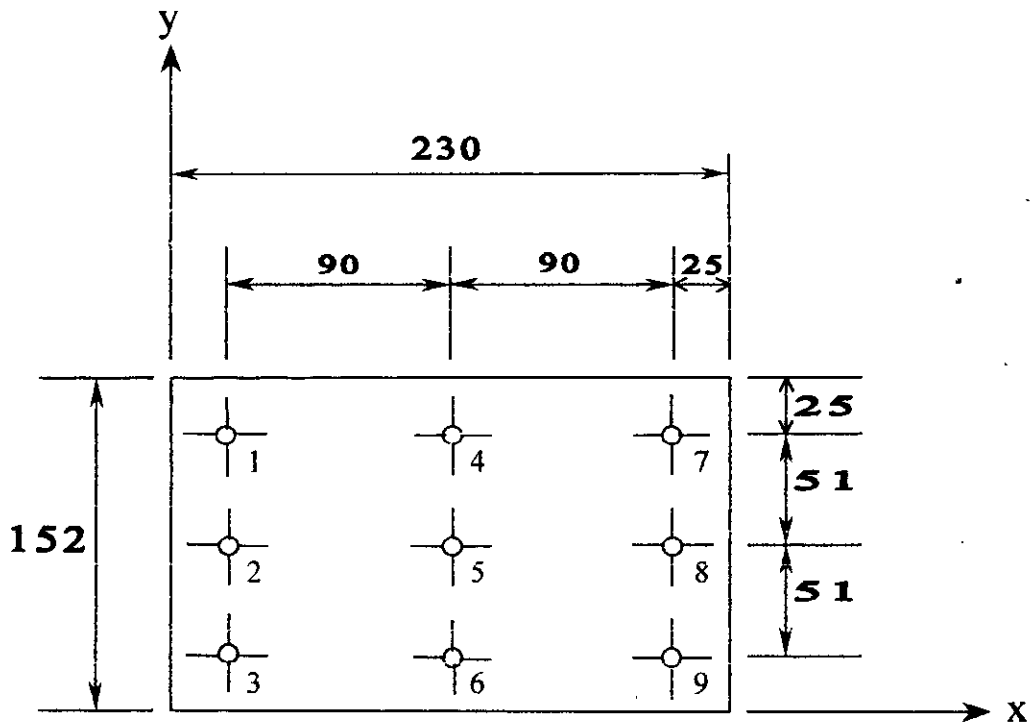


Fig. 4.9: The Supporting Frame.



94973

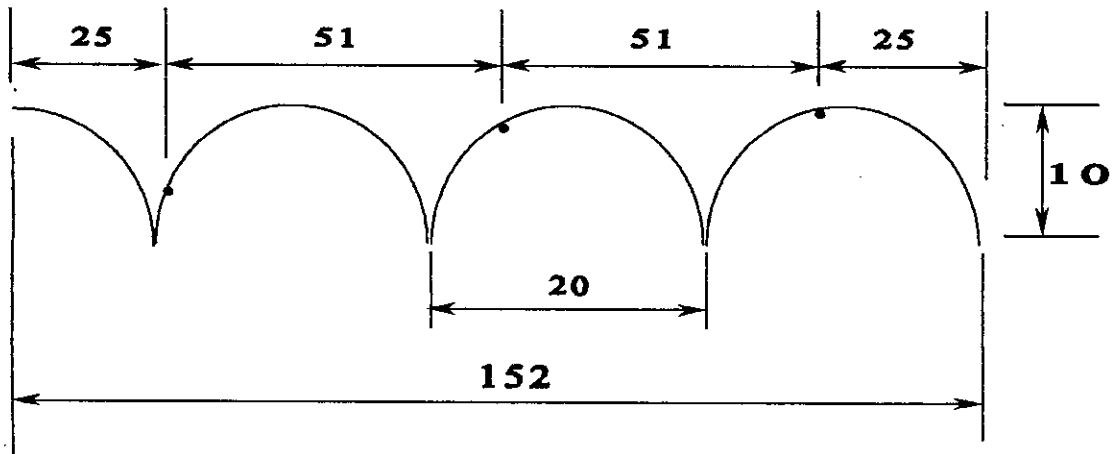


Fig. 5.1: Positions of thermocouples in the test section of hot semicircular corrugated plate.

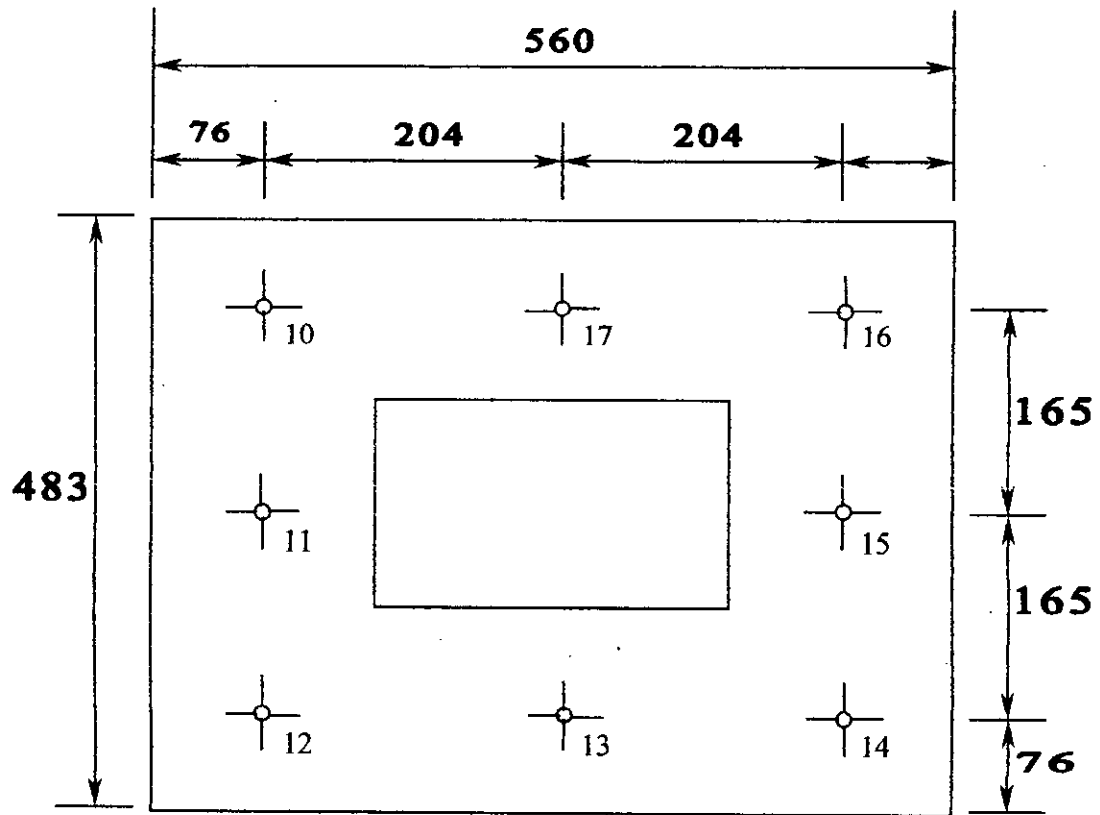


Fig. 5.2: Position of thermocouples in outer end and side guard heater sections.

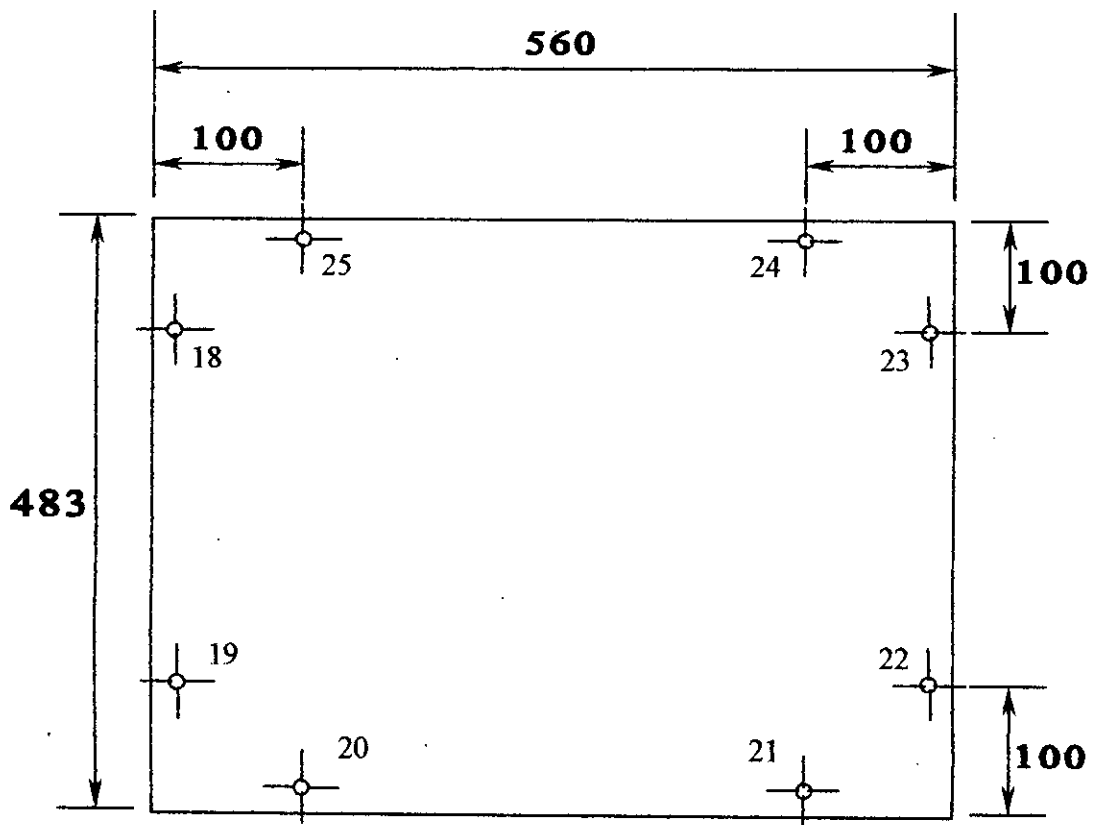


Fig. 5.3: Position of thermocouples in upper outer guard heater ring.

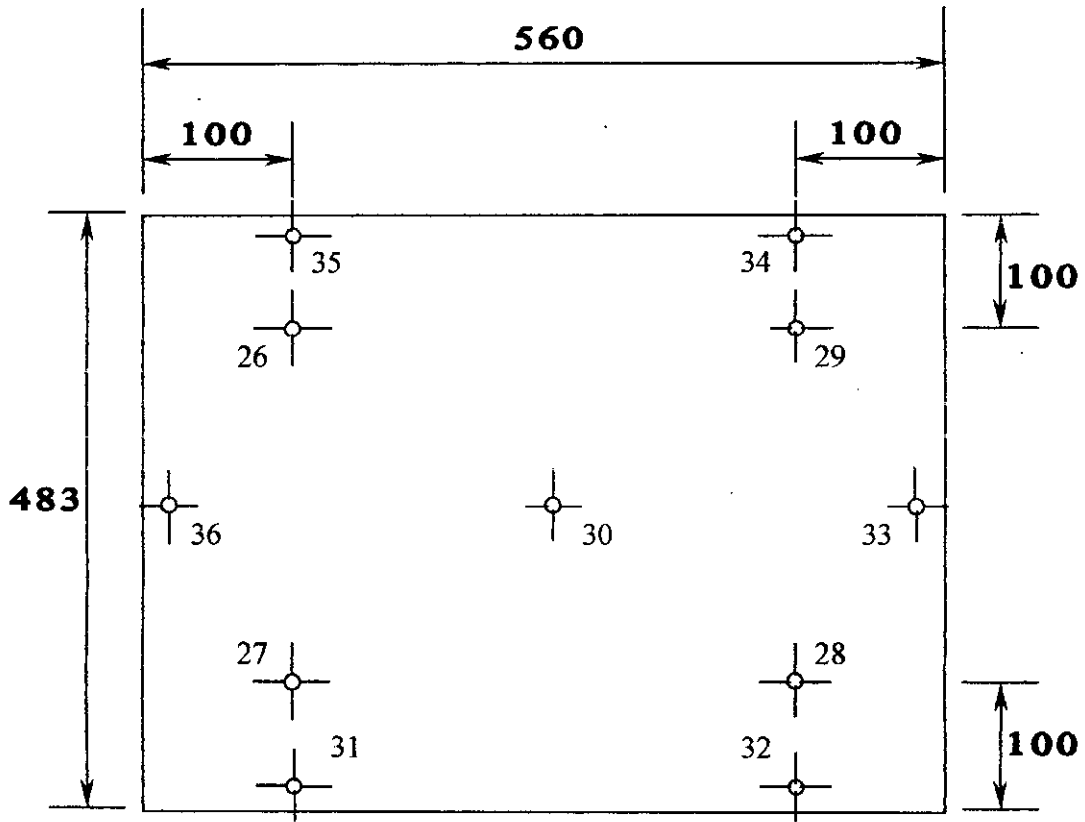


Fig. 5.4: Position of thermocouples in lower outer guard heater box.

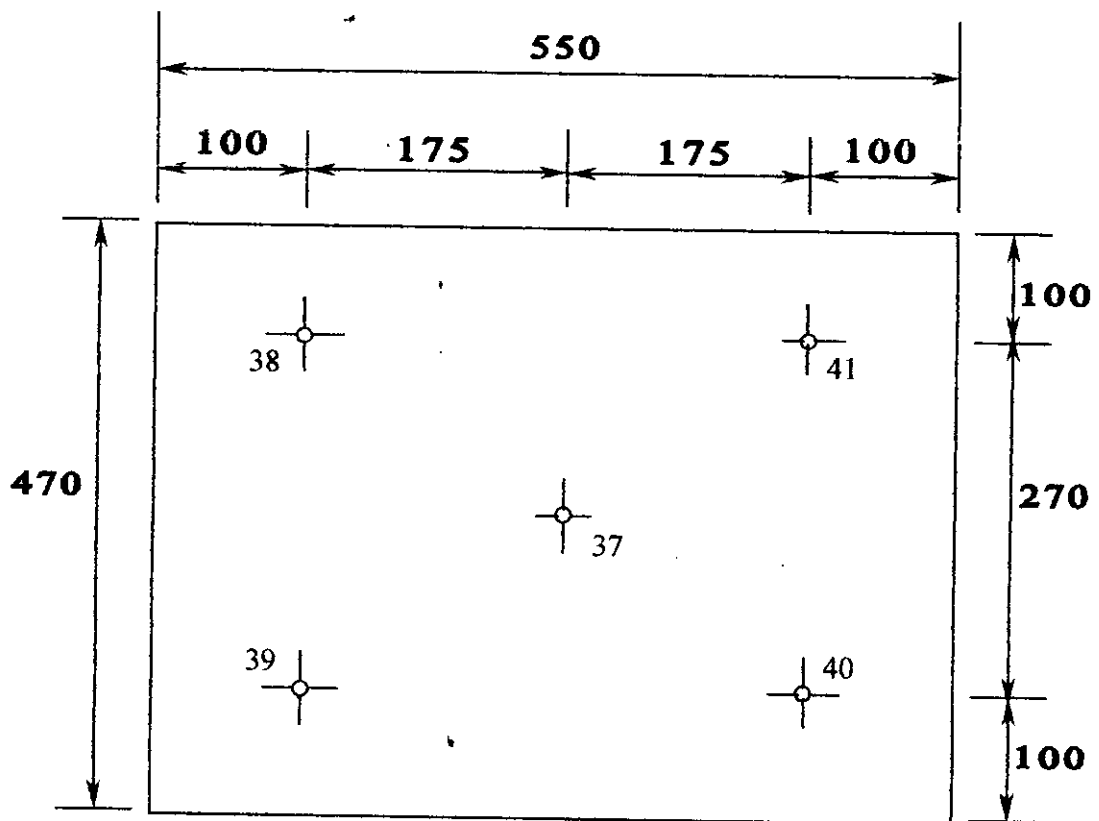


Fig. 5.5: Position of thermocouples in cold flat plate.

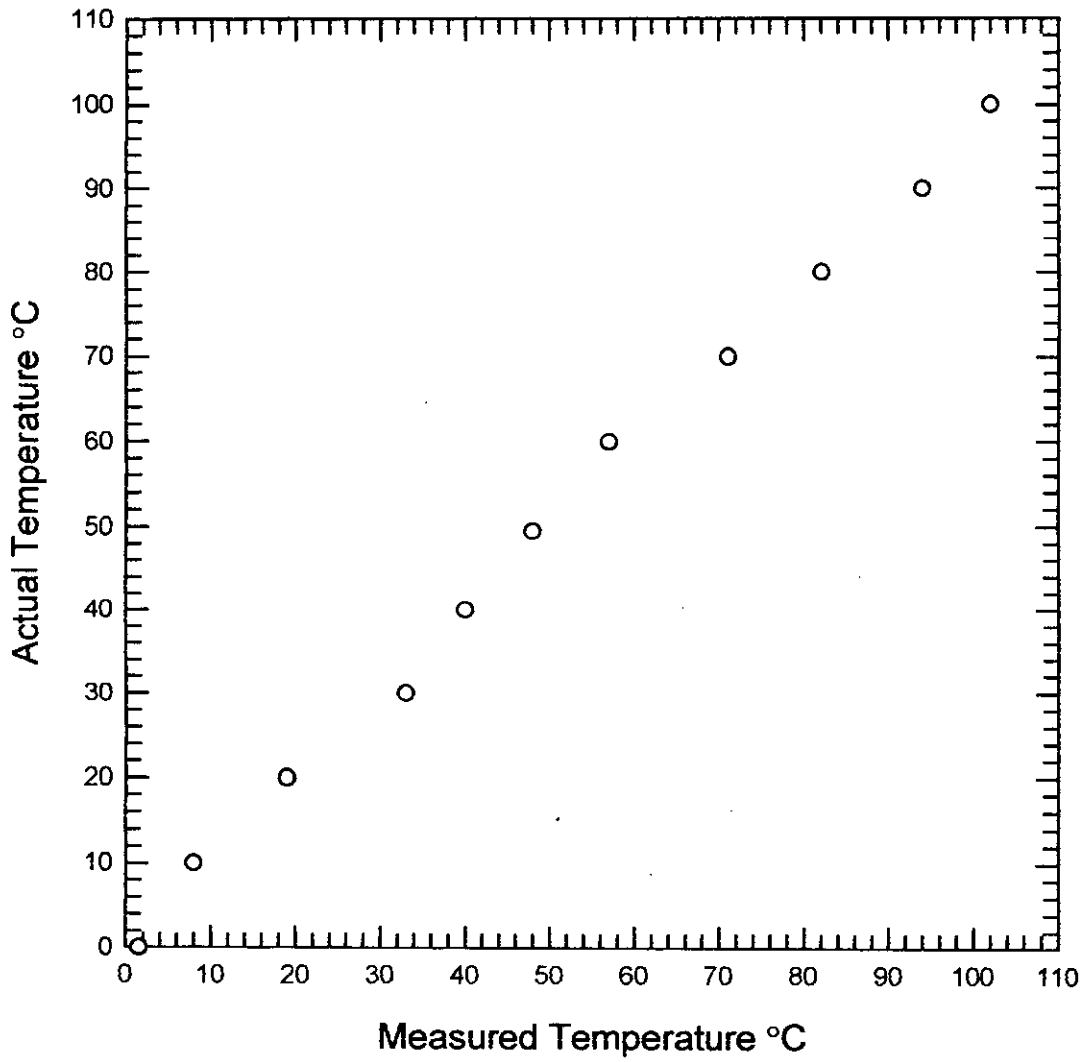


Fig. 5.6: Thermocouple calibration curve for Thermocouple No. 5.

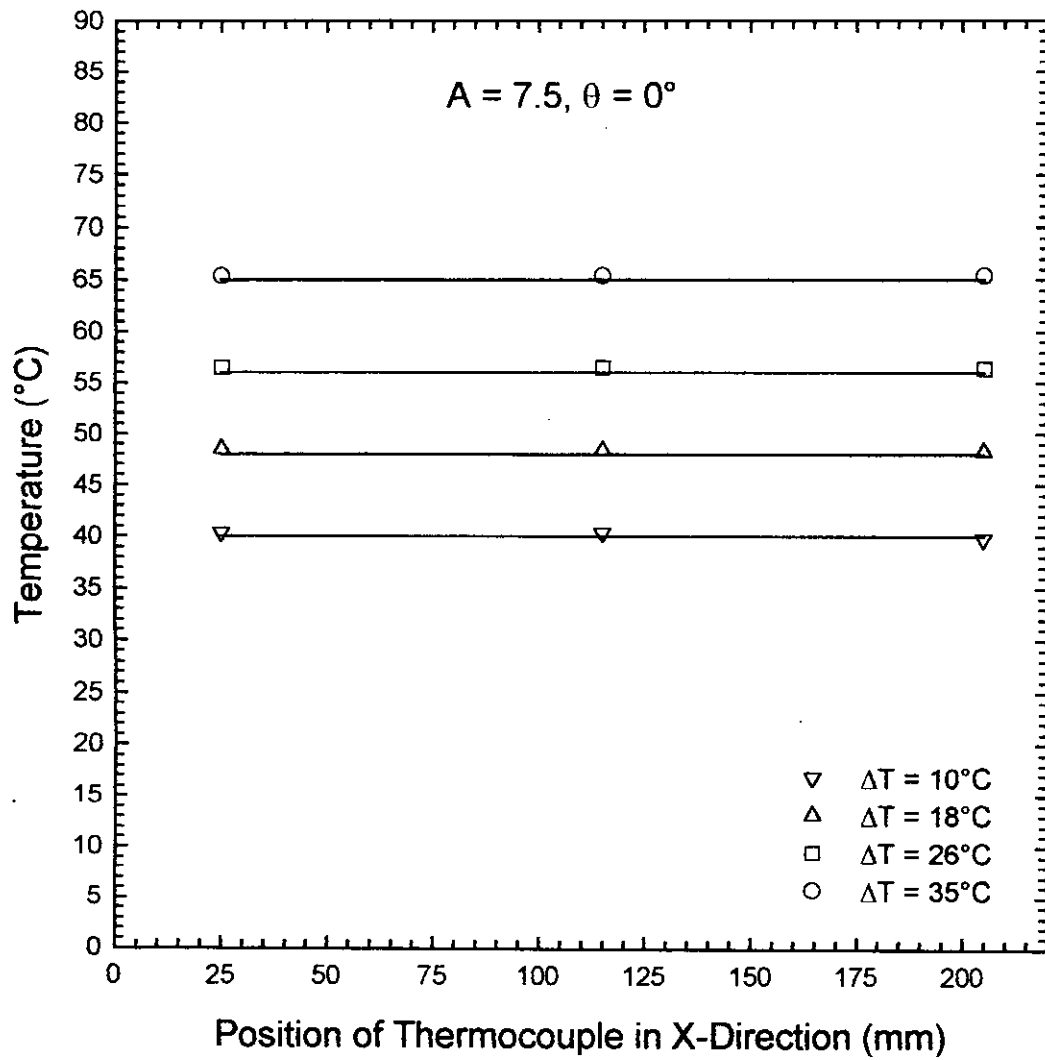


Fig. 6.1: Temperature distribution over the hot corrugated plate for $A = 7.5$ at $\theta = 0^\circ$.

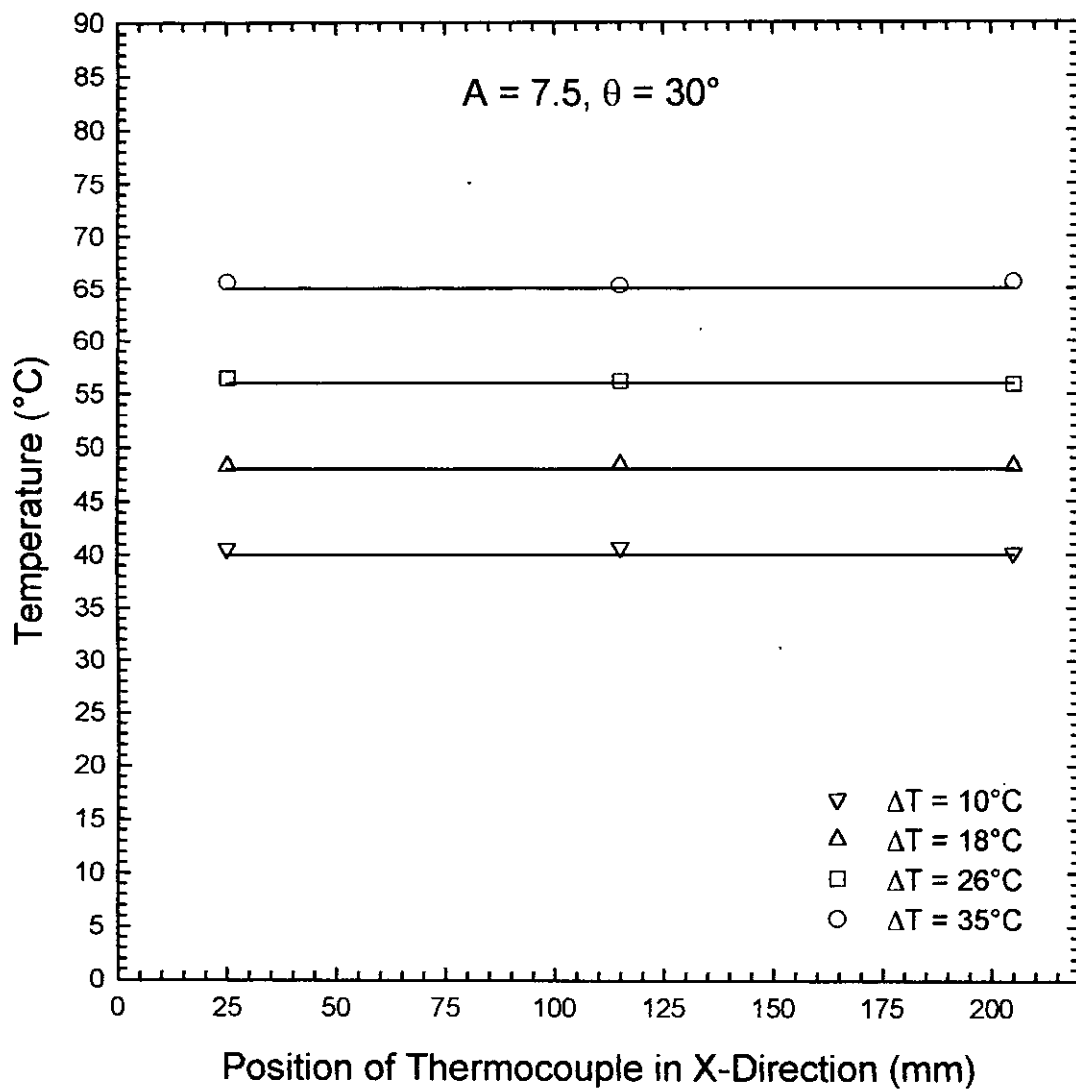


Fig. 6.2: Temperature distribution over the hot corrugated plate for $A = 7.5$ at $\theta = 30^\circ$.

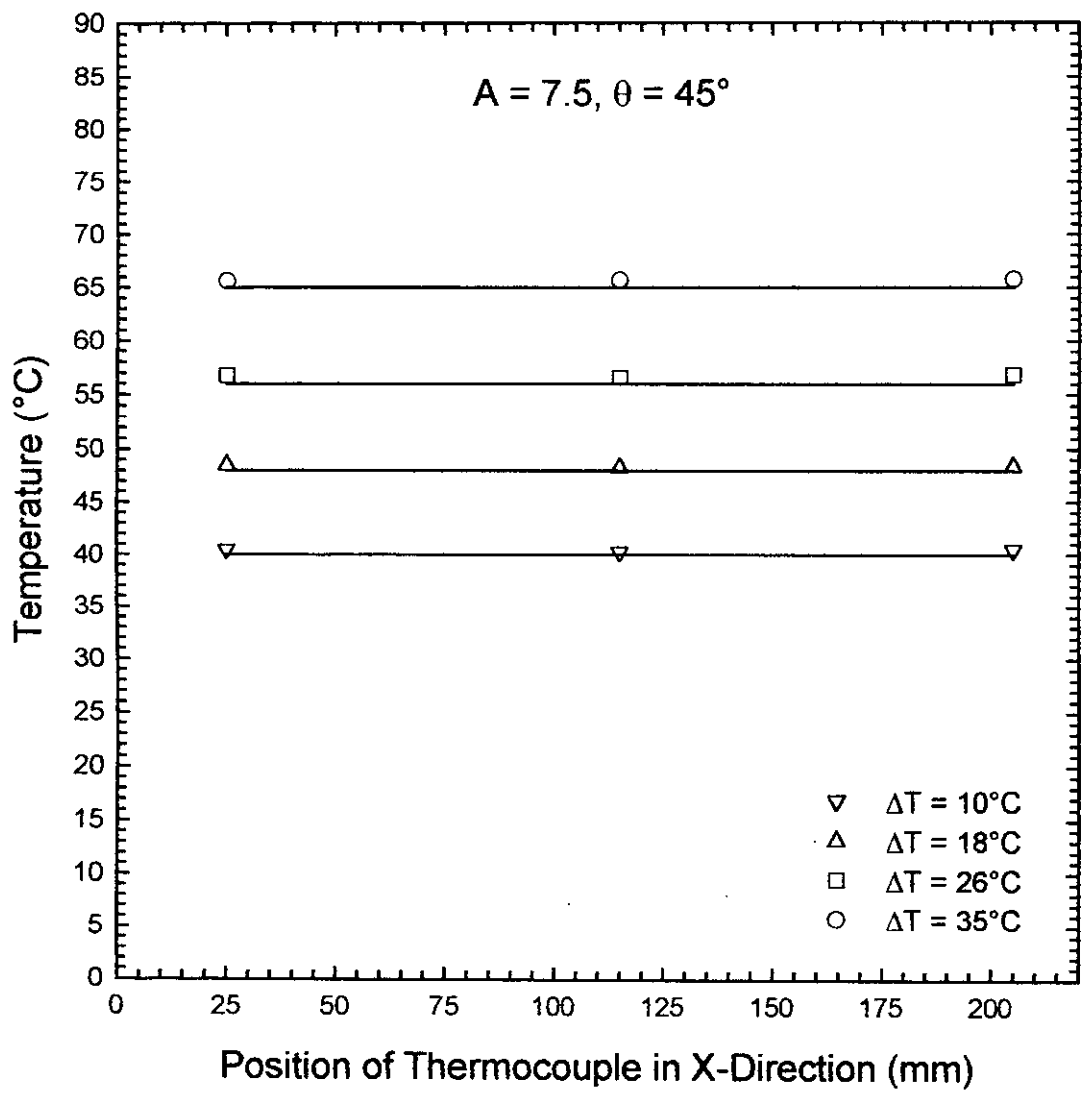


Fig. 6.3: Temperature distribution over the hot corrugated plate for $A = 7.5$ at $\theta = 45^\circ$.

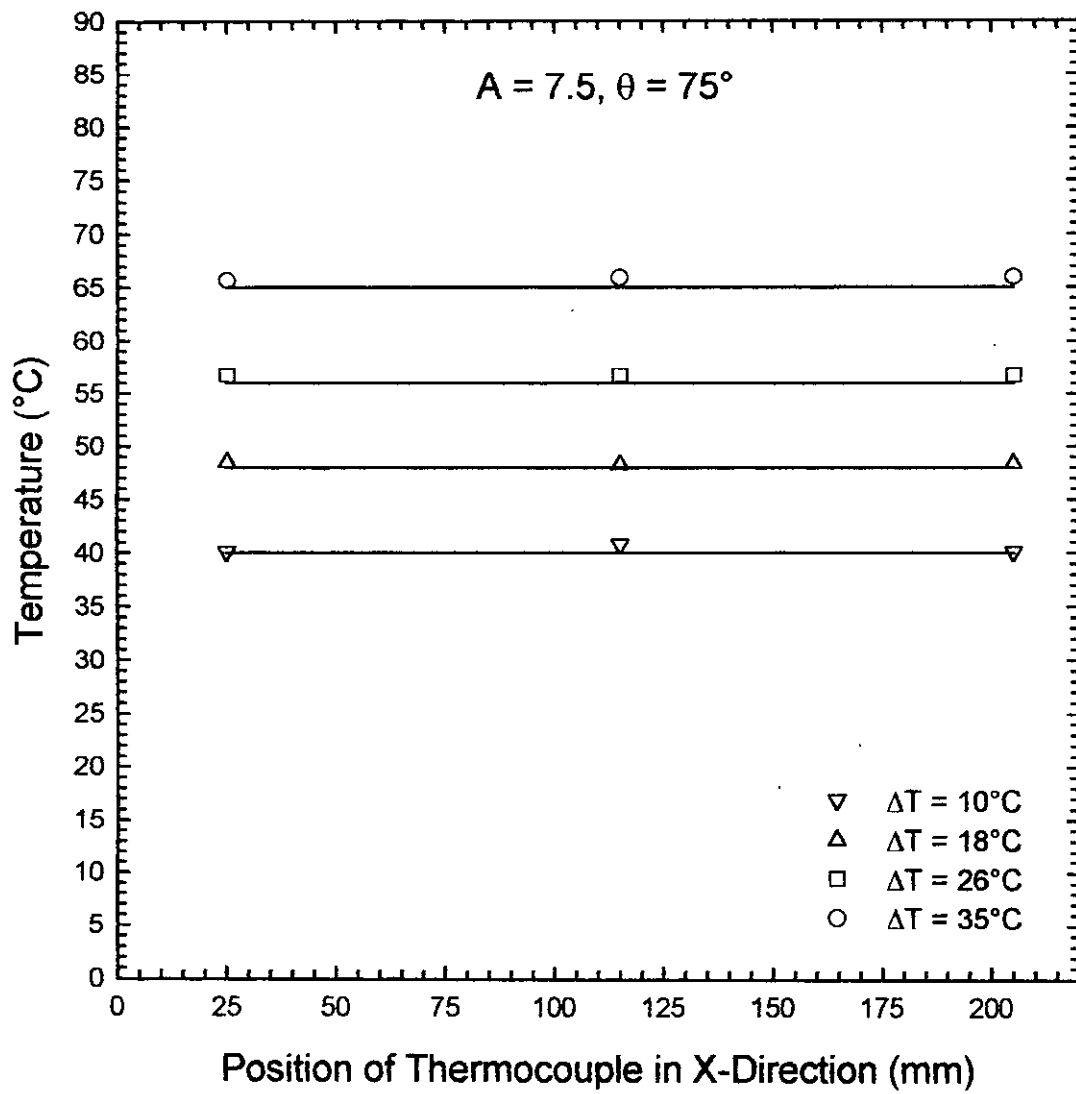


Fig. 6.4: Temperature distribution over the hot corrugated plate for $A = 7.5$ at $\theta = 75^\circ$.

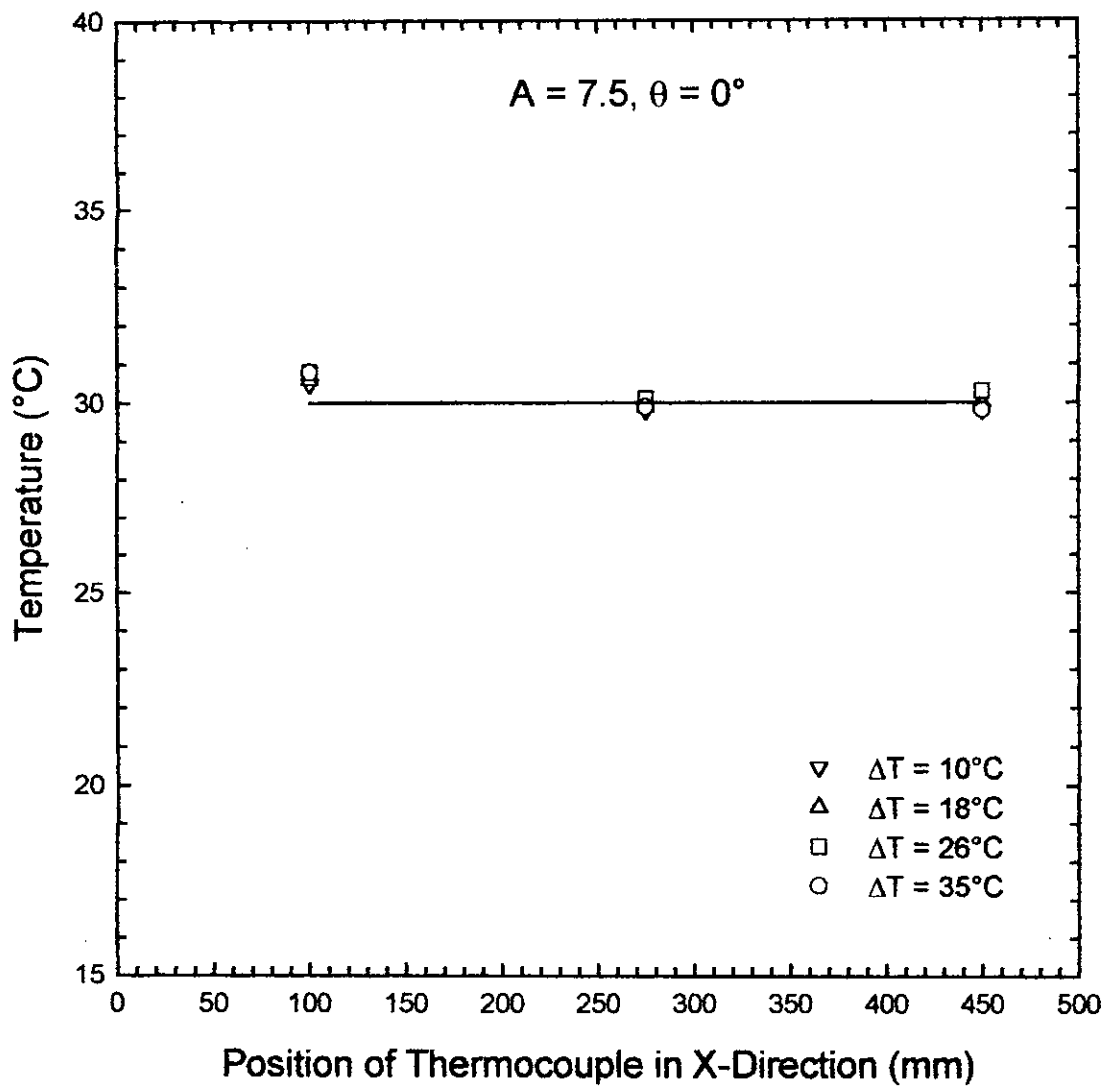


Fig. 6.5: Temperature distribution over the cold flat plate for $A = 7.5$ at $\theta = 0^\circ$.

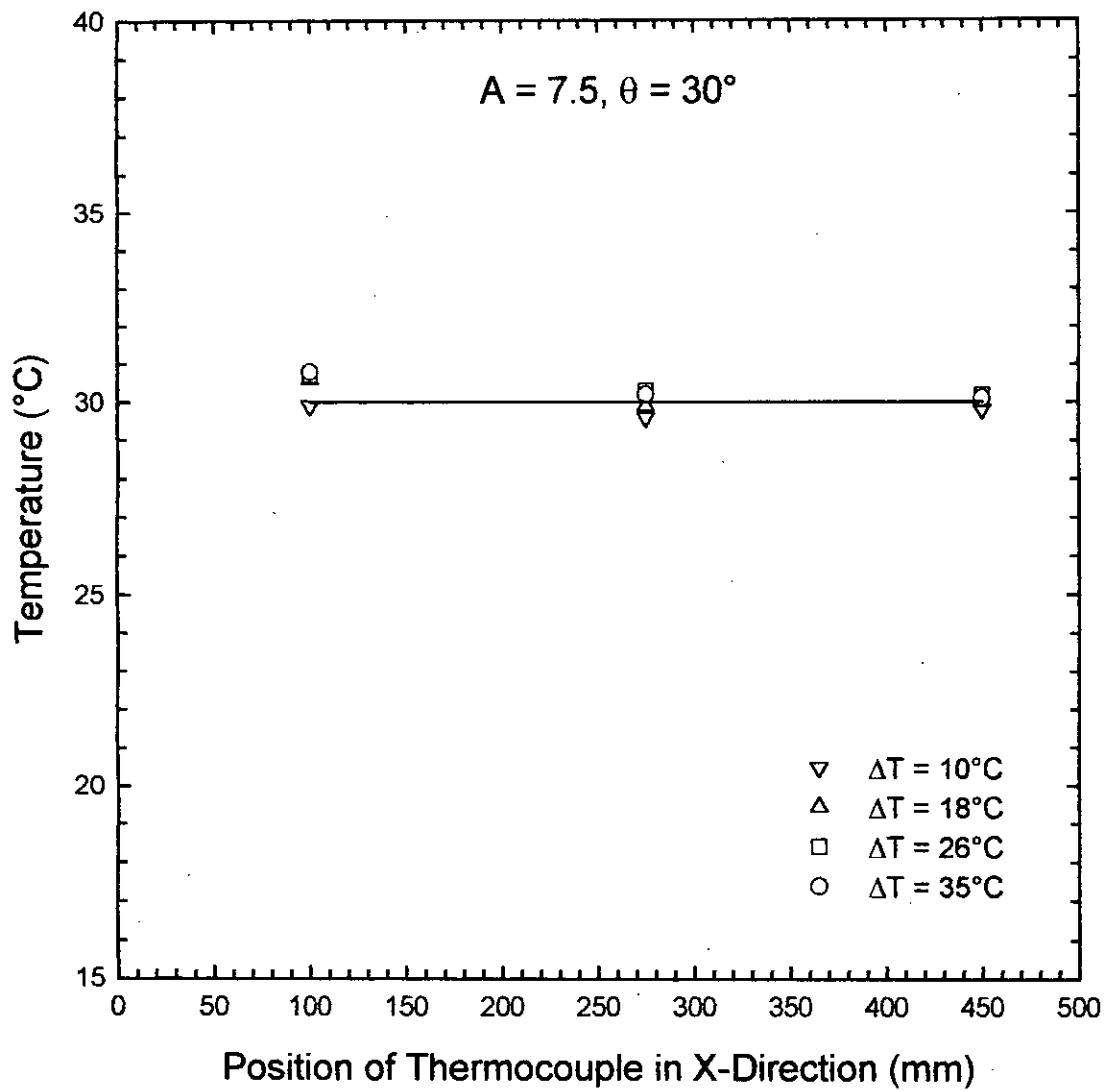


Fig. 6.6: Temperature distribution over the cold flat plate for $A = 7.5$ at $\theta = 30^\circ$.

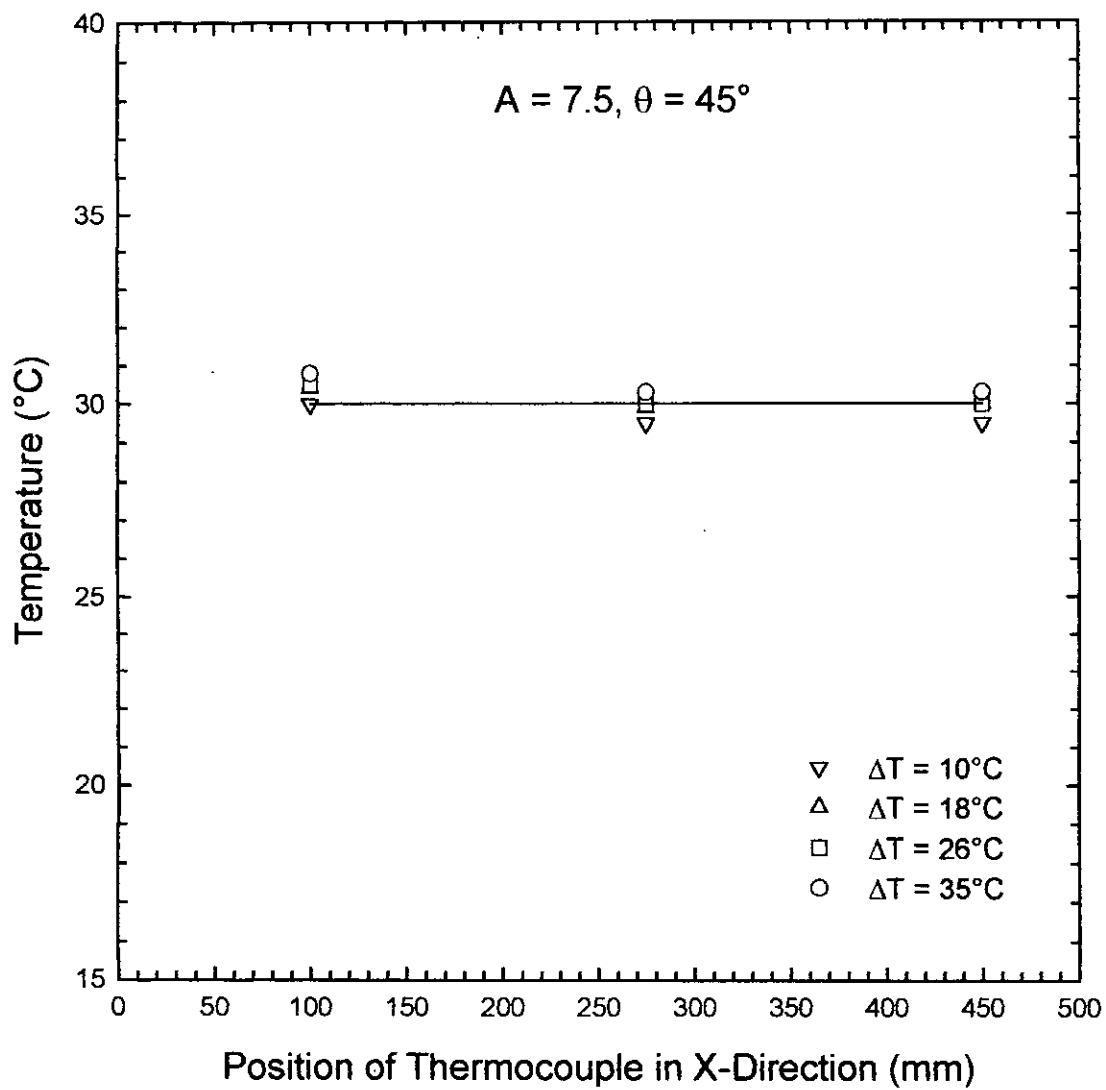


Fig. 6.7: Temperature distribution over the cold flat plate for $A = 7.5$ at $\theta = 45^\circ$.

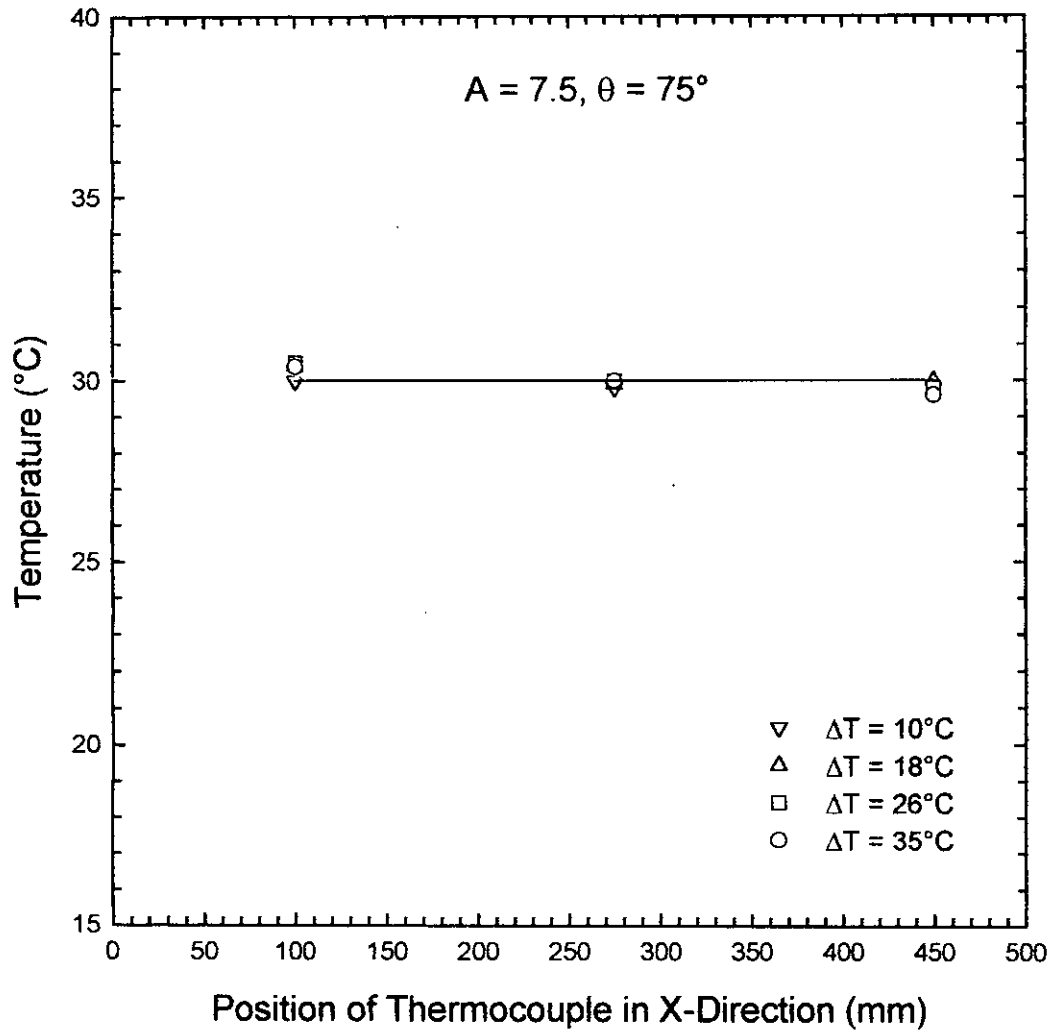


Fig. 6.8: Temperature distribution over the cold flat plate for $A = 7.5$ at $\theta = 75^\circ$.

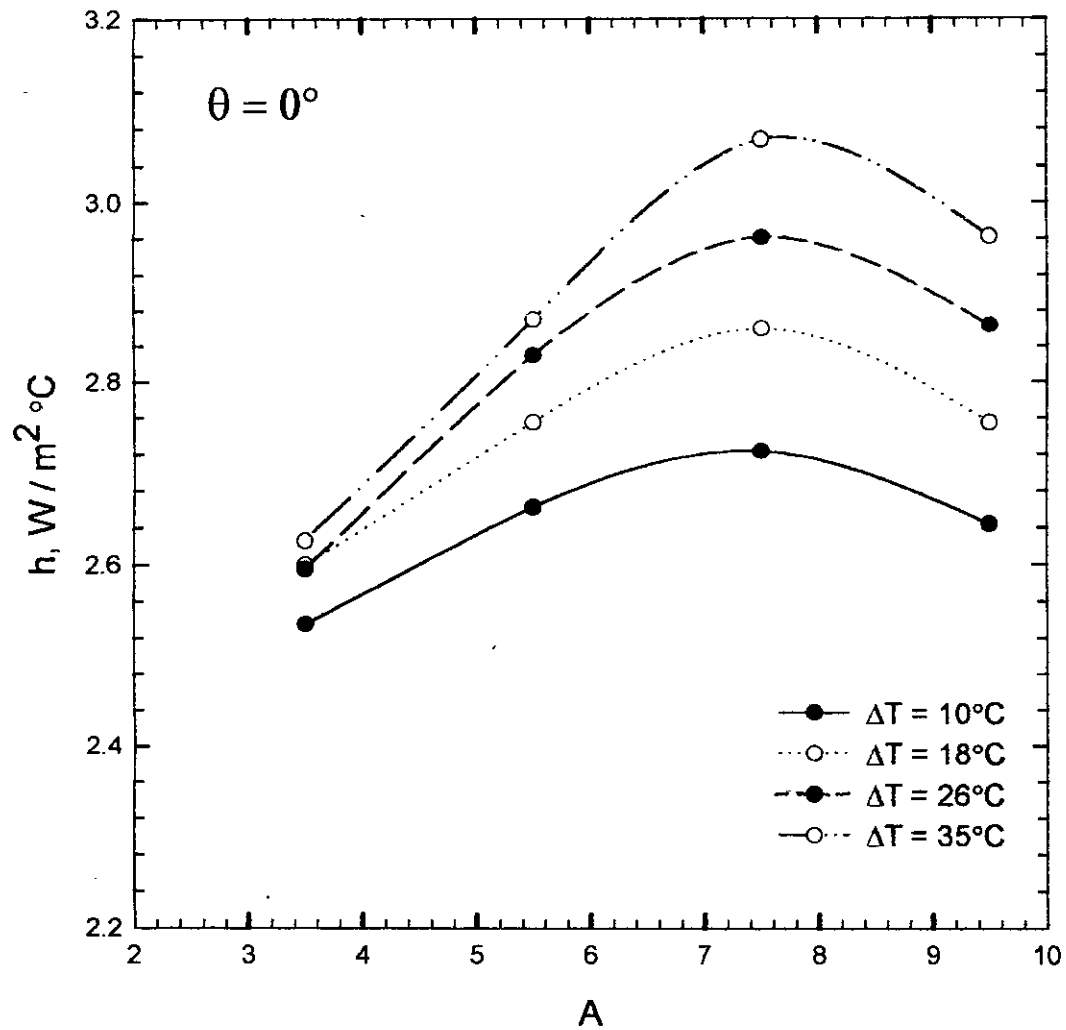


Fig. 6.9: Effect of aspect ratio, A on average heat transfer coefficient for $\theta = 0^\circ$.

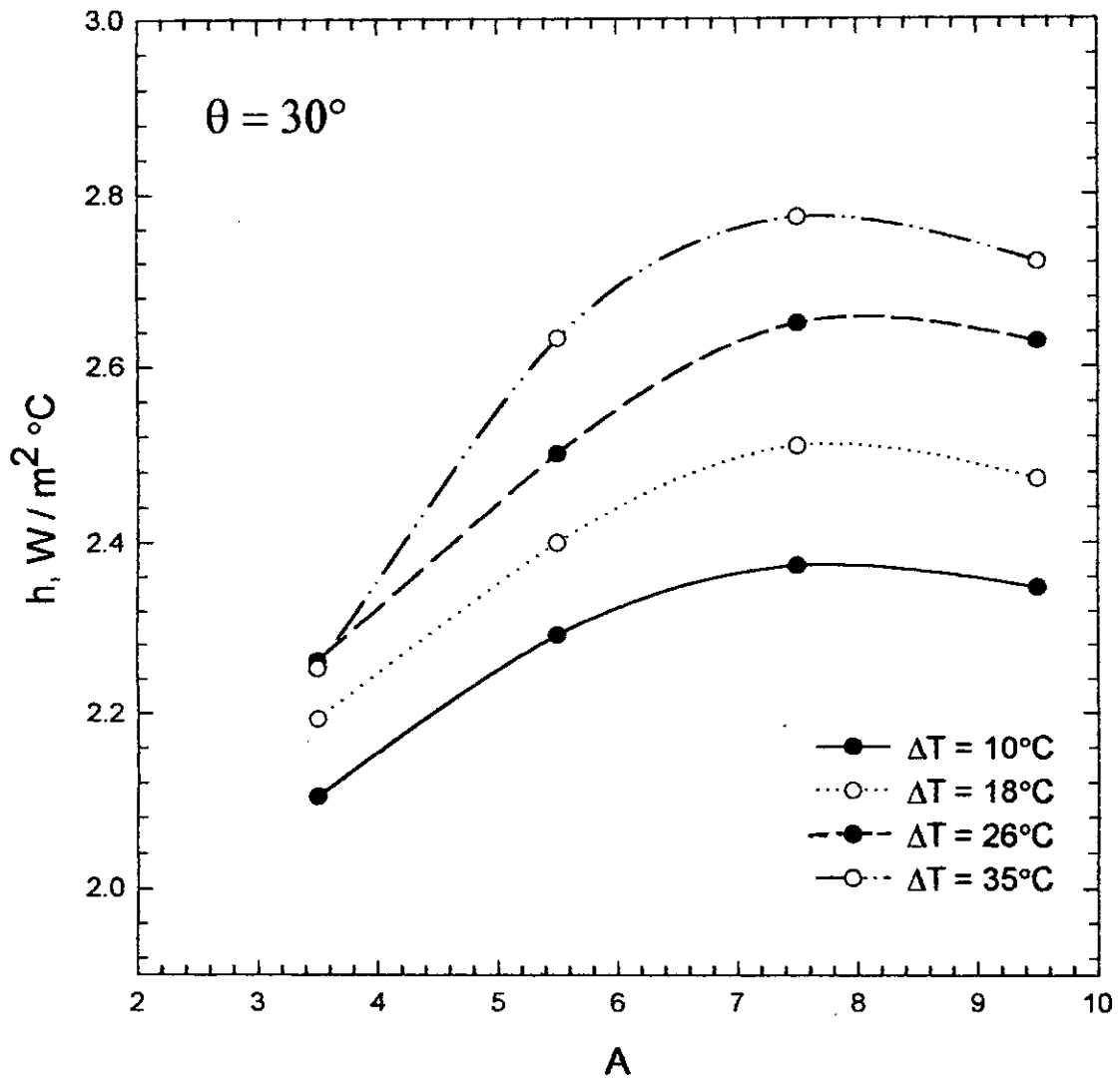


Fig. 6.10: Effect of aspect ratio, A on average heat transfer coefficient for $\theta = 30^\circ$.

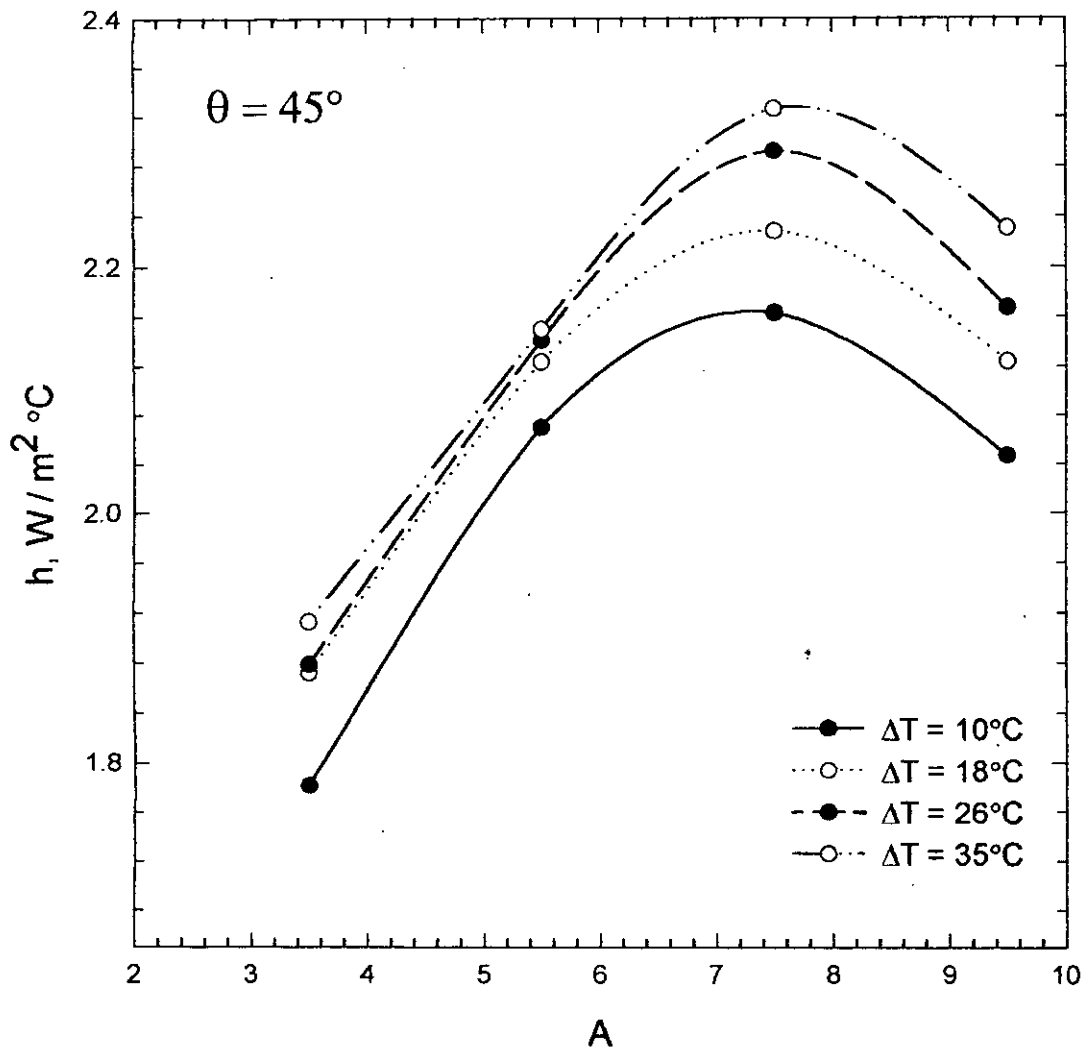


Fig. 6.11: Effect of aspect ratio, A on average heat transfer coefficient for $\theta = 45^\circ$.

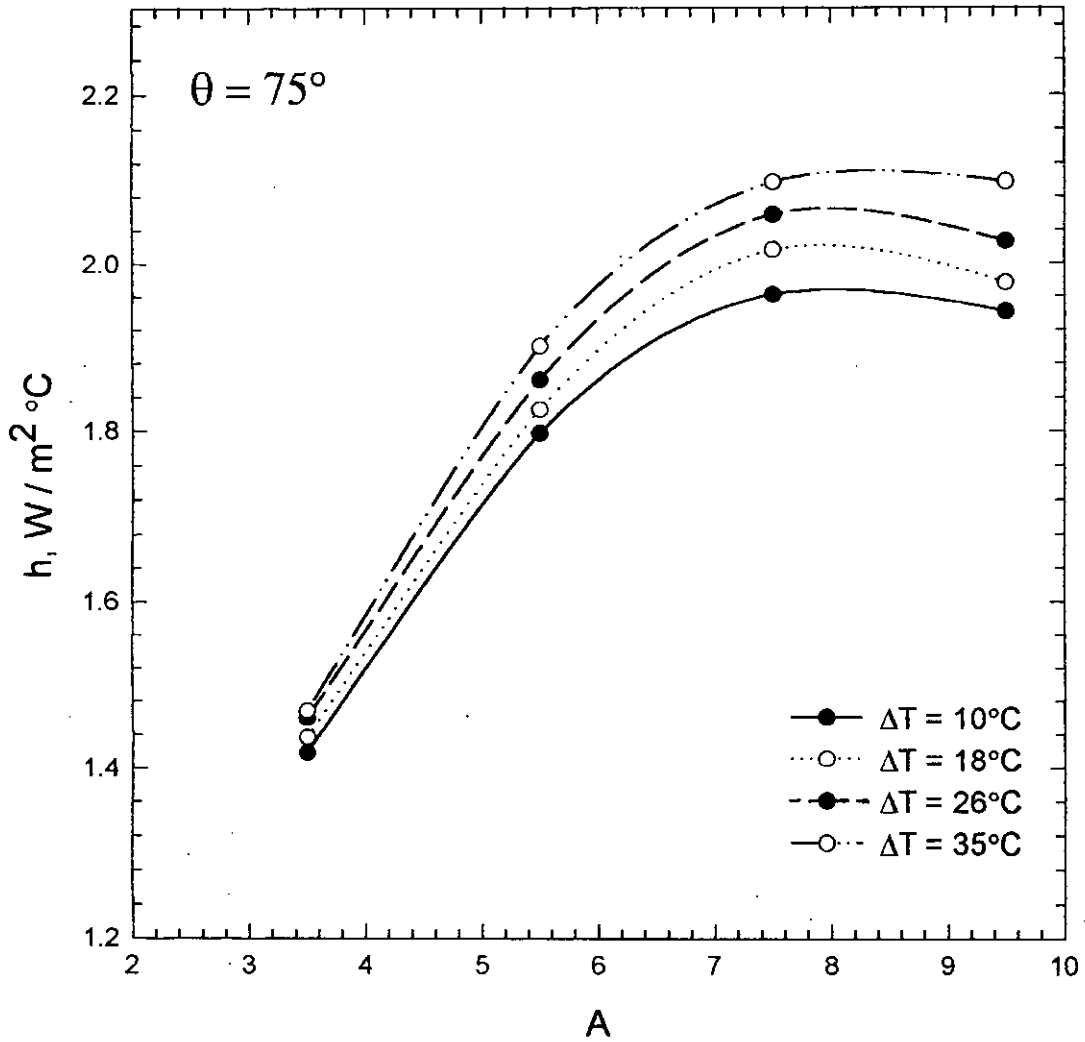


Fig. 6.12: Effect of aspect ratio, A on average heat transfer coefficient for $\theta = 75^\circ$.

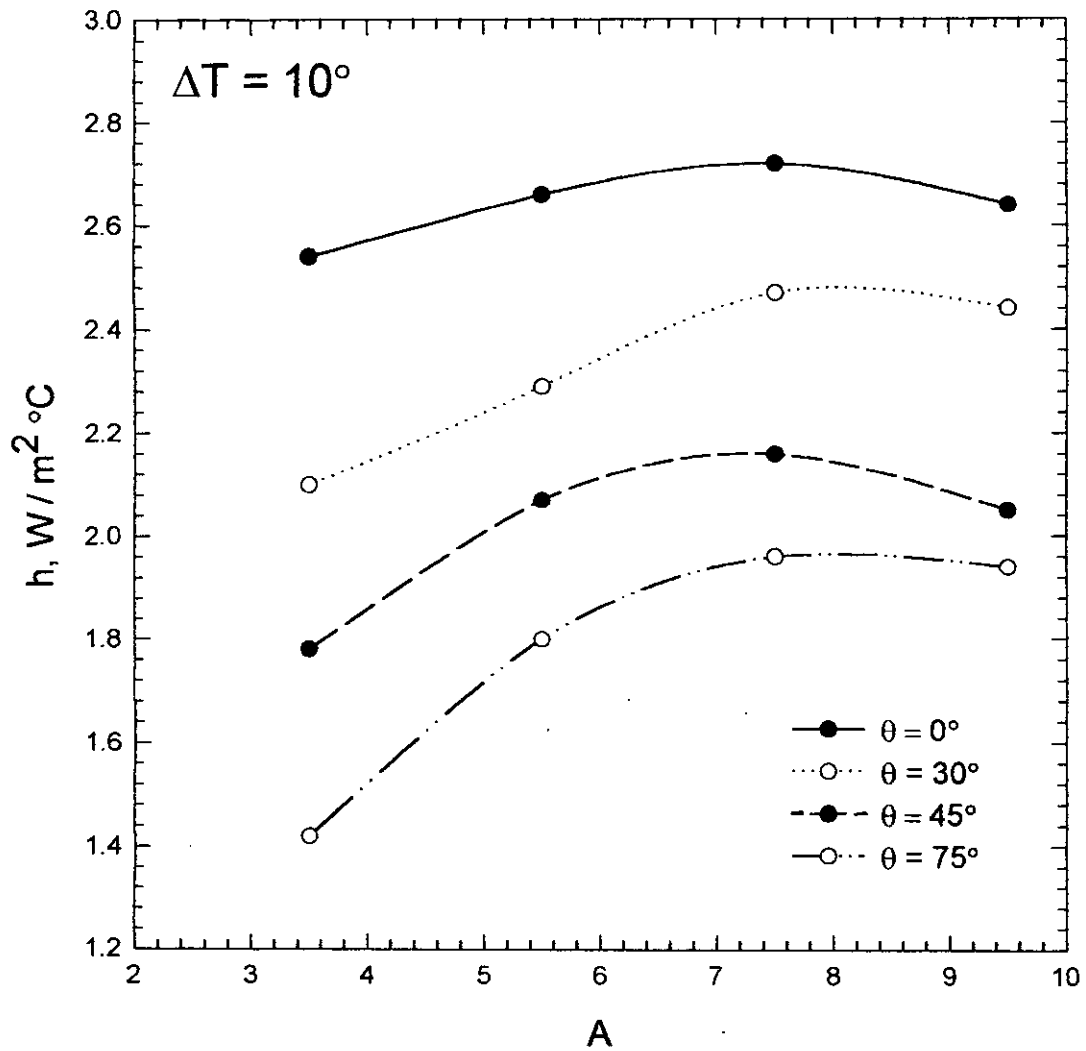


Fig. 6.13: Effect of aspect ratio, A on average heat transfer coefficient for different angles of inclination, θ for $\Delta T = 10^\circ$.

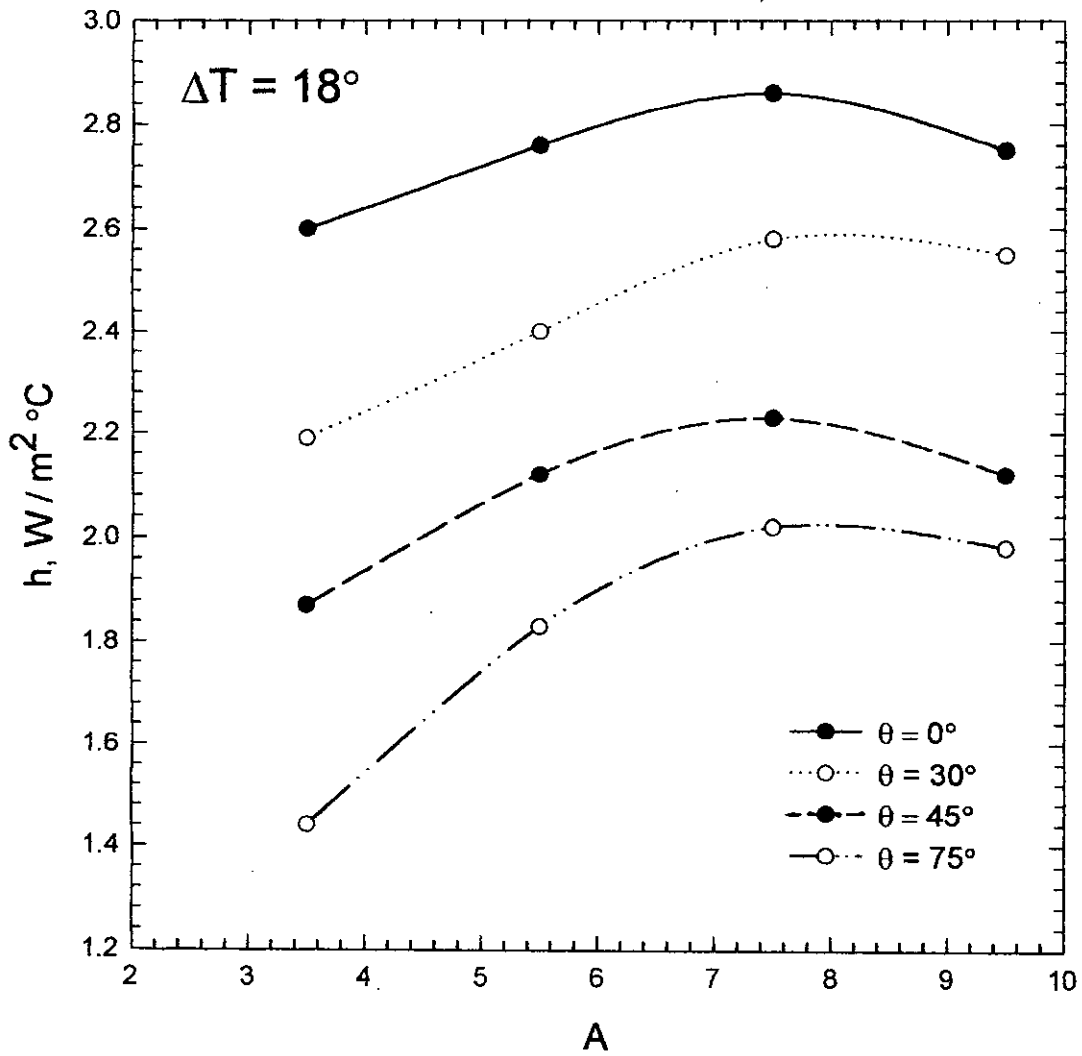


Fig. 6.14: Effect of aspect ratio, A on average heat transfer coefficient for different angles of inclination, θ for $\Delta T = 18^\circ$.

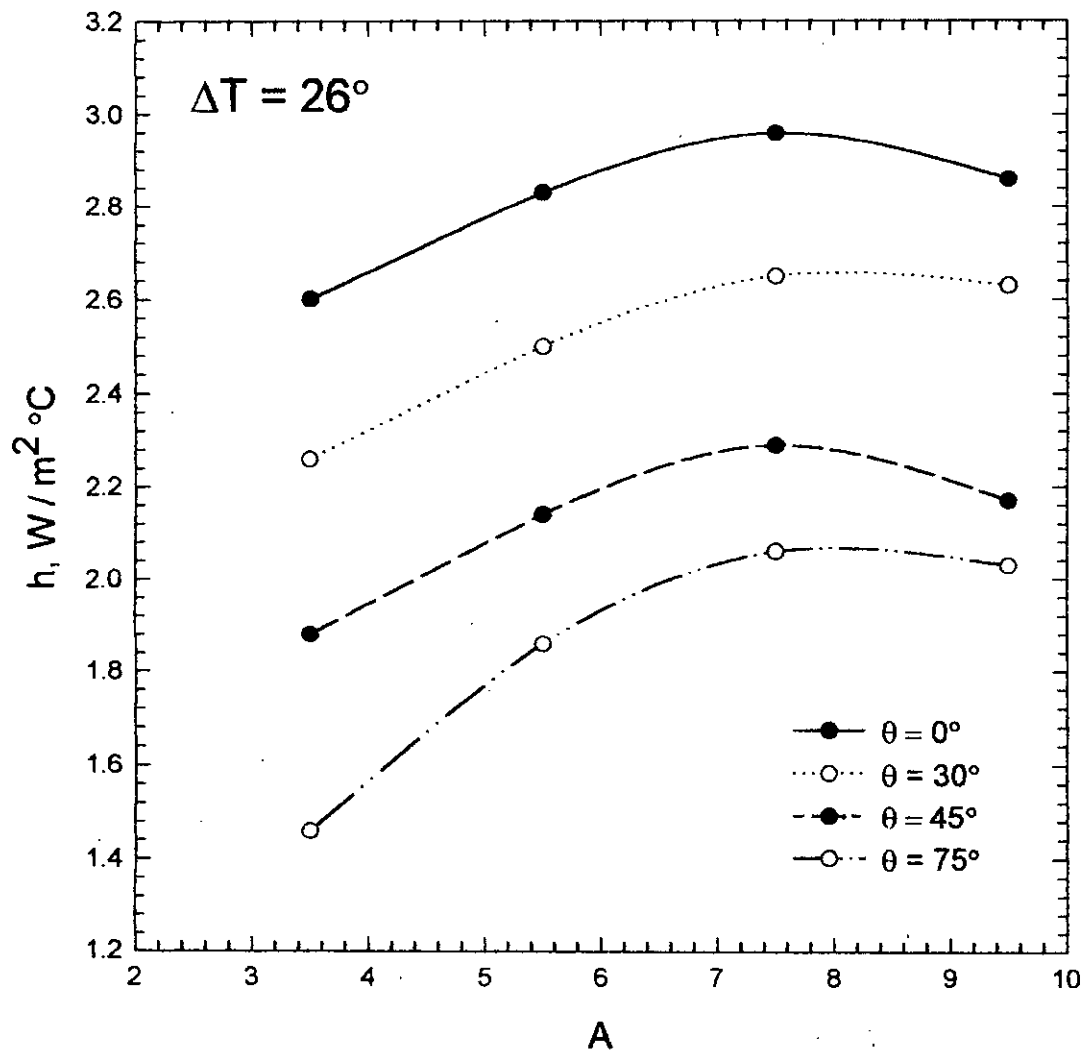


Fig. 6.15: Effect of aspect ratio, A on average heat transfer coefficient for different angles of inclination, θ for $\Delta T = 26^\circ$.

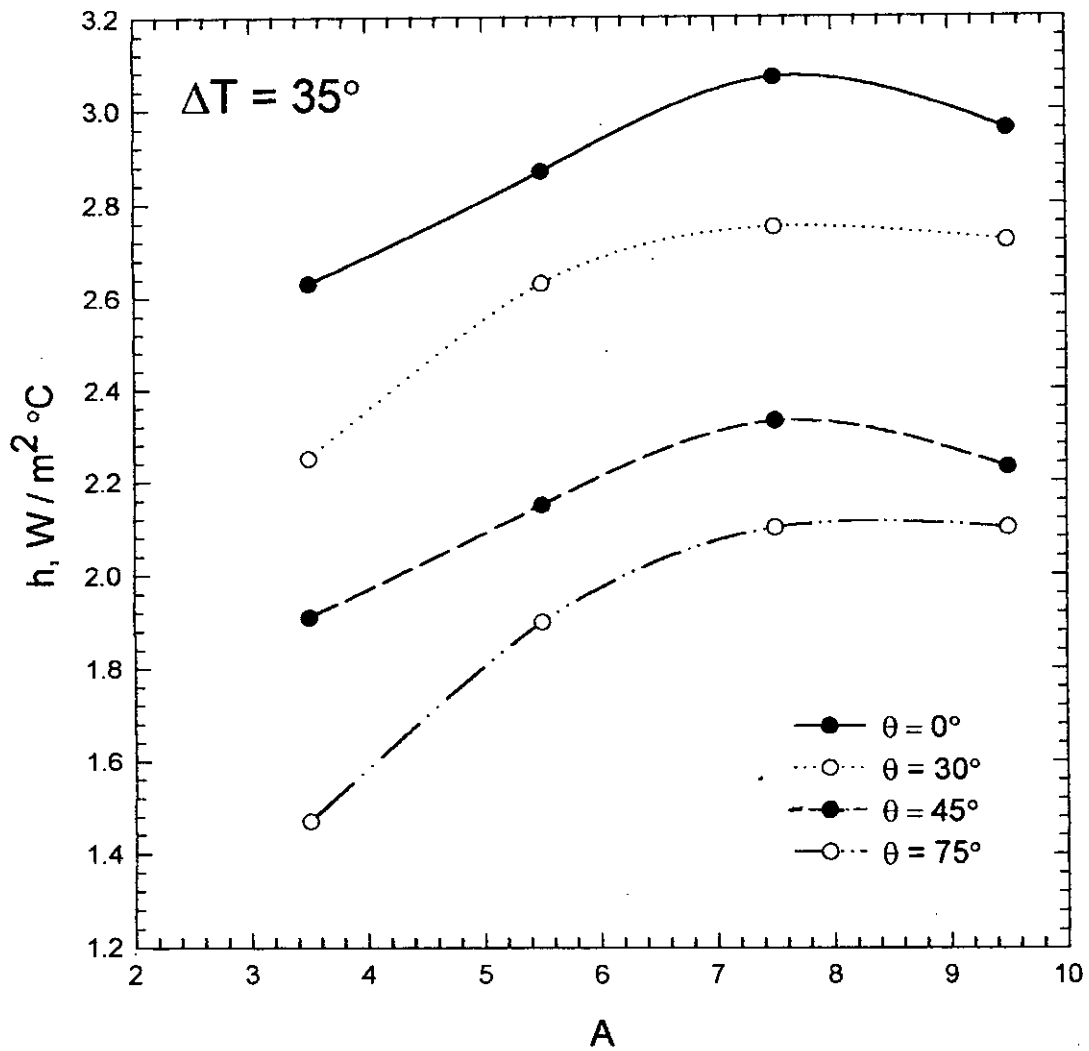


Fig. 6.16: Effect of aspect ratio, A on average heat transfer coefficient for different angles of inclination, θ for $\Delta T = 35^\circ$.

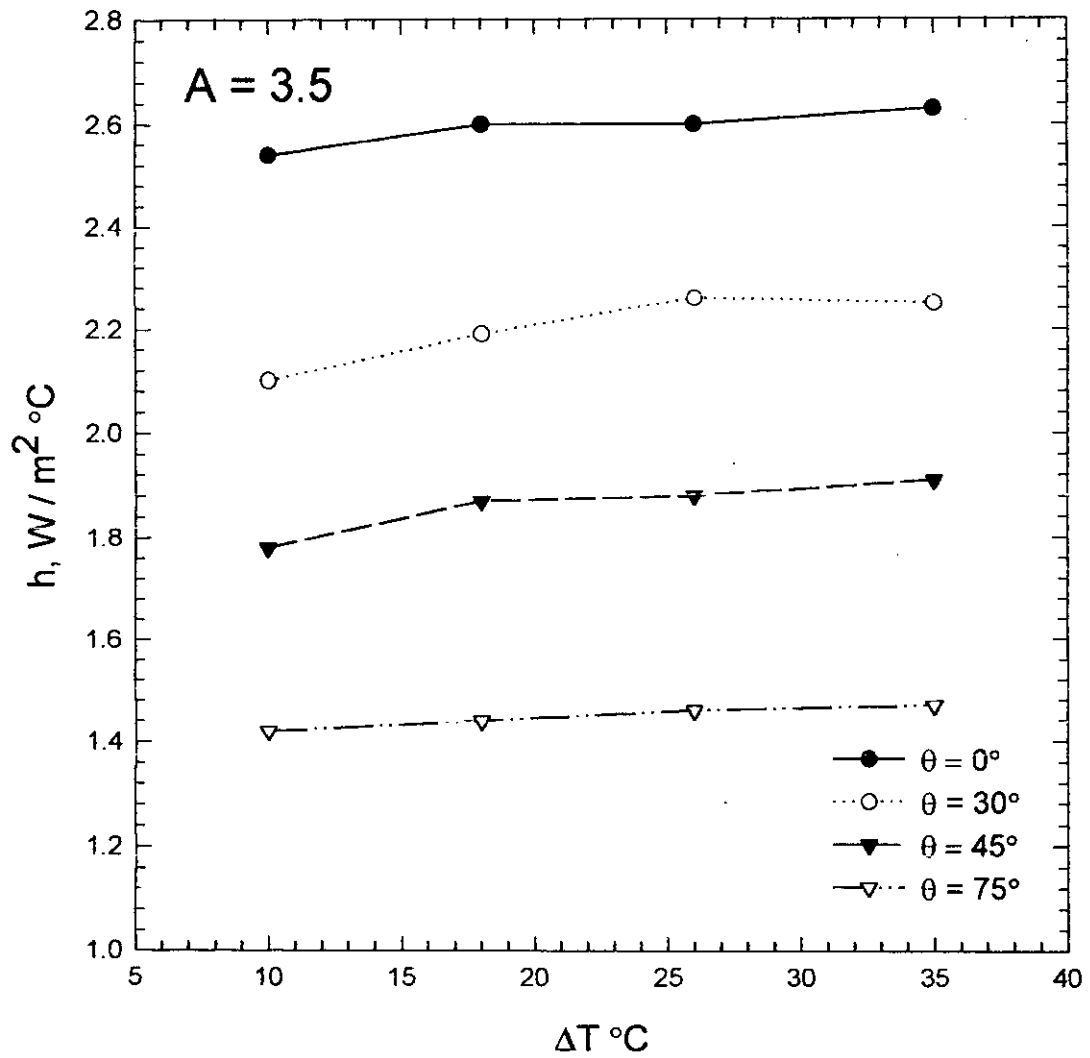


Fig. 6.17: Effect of temperature potential, ΔT on average heat transfer coefficient for $A = 3.5$.

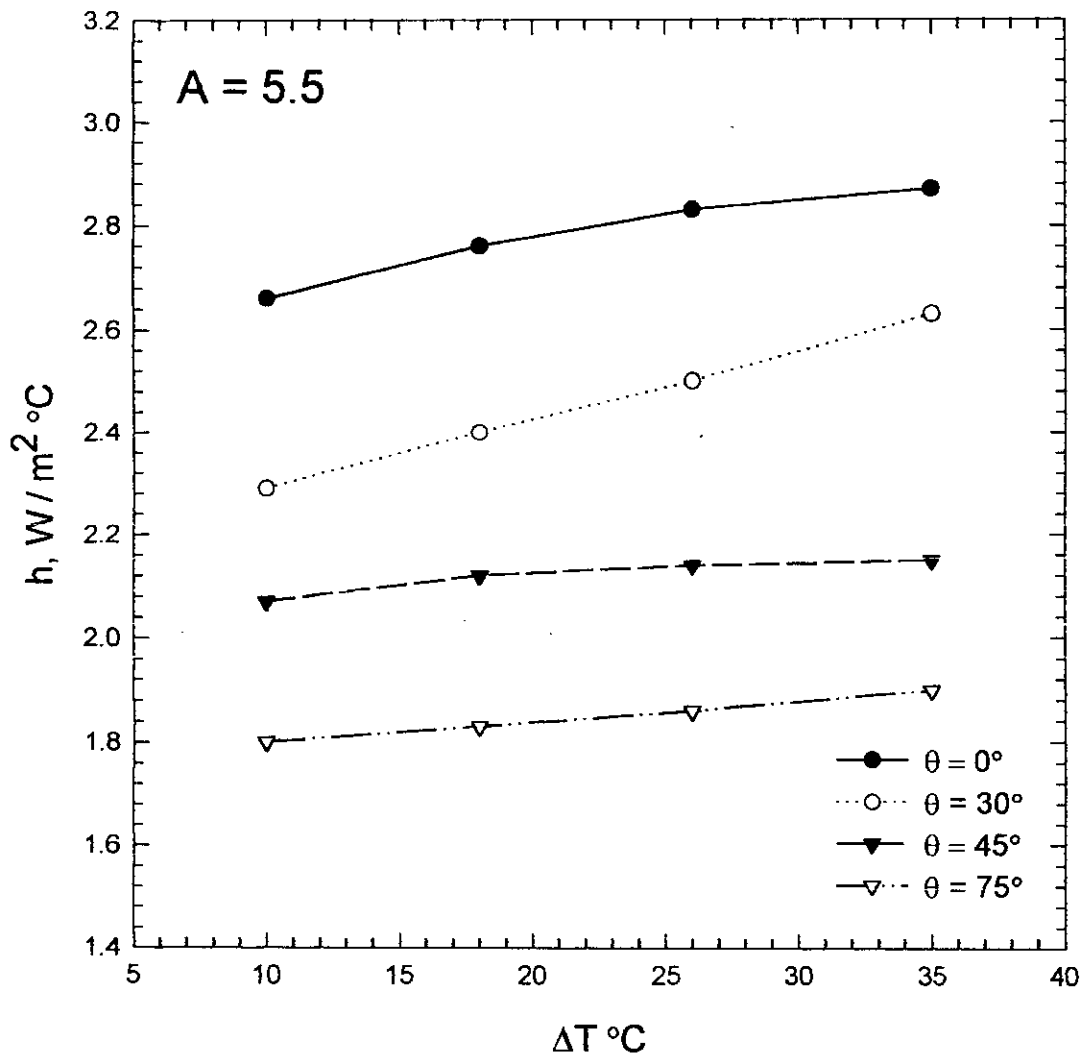


Fig. 6.18: Effect of temperature potential, ΔT on average heat transfer coefficient for $A = 5.5$.

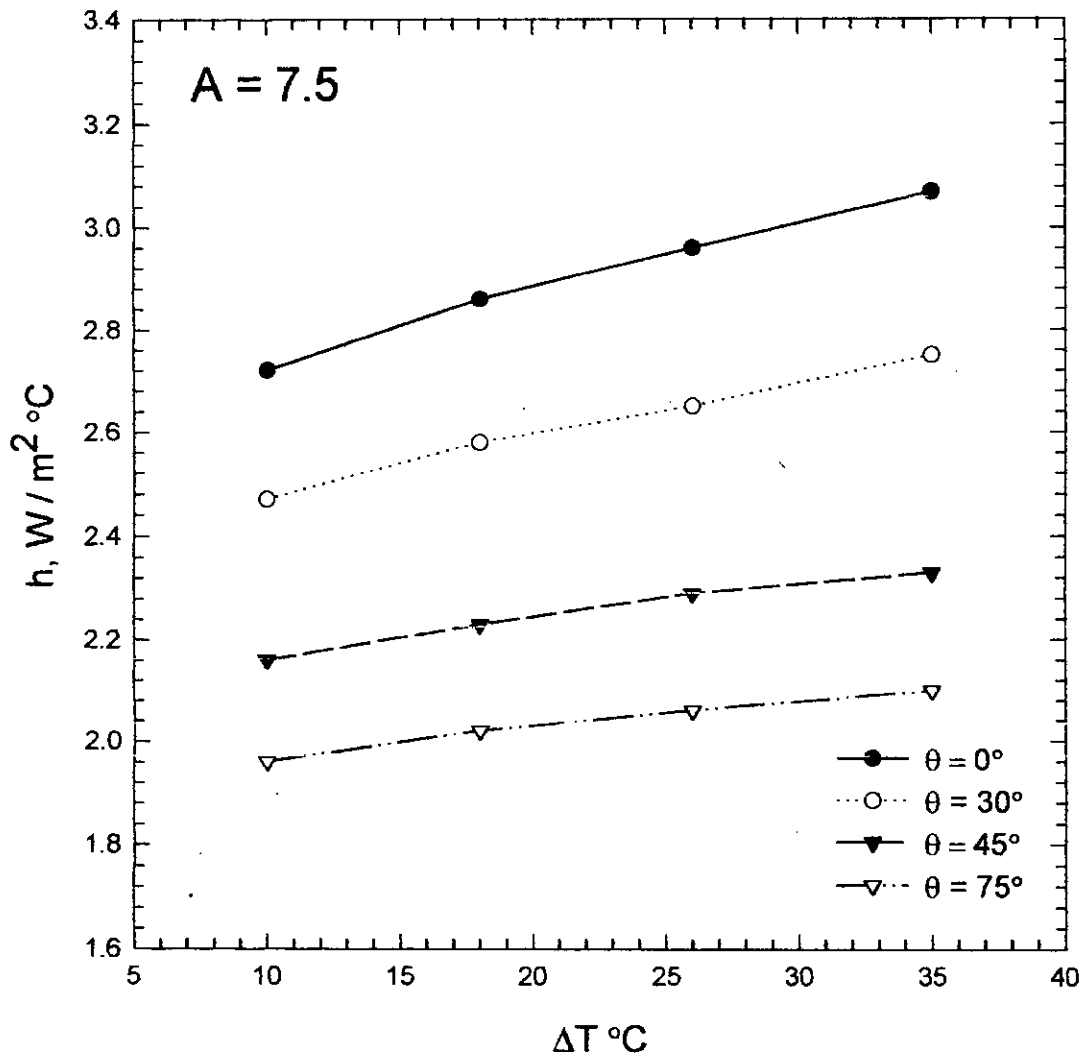


Fig. 6.19: Effect of temperature potential, ΔT on average heat transfer coefficient for $A = 7.5$.

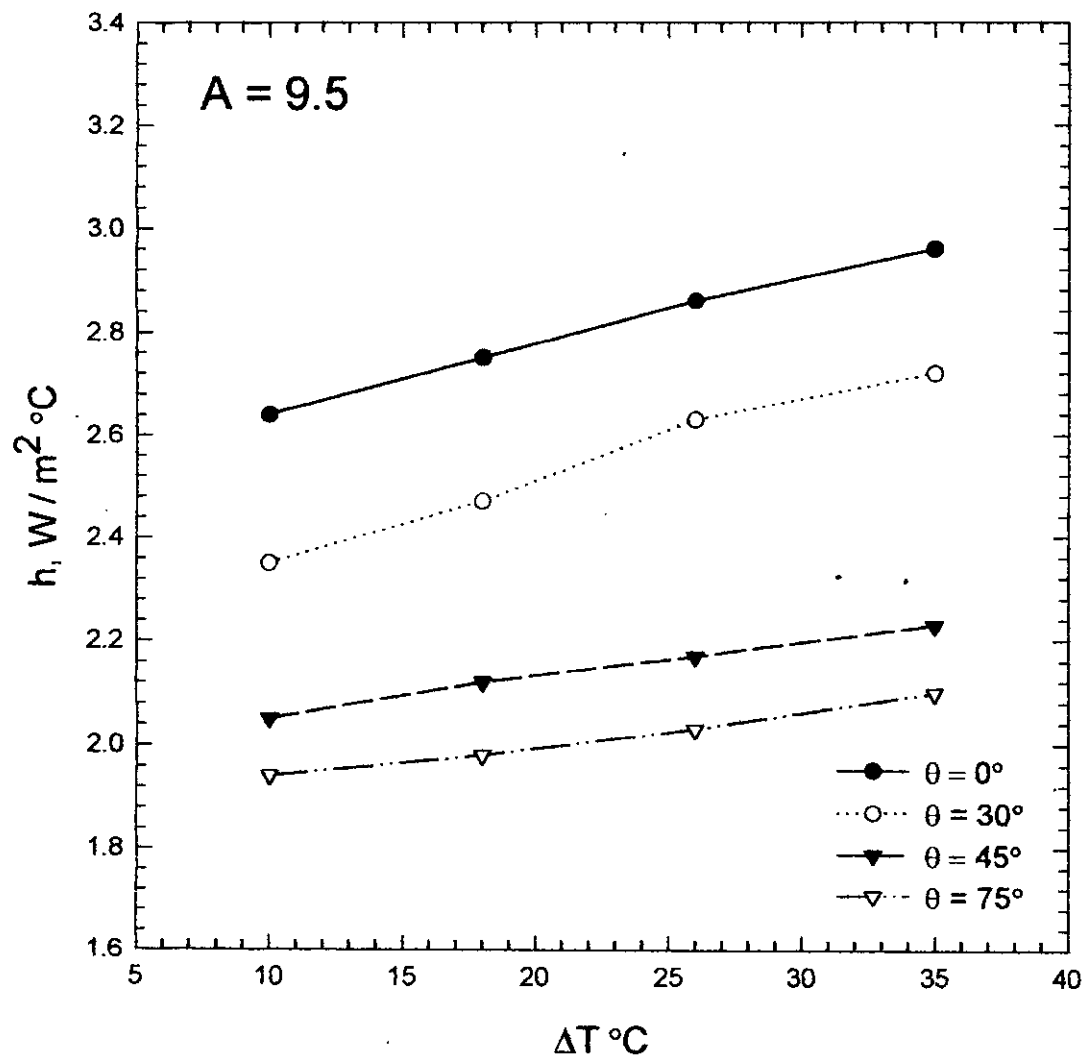


Fig. 6.20: Effect of temperature potential, ΔT on average heat transfer coefficient for $A = 9.5$.

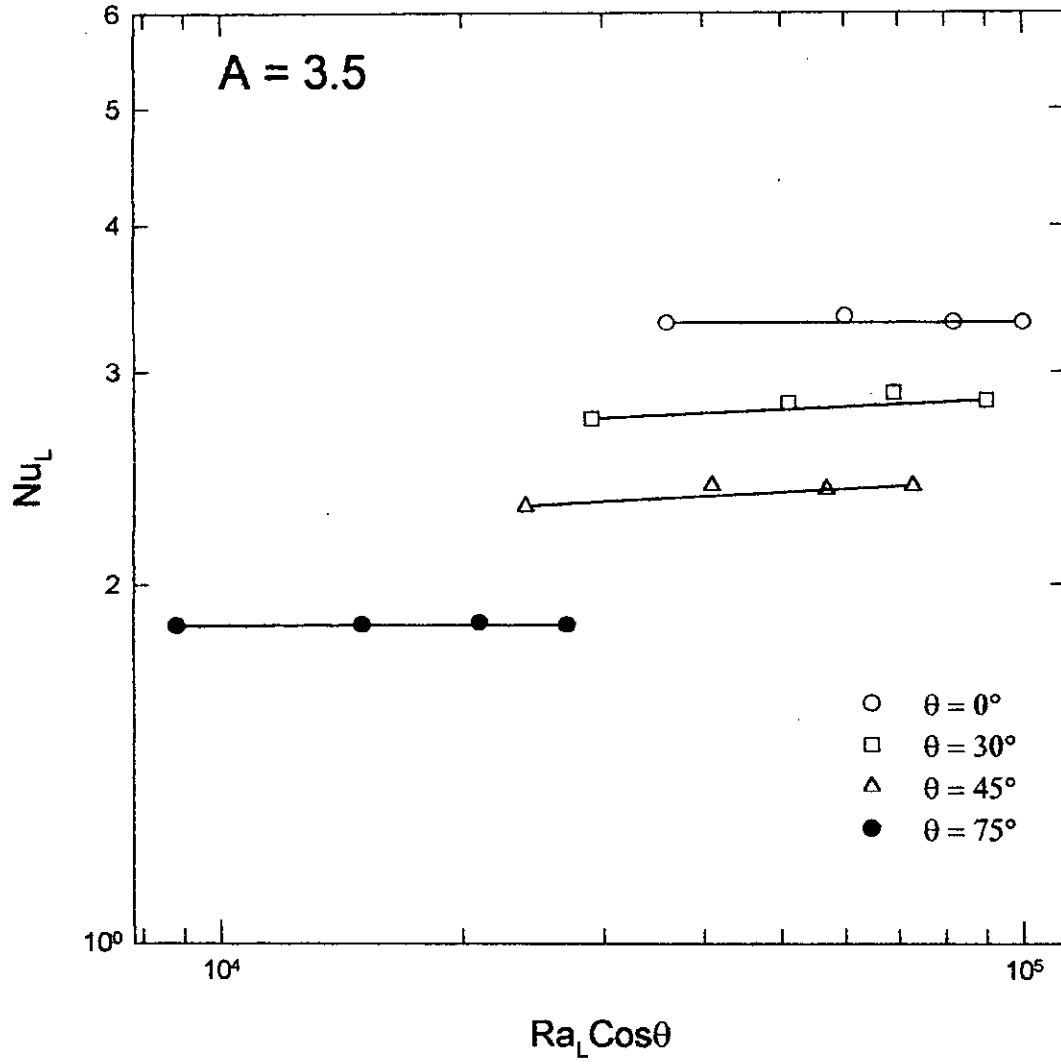


Fig. 6.21: Effect of average Nusselt number on $Ra_L \cos \theta$ at all inclinations for $A = 3.5$.

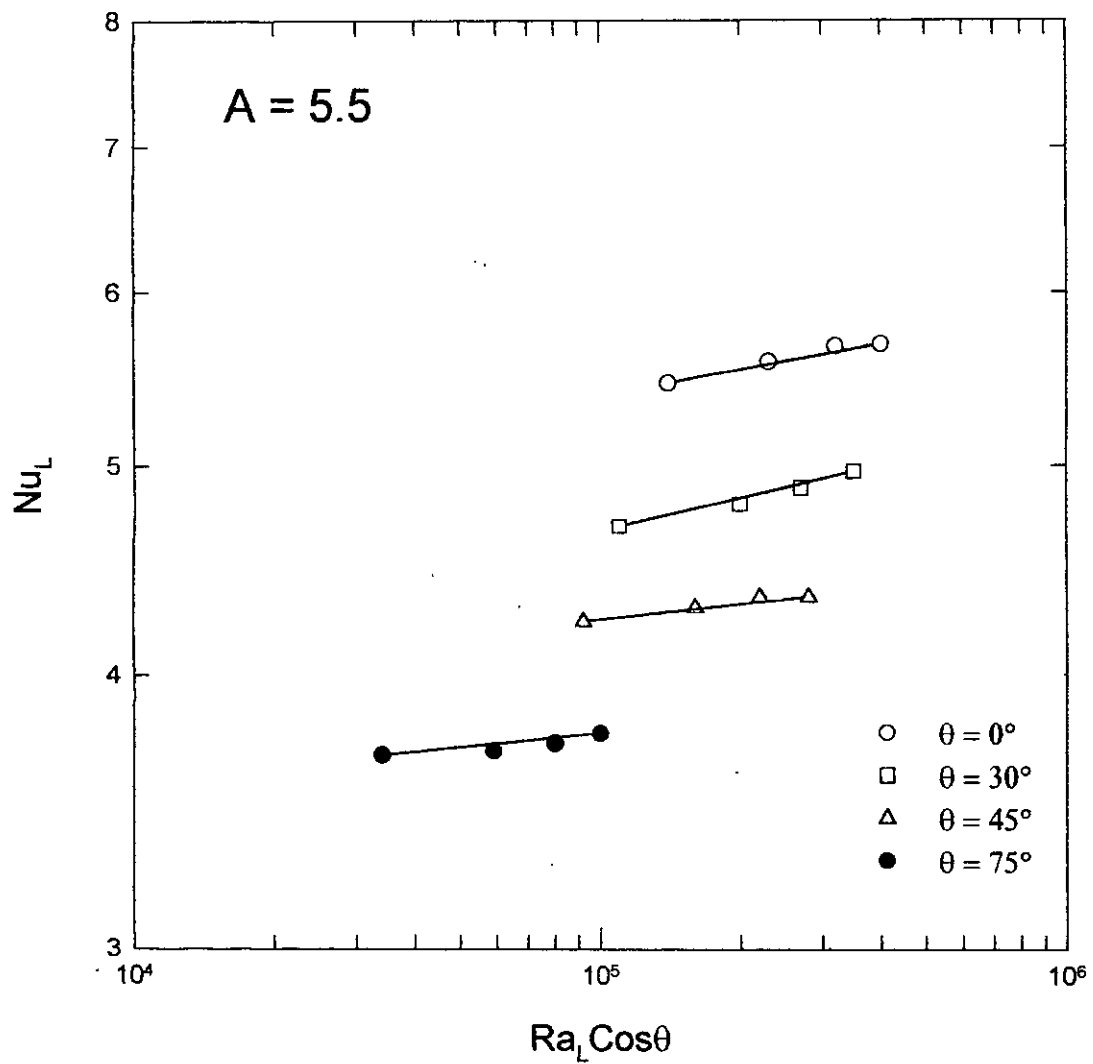


Fig. 6.22: Effect of average Nusselt number on $Ra_L \cos \theta$ at all inclinations for $A = 5.5$.

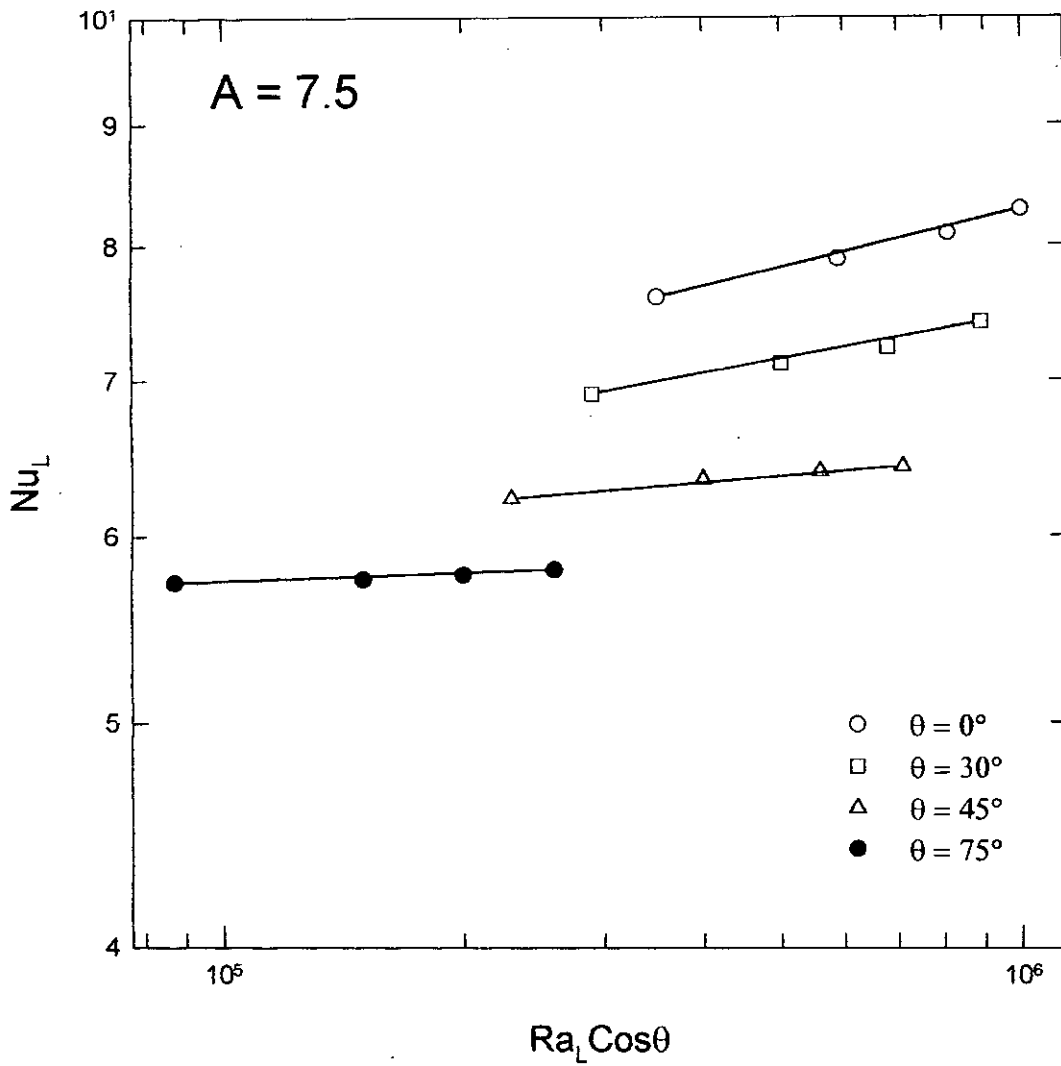


Fig. 6.23: Effect of average Nusselt number on $Ra_L \cos\theta$ at all inclinations for $A = 7.5$.

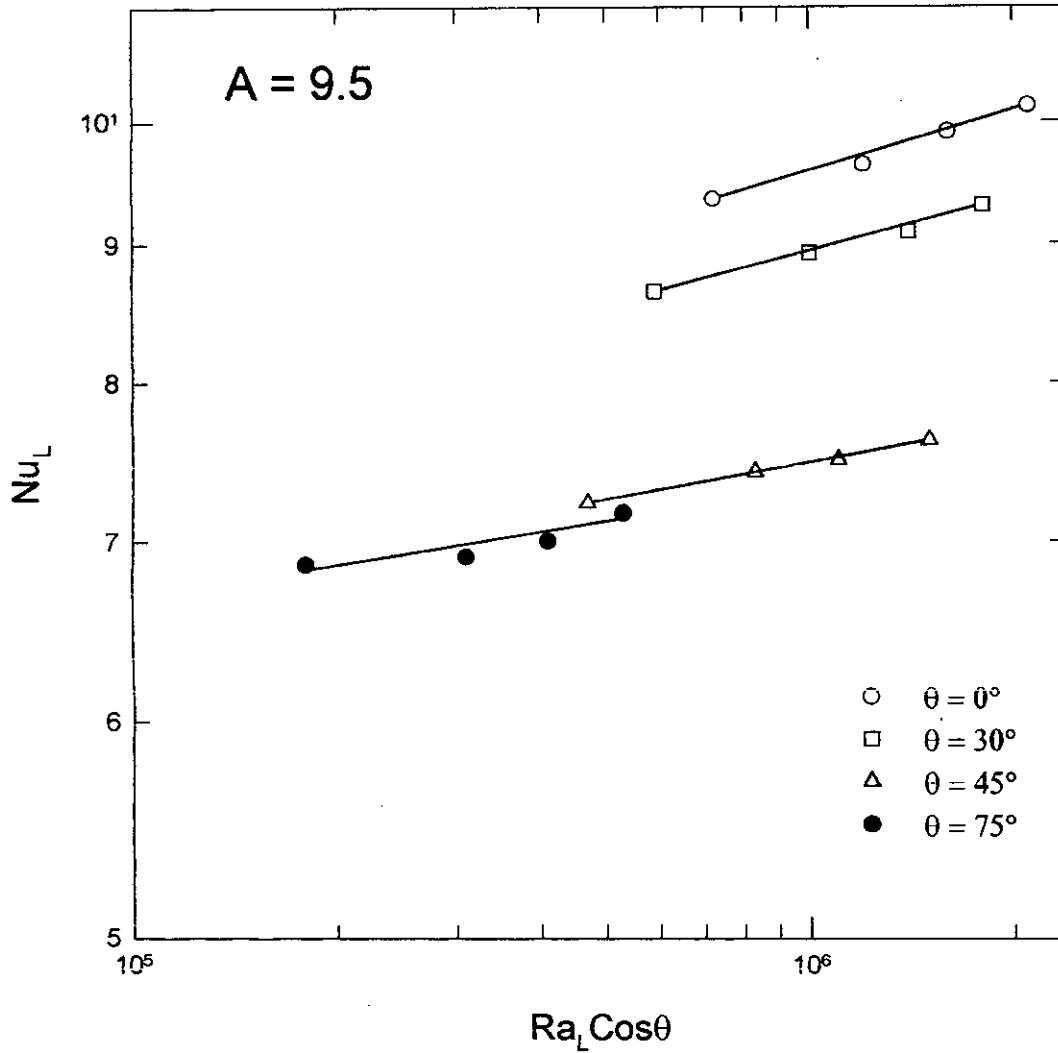


Fig. 6.24: Effect of average Nusselt number on $Ra_L \cos\theta$ at all inclinations for $A = 9.5$.

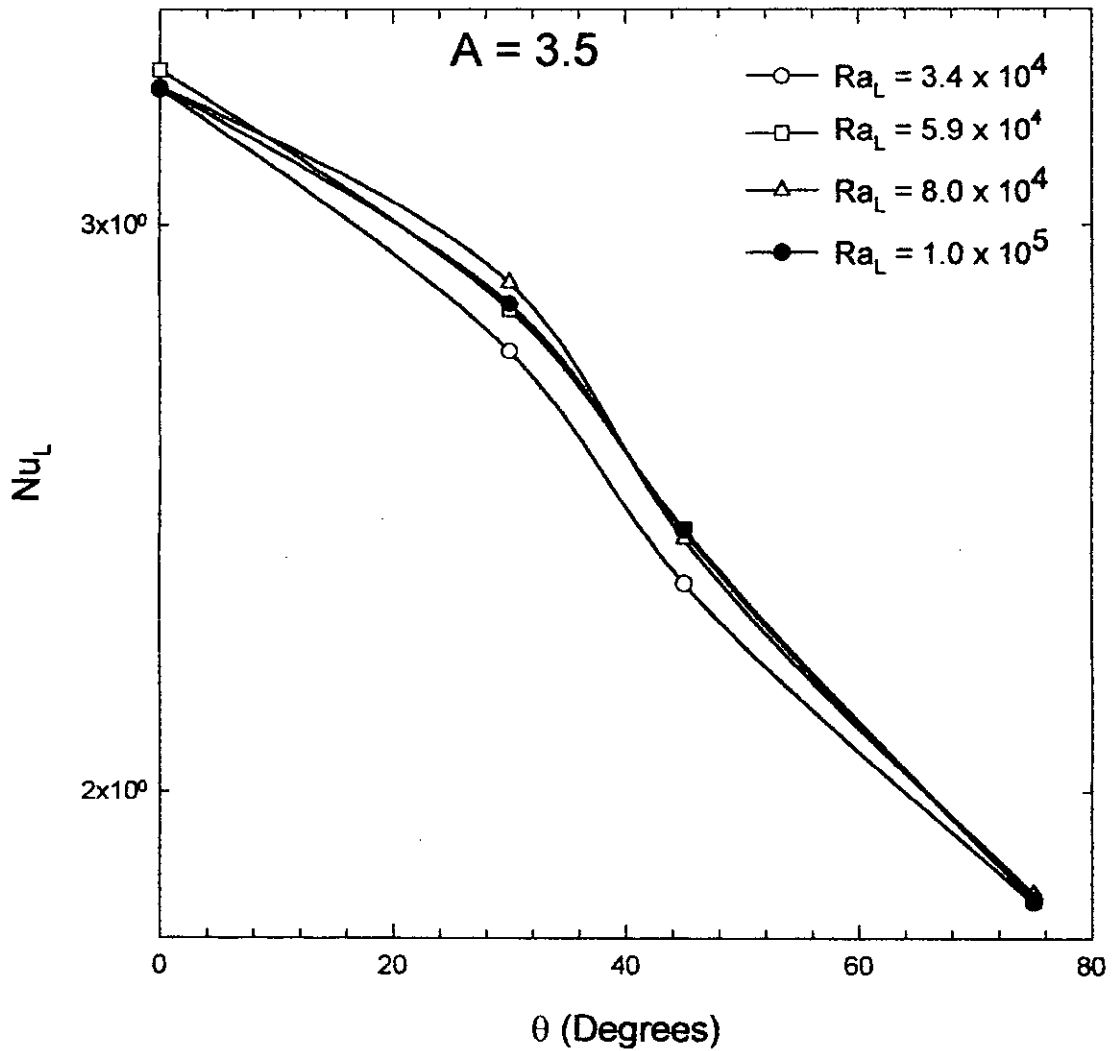


Fig. 6.25: Effect of angle of inclinations on average Nusselt number at various Ra_L for $A = 3.5$.

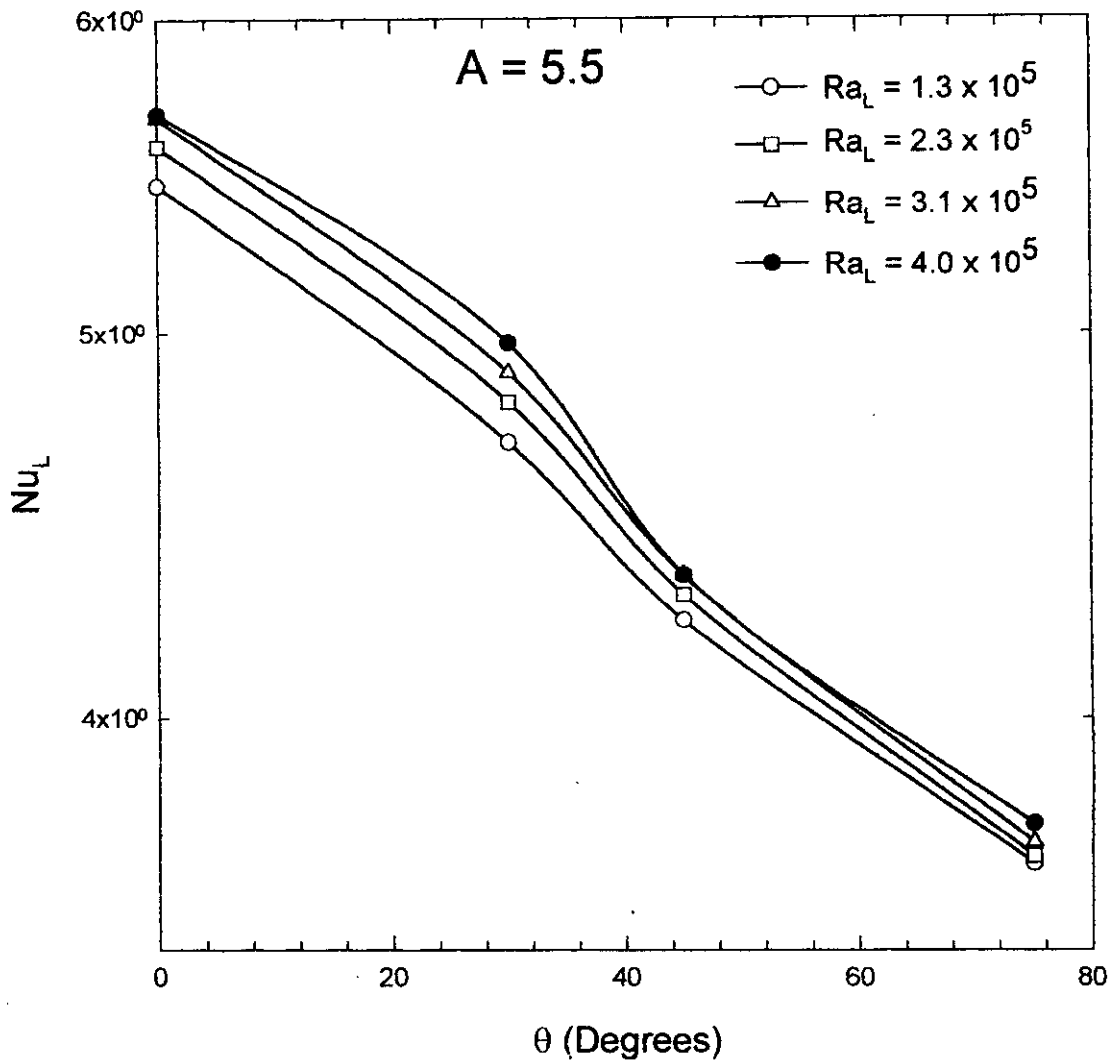


Fig. 6.26: Effect of angle of inclinations on average Nusselt number at various Ra_L for $A = 5.5$.

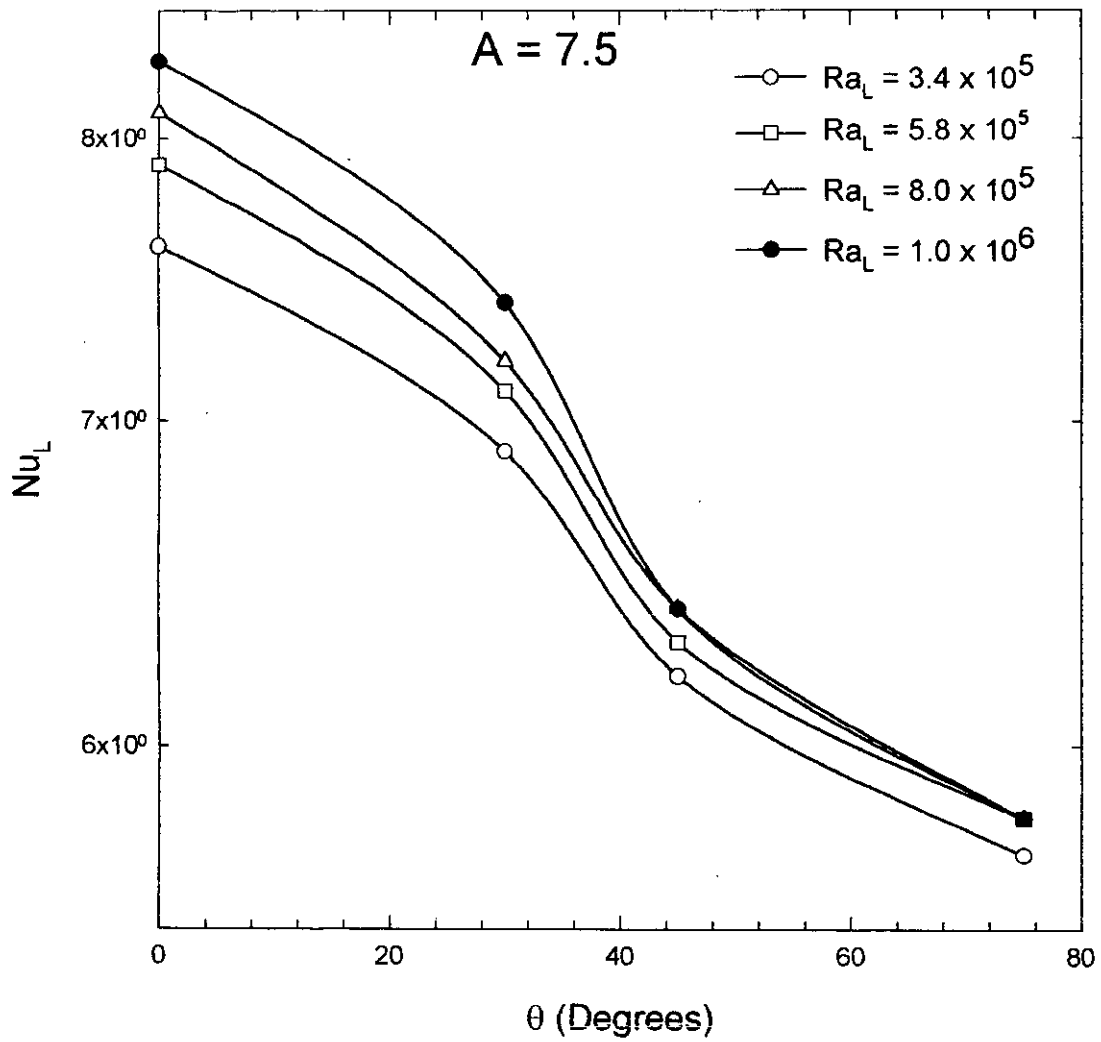


Fig. 6.27: Effect of angle of inclinations on average Nusselt number at various Ra_L for $A = 7.5$.

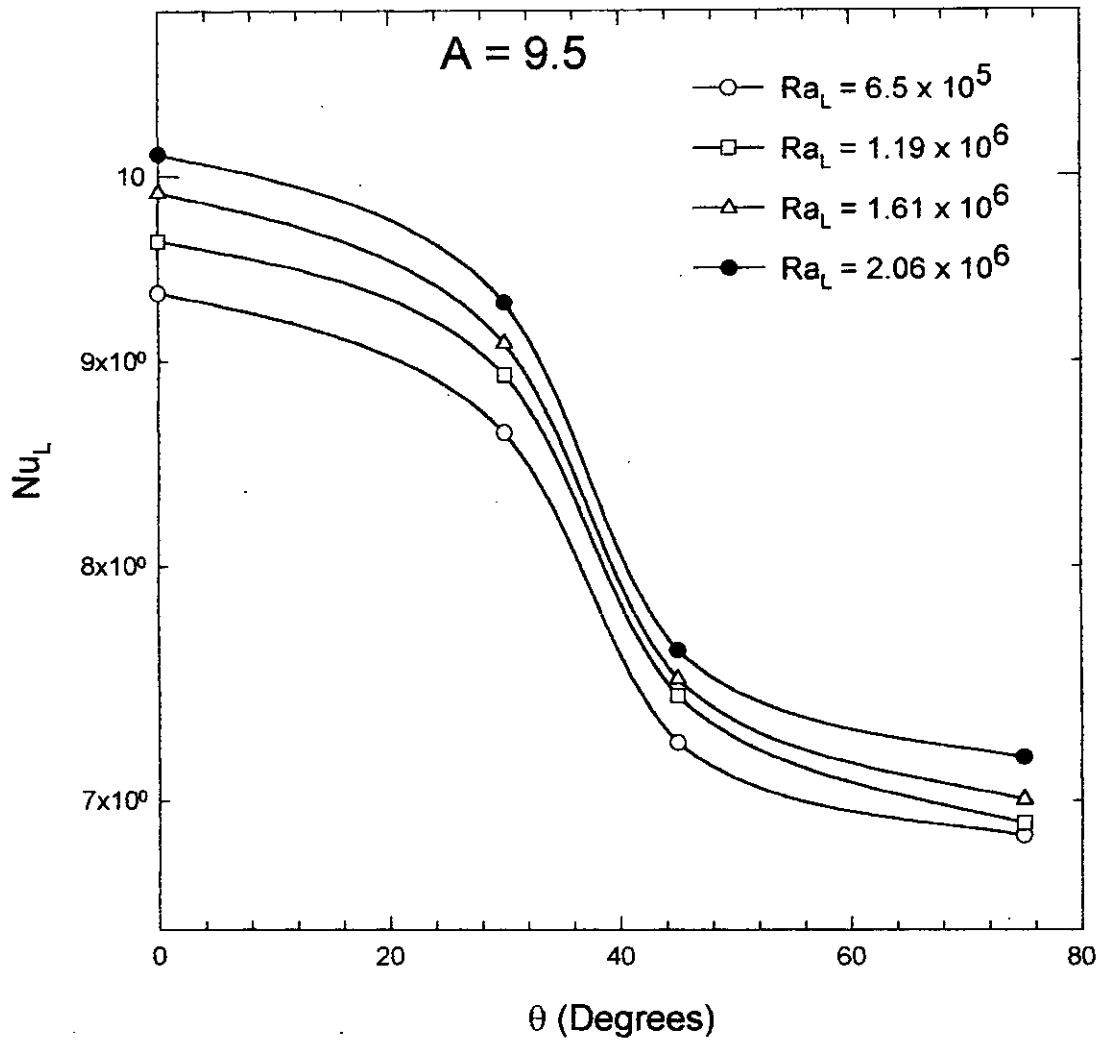


Fig. 6.28: Effect of angle of inclinations on average Nusselt number at various Ra_L for $A = 9.5$.

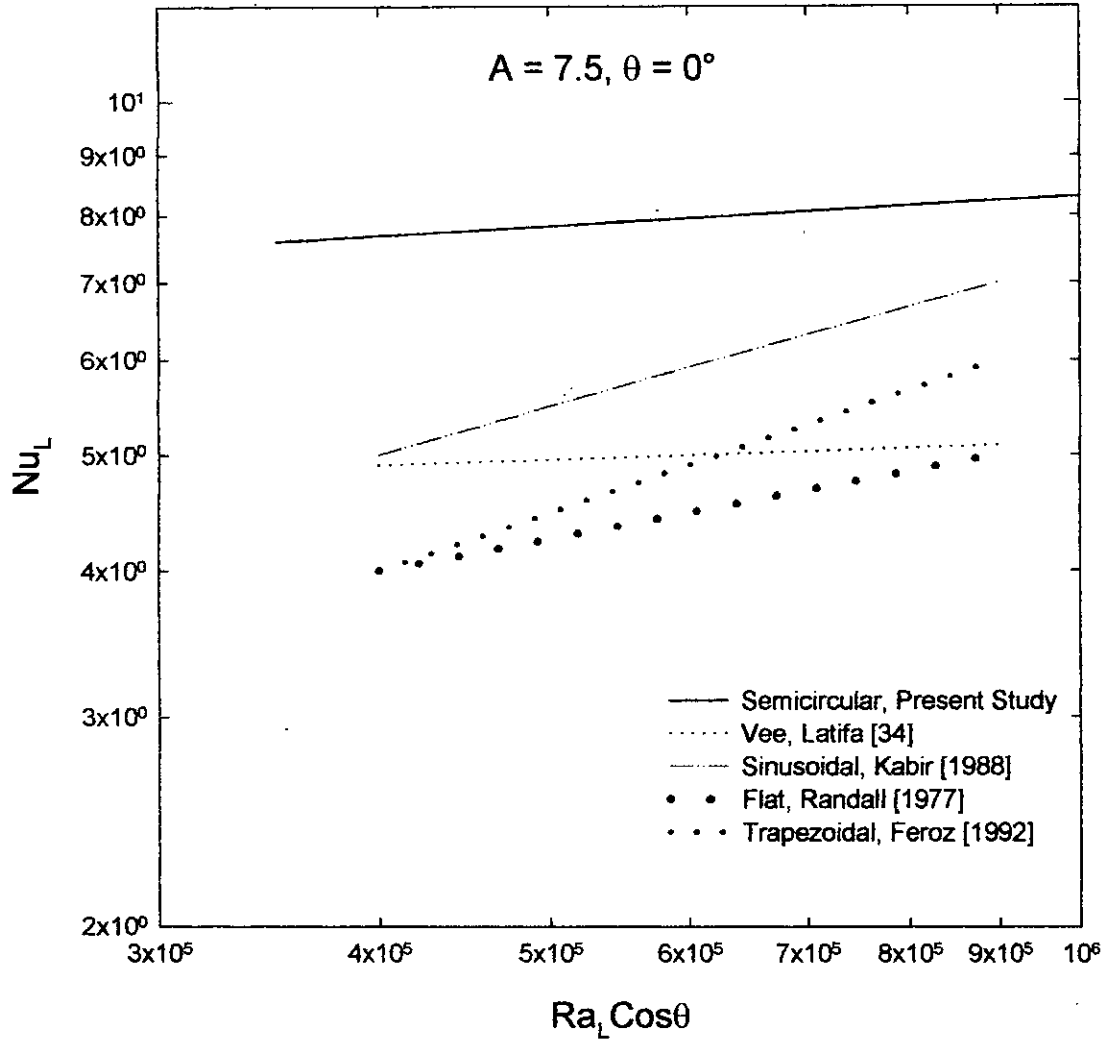


Fig. 6.29: Comparison of Nusselt number of the present study with Nusselt number of other related works for $A = 7.5$ at $\theta = 0^\circ$.

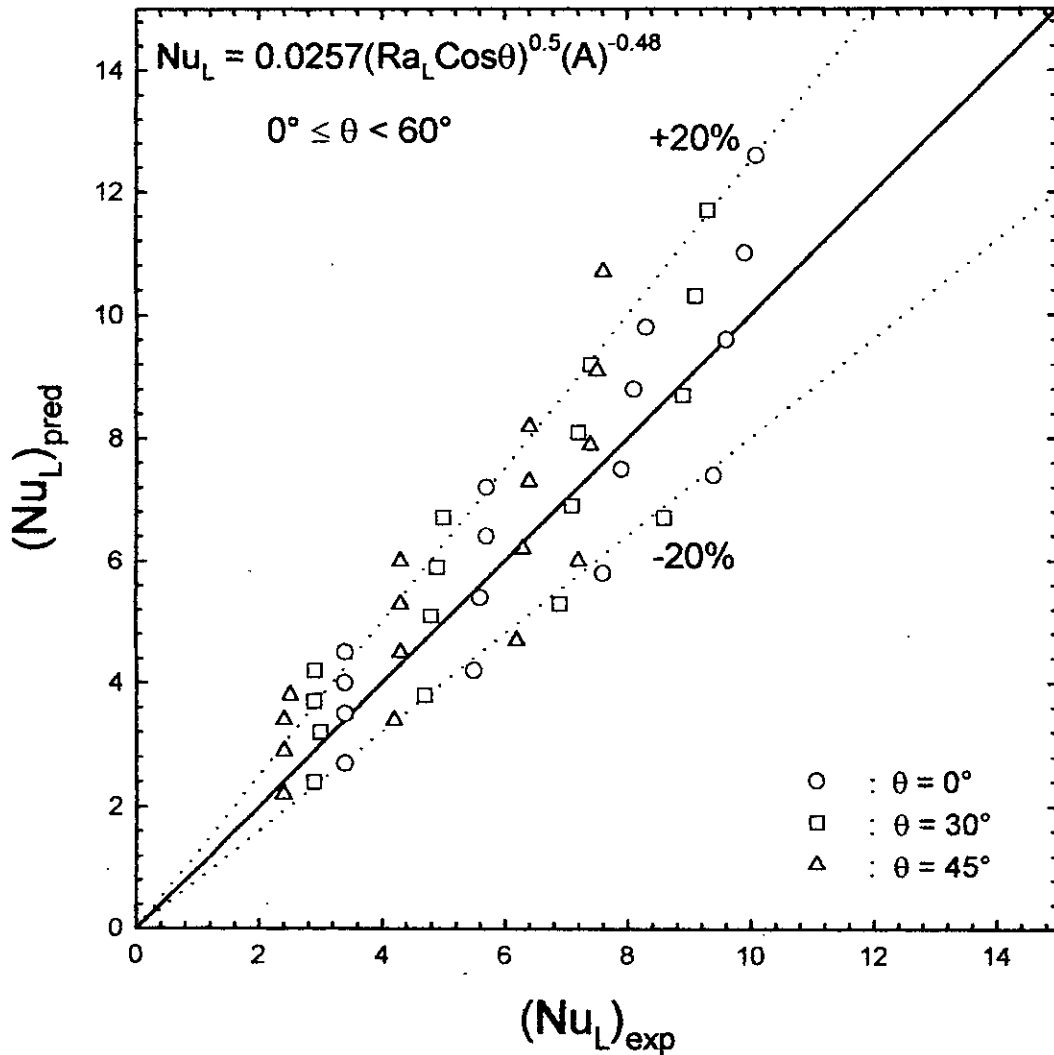


Fig. 6.30: Comparison of measured heat transfer coefficients with proposed correlation developed for free convection heat transfer across air layers with one surface semicircular corrugated for $0^\circ < \theta < 60^\circ$.

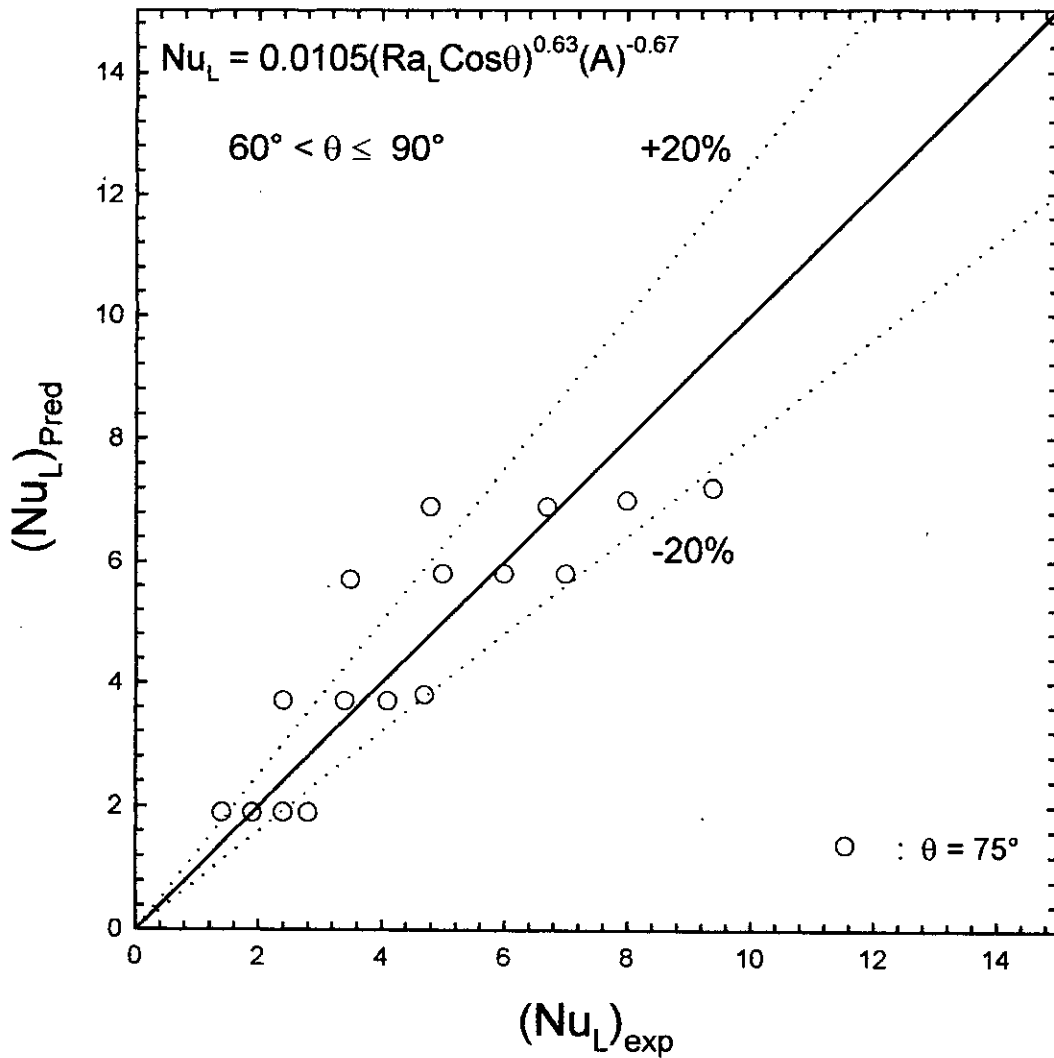


Fig. 6.31: Comparison of measured heat transfer coefficients with proposed correlation developed for free convection heat transfer across air layers with one surface semicircular corrugated for $60^\circ < \theta < 90^\circ$.

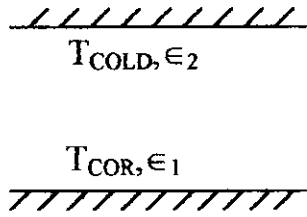


Fig. A.1

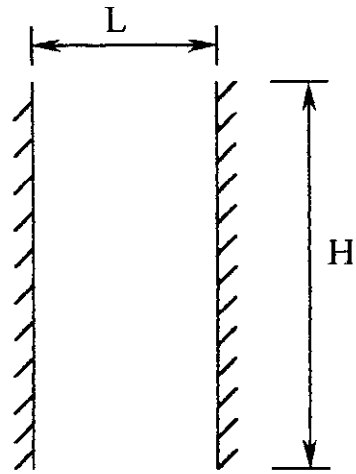


Fig. A.2

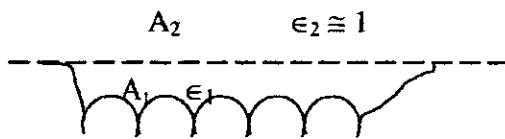


Fig. A.3

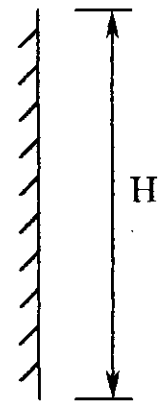


Fig. A.4

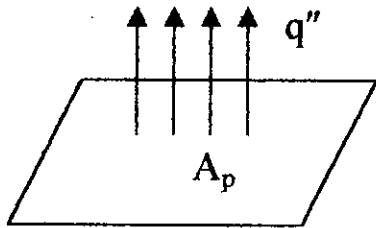


Fig. A.5

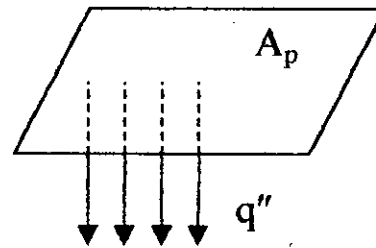


Fig. A.6

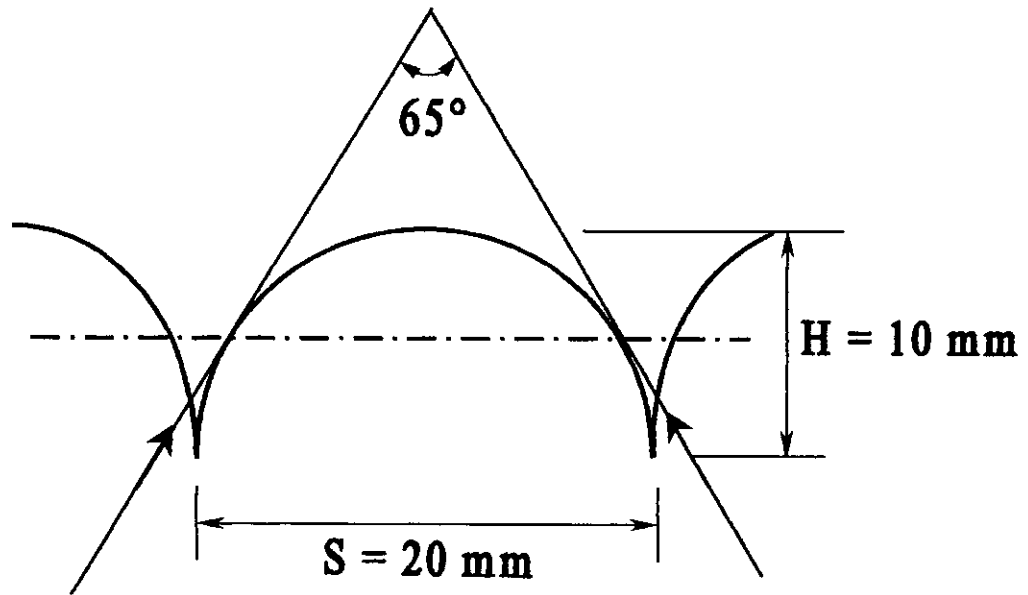


Fig. C.1: Corrugation geometry.

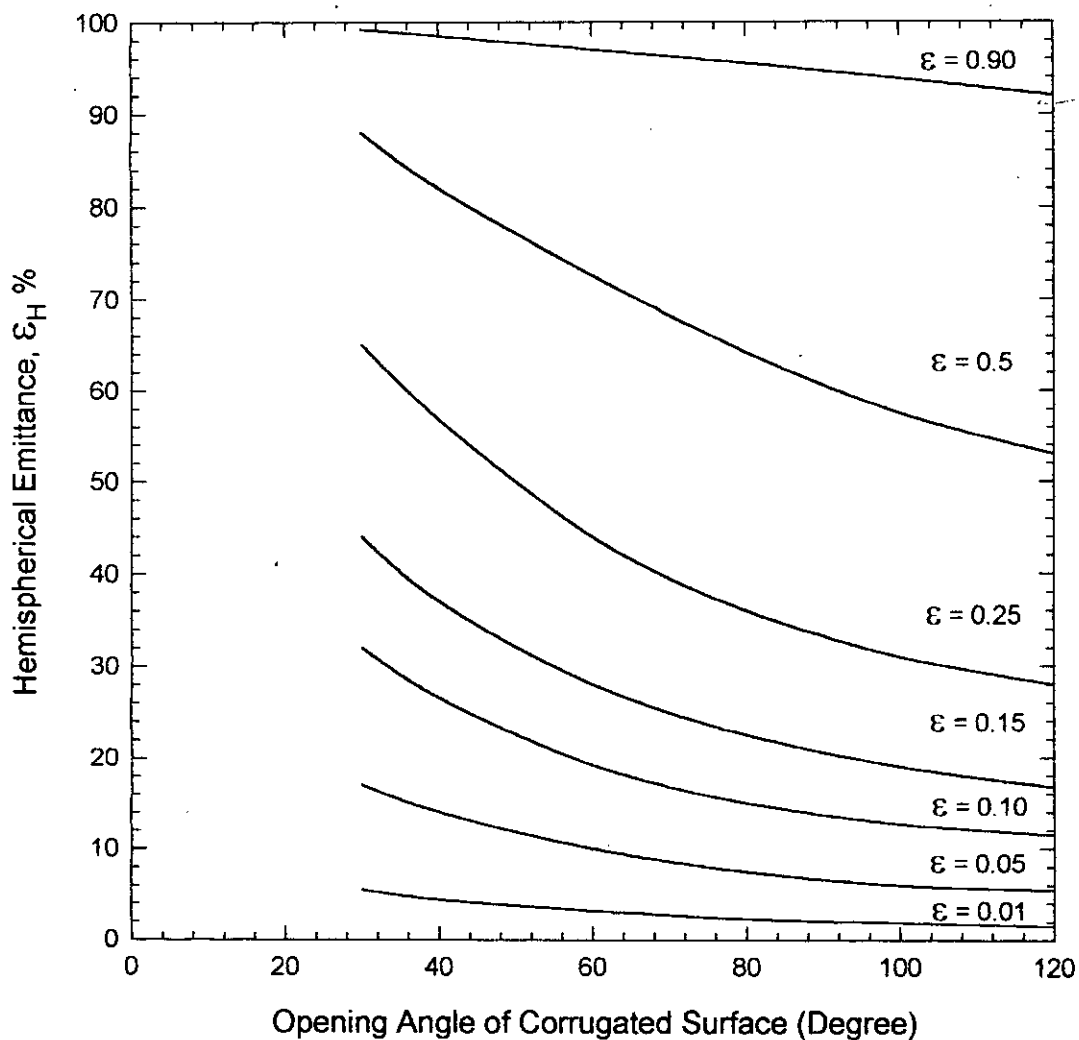


Fig. C.2: Hemispherical emittance versus angle of opening for several plane long wave emissivities [Hollands, 1963].

